INFORMATION TO USERS

This reproduction was made from a copy of a document sent to us for microfilming. While the most advanced technology has been used to photograph and reproduce this document, the quality of the reproduction is heavily dependent upon the quality of the material submitted.

The following explanation of techniques is provided to help clarify markings or notations which may appear on this reproduction.

1. The sign or "target" for pages apparently lacking from the document photographed is "Missing Page(s)". If it was possible to obtain the missing page(s) or section, they are spliced into the film along with adjacent pages. This may have necessitated cutting through an image and duplicating adjacent pages to assure complete continuity.

2. When an image on the film is obliterated with a round black mark, it is an indication of either blurred copy because of movement during exposure, duplicate copy, or copyrighted materials that should not have been filmed. For blurred pages, a good image of the page can be found in the adjacent frame. If copyrighted materials were deleted, a target note will appear listing the pages in the adjacent frame.

3. When a map, drawing or chart, etc., is part of the material being photographed, a definite method of "sectioning" the material has been followed. It is customary to begin filming at the upper left hand corner of a large sheet and to continue from left to right in equal sections with small overlaps. If necessary, sectioning is continued again–beginning below the first row and continuing on until complete.

4. For illustrations that cannot be satisfactorily reproduced by xerographic means, photographic prints can be purchased at additional cost and inserted into your xerographic copy. These prints are available upon request from the Dissertations Customer Services Department.

5. Some pages in any document may have indistinct print. In all cases the best available copy has been filmed.

University Microfilms International
300 N. Zeeb Road
Ann Arbor, MI 48106

Dresdner, Karl P., Jr.

CELLULAR CALCIUM ION UPTAKE AND EXTRACELLULAR (CALCIUM ION) DEPLETION IN FROG VENTRICULAR MUSCLE

City University of New York PH.D. 1983

PLEASE NOTE:

In all cases this material has been filmed in the best possible way from the available copy. Problems encountered with this document have been identified here with a check mark __✓__.

1. Glossy photographs or pages _____
2. Colored illustrations, paper or print _____
3. Photographs with dark background _____
4. Illustrations are poor copy __✓__
5. Pages with black marks, not original copy __✓__
6. Print shows through as there is text on both sides of page _____
7. Indistinct, broken or small print on several pages __✓__
8. Print exceeds margin requirements _____
9. Tightly bound copy with print lost in spine _____
10. Computer printout pages with indistinct print _____
11. Page(s) _____ lacking when material received, and not available from school or author.
12. Page(s) _____ seem to be missing in numbering only as text follows.
13. Two pages numbered _____. Text follows.
14. Curling and wrinkled pages __✓__
15. Other _____

CELLULAR CA^{++} UPTAKE AND EXTRACELLULAR $[CA^{++}]$ DEPLETION IN FROG VENTRICULAR MUSCLE

by

KARL DRESDNER

A dissertation submitted to the Graduate Faculty in Pharmacology of the School of Biomedical Sciences at Mount Sinai School of Medicine in partial fulfillment of the requirements for the degree of Doctor of Philosophy, The City University of New York.

1983

This manuscript has been read and accepted for the Graduate Faculty in Pharmacology satisfaction of the dissertation requirement for the degree of Doctor of Philosophy.

8/31/83
Date

Richard P. Lin
Chairman of Examining Committee

8/31/83
Date

Terry Ann Krulwich
Executive Officer

Supervisory Committee

The City University of New York

ABSTRACT - CELLULAR Ca^{++} UPTAKE AND EXTRACELLULAR $[Ca^{++}]$ DEPLETION IN FROG VENTRICULAR MUSCLE by Karl Dresdner.

Advisor: Dr. Richard P. Kline

The extracellular calcium ion concentration ($[Ca^{++}]_o$) in contracting frog ventricular myocardium was directly and continuously measured with a Ca^{++} selective microelectrode (Ca-ISE). Frog (Rana pipiens) ventricular strips were superfused with 0.050 to 0.20 millimolar Ca^{++} Ringers to reduce muscle contraction. A few experiments were successful in higher Ca^{++} Ringers. For some positions of the Ca-ISE tip, the $[Ca^{++}]_o$ significantly decreased during the action potential. As fast repolarization of the membrane potential occurred, the depletion of $[Ca^{++}]_o$ stopped. Following repolarization, the $[Ca^{++}]_o$ increased rapidly toward baseline suggesting that the tip of the Ca-ISE was positioned in the small clefts surrounding the cells. At other Ca-ISE tip locations (presumably in larger clefts), the beat to beat $[Ca^{++}]_o$ fluctuations were small or absent.

We estimated the Ca^{++} flux/cm^2 cell membrane required to generate depletion. The estimated increase in the intracellular $[Ca^{++}]$ which would result from the transmembrane Ca^{++} influx was 0.5 to 8.8 micromoles per liter cells (with 0.050 to 1.0 Ca^{++} Ringers). This is comparable to the quanity of Ca^{++} required to catalyze muscle contraction.

During acute increase in the stimulation rate, the $[Ca^{++}]_o$ fell in 3 to 5 minutes to a minimum level. The minimum $[Ca^{++}]_o$ was attained sooner when the $[Ca^{++}]_o$ depletion was large, indicating that cellular Ca^{++} uptake turned off as the transmembrane $[Ca^{++}]$ gradient

was dissipated. $[Ca^{++}]_o$ depletion during repetitive stimulation was enhanced in low Na^+ Ringers and reduced by manganese or nickel ions. Catecholamines increased the rate and magnitude of $[Ca^{++}]_o$ depletion and were blocked by propranolol, nickel, or manganese ions. Contracture fluid (high K^+/low Na^+ Ringers) caused significant $[Ca^{++}]_o$ depletion. When interventions prolonged $[Ca^{++}]_o$ depletion beyond 4 minutes a cellular efflux of Ca^{++} was activated which caused a prolonged postdrive overshoot of $[Ca^{++}]_o$.

DEDICATION

To Susan

Whose love, encouragement, and advice have always been present.

ACKNOWLEDGMENT

I want to thank Dr. Richard P. Kline for the opportunity he gave me to learn to measure extracellular ion concentration fluctuations in heart muscle. Without his continuous encouragement and guidance throughout the project, this thesis could never have been done.

I also thank Dr. Joseph Goldfarb for his help and expert guidance during my graduate training. My appreciation also extends to scientific training I received from Dr. Ken Foster, Dr. Sherwin Wilk, Dr. Robert Barker, Dr. Marian Orlowski, Dr. Thomas Mittag, Dr. Zia Penefsky, Dr. Joel Kupersmith, and the other members of the Faculty of the Department of Pharmacology in Basic Sciences at Mount Sinai School of Medicine.

I wish to gratefully thank Dr. Jack Peter Green for his interest in my behalf and support of my stay here.

I am indebted to Dr. Mark J. Kane for his constant help and guidance during my graduate studies. Also, I am indebted to Dr. Thomas Maack for his assistance in my scientific development.

I am indebted to my wife and family for their continuous love and support throughout the years.

Lastly, I acknowledge with gratitude my financial support at Mount Sinai: PHS Grant #5T32 GM07163-07.

TABLE OF CONTENTS

LIST OF FIGURES

I INTRODUCTION

Over the last century growing awareness of the complex actions of calcium ions in cellular function has stimulated basic research on calcium ion homeostasis in biological cells and tissues. Many of the biological actions of calcium ions were discovered during frog heart studies. In 1883 Ringer discovered that the frog heart needed calcium ions to contract. Contractility also increased when the bathing solution $[Na^+]$ was reduced. Clark (1913) found that frog heart contractility was proportional to the the ratio of [Ca++]/([Na+] + [K+]) in the Ringers solution . Wilbrant and Koller (1948) observed that the contractility varied with the Ringers solution $[Ca^{++}]/[Na^+]^2$. Calcium was hypothesized to cause muscle contraction by binding to the cardiac cell membrane (Niedergerke, 1956).

This hypothesis has been disproven. The site of action of calcium ions is in the cytoplasm. Calcium ions (10^{-7} to 10^{-5} molar) bind to troponin-C, a cytosolic protein associated with the contractile proteins (Endo and Ebashi, 1968). This was shown by biochemical experiments with the isolated muscle proteins. Winegrad (1971) found a similar $[Ca^{++}]$ dependence to the contraction of EDTA-treated frog ventricular muscle strips. EDTA treatment rendered the cell membranes completely permeable to small molecules and ions including Ca^{++}. Frog ventricular muscle contraction was also activated by 10^{-7} to 10^{-5} molar $[Ca^{++}]$ Ringers in mechanically skinned muscle strips (Fabiato and Fabiato, 1978).

These experiments indicated that muscle contraction was controlled by the myoplasmic $[Ca^{++}]$.

Transmembrane Ca++ Movements

Frog heart cells accumulate calcium ions when depolarized or exposed to low sodium Ringers. During repetitive trains of action potentials, cellular uptake of $^{45}Ca^{++}$ increased in proportion to the Ringers $[Ca^{++}]/[Na^{+}]^2$ (Niedergerke, 1963b). During continuous membrane depolarization by high $[K^{+}]$ Ringers, contracture tension (Luttgau & Niedergerke, 1958), and cellular uptake of $^{45}Ca^{++}$ were increased in proportion to the Ringers $[Ca^{++}]/[Na^{+}]^2$ (Niedergerke, 1963a). Low $[Na^{+}]$ Ringers also induced contractures (Luttgau and Niedergerke, 1958), and increased cellular $^{45}Ca^{++}$ uptake in proportion to the Ringers $[Ca^{++}]/[Na^{+}]^2$ (Niedergerke, 1963a). When a low $[Na^{+}]$ Ringers solution, caused a submaximal contracture, tension could be increased by membrane depolarization (Luttgau and Niedergerke, 1958). However, with zero $[Na^{+}]$ Ringers, membrane depolarization could not increase the tension (Luttgau and Niedergerke, 1958).

The largest cellular $[Ca^{++}]$ accumulations during these manuevers, estimated from $^{45}Ca^{++}$ movements, was 1.6 millimolar (Niedergerke, 1963a). Since contracture tension was transient, the free cytoplasmic $[Ca^{++}]$ of the relaxed tissue was estimated to be 0.1 micromolar, although the total cell $[Ca^{++}]$ was higher. Niedergerke (1963a) concluded that: 1) frog ventricular cells could store large amounts of calcium ions inside the cells in an inactive state, and 2) a small transmembrane Ca^{++} influx is associated with all protocols which cause frog ventricular muscle tension.

The average net cellular calcium ion accumulation per action potential, estimated from $^{45}Ca^{++}$ uptake in beating frog ventricles perfused in 1 mM Ca^{++}Ringers, was 1 to 2 micromolar (Niedergerke, 1963b). It was erroneously assumed that accurate measurements of the average Ca^{++} uptake per beat in frog ventricular cells could be obtained with tracer flux methods for the following reasons.

First, in an isotope uptake experiment the extracellular fluid would ideally be immediately equilibrated with isotope. Ideally as the radioisotope enters the cell, it is infinitely diluted so that backflux of isotope out of the cell is not significant (Attwell et al., 1979). However, several minutes were required before the $^{45}Ca^{++}$ equilibrated in the extracellular spaces in the frog experiments of Niedergerke (1957, 1963a,b). Isotope uptake was measured after 10 and 60 minutes time when the rate of uptake over time was markedly decreased indicating the cells were approaching saturation with $^{45}Ca^{++}$. The backflux of $^{45}Ca^{++}$ from the cells would cause an underestimation of the average beat to beat Ca^{++} influx.

Secondly, in frog ventricle radioisotope $^{45}Ca^{++}$ experiments, the time resolution for the determination of the Ca^{++} uptake per beat was not better than 10 to 20 seconds because of impeded simple diffusion in the extracellular compartments of the frog ventricle. Transient $^{45}Ca^{++}$ uptake lasting less than 10 to 20 seconds would be missed (Niedergerke et al., 1976).

Thirdly, assumptions were made regarding the amount of $^{45}Ca^{++}$ which was binding to passive fibre structures such as connective tissue, injured cells, or cell membranes (Niedergerke, 1957). These assumptions arose from the observation that the attainment of twitch tension and

extracellular [Ca^{++}] equilibrium was much slower than theoretically expected in frog ventricular muscle strips. The slow attainment of equilibrium was probably due to cellular uptake of Ca^{++} as it diffused into the strips. However, Niedergerke (1957, 1963b) attributed the slow attainment of equilibrium to extracellular adsorption of Ca^{++} to membranes and connective tissue. The cellular uptake of $^{45}Ca^{++}$ was reduced by about 25% when the $^{45}Ca^{++}$ tracer fluxes were corrected for $^{45}Ca^{++}$ assumed to be bound to connective tissue and to the outer surface membranes of cells (Niedergerke, 1963a,b).

Several years later it was realized that the estimates of Ca^{++} influx into frog ventricular cells per action potential, by $^{45}Ca^{++}$ flux studies, were too low to account for the observed tension generated. Alternatively, this estimate suggested to some investigators in the field that intracellular Ca^{++} sources might be involved in contraction (Page and Niedergerke, 1972, and Niedergerke et al., 1976). About 10 micromolar cytosolic [Ca^{++}] per action potential was needed for physiological contraction (Morad and Orkand, 1971; Niedergerke et al., 1976). This was about five times larger than the transmembrane $^{45}Ca^{++}$ flux measurements.

Frog ventricular cells are organized into groups of 10 to 100 cells and loosely surrounded by a sheath of porous endothelial cells (Staley and Benson, 1968). The endothelial cell sheath of these trabecula was predicted to function as a barrier to the free diffusion of ions in extracellular fluid (Page and Niedergerke, 1972). An instantaneous [Ca^{++}] change in the extratrabecular space (ETS) was calculated from electron micrographs to equilibriate in the subendothelial extracellular fluid outside the cell membranes by diffusion with a T 1/2 of 2.3 ± 0.8

seconds (Page and Niedergerke, 1972). The ETS itself would be expected to equilibrate with T 1/2 of 1 to 2 minutes. Chapman and Niedergerke (1970a) found that the twitch tension declined with a rapid exponential phase (T 1/2 = 3 to 10 seconds) and a slow exponential phase (T 1/2 = 50 to 180 seconds) when the Ringers [Ca^{++}] was rapidly decreased by the rapid superfusion method of Lamb and McGuigan (1966). The phase of rapid tension decline was similar to the time required for the [Ca^{++}] to re-equilibrate in the subendothelial space (SES). Using a choline gap voltage clamp to step the membrane potential, of a piece of frog ventricle to 0 mV for 10 seconds, Kavaler (1974) showed that a rapid change in the Ringers [Ca^{++}] altered muscle tension in less than 10 seconds. The rapid contractile sensitivity of frog ventricular muscle to the extracellular [Ca^{++}] indicated that this Ca^{++} source was important.

Hypodynamic Tension State

The isolated frog heart becomes hypodynamic. The ventricular contractions weaken over several hours (Clark, 1913) as the heart muscle loses stored Ca^{++} (Lieb and Loewi, 1918; Winegrad, 1973). The frog ventricle can become hypodynamic more quickly if the Ringers [Ca^{++}] or the heart rate is lowered sufficiently (Chapman & Niedergerke, 1970b). The development of the hypodynamic condition is rate-limited by an intracellular reaction, because the rate of this process was slower than the rate of exchange of the extracellular Ringers [Ca^{++}]. Proposed intracellular modulators of frog ventriclular contractility include: 1) an intracellular molecular complex with Ca^{++} (Clark, 1913; Chapman and Niedergerke, 1970 a,b); 2) Ca^{++} association with the inner face of the

cell membrane (Orkand, 1968); 3) the intracellular [Na^+] (Chesnais et al., 1978); and 4) the intracellular [Cyclic AMP]: [Cyclic GMP] ratio (Flitney and Singh, 1978).

Role of Ion Selective Electrodes

Rapid, accurate, and continuous measurements of transmembrane ion flux were needed. Potassium ion selective microelectrodes were developed by Walker (1971). These were used to measure rapid extracellular [K^+] fluctuations in nervous tissue (Neher and Lux, 1973; Prince et al., 1973) and in frog ventricle (Kline, 1975; Kline and Morad 1976, 1978).

Using potassium ion selective microelectrodes Kline (1975) found that the free potassium ion concentration in the subendothelial space (SES) of frog ventricular muscle increased during the cardiac action potential. At steady state the beat to beat extracellular potassium accumulations were observed to completely decay in the time interval between the action potentials. Transient, extracellular potassium ion concentration oscillations in beating frog ventricle are caused by several factors: 1) Narrow and tortuous extracellular spaces occur between cardiac cells and trabecula. The trabecular endothelial sheath restricts simple diffusion of ions (Page and Niedergerke, 1972). The attainment of equilibrium of the [K^+] in the extracellular spaces by diffusion is thus predictably delayed (Johnson and Liebermann, 1971; Attwell et al., 1979; Cohen and Kline, 1982). 2) The large ratio of the cardiac cell membrane surface area to extracellular cleft volume increases the extracellular ionic concentration fluctuation for a given membrane current density (Cohen and Kline, 1982). 3) The long duration of the frog ventricular action potential causes integration of the net potassium ion efflux over a long

period of time (Cohen and Kline, 1982). 4) Because the concentration of potassium ions outside the myocardial cell is low it changes by a larger percentage than the extracellular sodium ion concentration for the same membrane flux (Johnson and Liebermann, 1971; Attwell and Cohen, 1979).

When a Ca^{++} selective resin with low selectivity to Na^{+}, K^{+}, and Mg^{++} was synthesized by Oehme, Kessler and Simon (1976), calcium selective microelectrodes (CaISES) could be made and adapted to procedures developed previously for potassium ion selective microelectrodes (Walker, 1971; Lux and Neher, 1973; Prince et al., 1973; Kline, 1975). The measurement of the extracellular $[Ca^{++}]$ by calcium ion selective microelectrodes would allow studies of the net transmembrane calcium ion flux.

Frog ventricular strips were the ideal preparation for this study. Kline and Morad (1976, 1978) and Martin and Morad (1982) have characterized the major features of extracellular potassium ion accumulation and depletion in this preparation. Their data analyses were facilitated by the earlier detailed studies of Staley and Benson (1968) and Page and Niedergerke (1972) on the histology and the theoretical diffusion of extracellular Ca^{++} ions across the trabecular endothelial sheath. In addition, Kline (1975) and Cohen and Kline (1982) have performed computer simulations of the subendothelial and extratrabecular space $[K^{+}]$ changes during single and trains of frog ventricular action potentials.

A direct role of the extracellular calcium ion concentration in the process of excitation-contraction in frog ventricle (versus a direct role of an intracellular calcium source) is the prevailing hypothesis (Morad and Orkand, 1971; Morad and Goldman, 1973; Kavaler, 1974; Anderson et al.

1977; Fabiato and Fabiato, 1978a,; Kavaler et al., 1978). Tension is altered in 10 to 20 seconds by changing the Ringers [Ca^{++}] (Chapman and Niedergerke, 1970a, b; Kavaler, 1974; Anderson et al., 1977; Chesnais et al., 1978; Kavaler, 1978). In skeletal and mammalian cardiac muscle the sarcoplasmic reticulum is well developed and thought to release large quanities of Ca^{++} during membrane depolarization. In frog ventricle there is one-fifthteenth the volume of sarcoplasmic reticulum found in mammalian heart cells (Page et al., 1971; Page and Niedergerke, 1972). Frog ventricular cells have a larger surface area to volume than mammalian cardiac and skeletal muscle cells. While these observations support the hypothesis, the net transmembrane Ca^{++} influx per action potential (estimated to date only by $^{45}Ca^{++}$ fluxes) is apparently too low. Therefore, new estimates of the frog ventricle net transmembrane Ca^{++} influx per beat are needed.

Negative Twitch Tension Staircase

Brown and Orkand (1968) have reported that frog ventricular strips produce a biphasic twitch tension staircase when the strips are superfused in Ringer containing less than one millimolar calcium. After a rest period, repetitive stimulation evokes, a 1 to 3 minute period of subnormal twitch tension (reduced by as much as 60%) followed by a slowly developing positive twitch tension staircase. The negative twitch tension phase occurs even though the action potential duration is not shortened by an increase in heart rate. Maneuvers thought to increase the intracellular calcium concentration abolish the negative twitch tension phase. Brown and Orkand (1968) have proposed that altered excitation-coupling occurs during the early negative phase of the

staircase. The present study proposition is that depletion of the extracellular calcium ion concentration was occurring. If so, the early time course of extracellular [Ca^{++}] depletion should correlate with the early negative tension staircase of frog ventricular muscle elicited by repetitive stimulation in low bath calcium solutions.

Certain limitations are present in the experimental approach selected: 1) The calcium ion selective microelectrode response is slow (time constant 0.3 to 0.6 seconds). 2) The CaISE tip diameter (1.5-3 microns) cannot enter small intercellular clefts without causing significant distortion. In these clefts the largest extracellular ionic fluctuations are expected to occur because the cell membrane surface area : extracellular volume is the greatest (Kline and Morad, 1978; Cohen and Kline, 1982). 3) The Ringers calcium ion concentraton had to be lowered from normal (1mM) to 0.05-0.20 mM to reduce the twitch tension and permit stable and prolonged extracellular CaISE impalements.

In this dissertation new and direct evidence for the depletion of the extracellular fluid calcium ion concentration in beating frog ventricular muscle is presented. Some of the physiological consequences of this extracellular [Ca^{++}] depletion have been investigated. In addition, some of the pharmacology of the membrane transport of Ca^{++} was studied by using the depletion of the extracellular [Ca^{++}] as the control response.

II METHODS

A. Preparation of Frog Ventricular Muscle Strips

Frogs (Rana pipiens) were obtained from Hazen & Co., Vermont, during March to December months, and were 2.5 to 3.5 inches body length. Frogs were stored in tap water at 22-23°C (not fed) and used within a month of purchase.

To isolate a ventricular muscle strip, a frog was decapitated and its spinal column was pithed. Once the ventricle was in view by dissection, the ventricular apex was held by twissors. The whole ventricle was freed from the body by a cut just dorsal to the atrio-ventricular junction. With 0.2-1.0 mM Ca^{++}Ringers the whole ventricle was rinsed free of blood using a pasteur pipette. The apex and top third of the ventricle were discarded. The ring of midventricular muscle was cut into 2 to 4 strips while preserving the ventricular wall thickness. The dimensions of the strips were 1-2 millimeters in diameter and 2-4 millimeters long.

Strips were mounted (endocardial face up) in a translucent plexiglass tissue bath with stainless steel insect pins or under an overhead silk thread grill so that deformation of the muscle strip was minimal. In early experiments the bath volume was 3 mls. and the Ringers solution flow rate was 1 to 5 mls. per minute. The later experiments employed a bath like that of Hodgkin & Horowicz (1959) with a volume of 0.2 mls. A Ringers solution flow rate of 1 to 5 mls. per minute was used to obtain complete bath changes in less than 20 seconds.

Before starting the experiment with a calcium microelectrode the muscle strips were continuously superfused with 0.2-1.0 mM Ca^{++}Ringers solution at 22°C for 30-60 minutes. This was followed by superfusion in

0.05-0.20 mM Ca^{++}Ringers solution for 2 hours. During this time, the muscle strips were continuously stimulated using brief electric shocks to trigger membrane action potentials at a rate of 3-12 per minute. The electric shocks were delivered by two Ag-AgCl wires which lay near and parallel to the outside of the muscle strips. The field stimulation had a duration of 1.5 to 10 milliseconds and a current of 1-10 milliamperes (about 150% the minimum required stimulus). Obvious contractile motion in the mounted muscle strips slowly disappeared after the bath calcium ion concentration was lowered from 1.0 to 0.05-0.20 mM.

B. Superfusion Solutions

In the early experiments the frog Ringers solution (Ringer, 1883; Kline and Morad, 1978) had the following composition in millimoles per liter: NaCl 116, KCl 3, $NaHCO_3$ 2, and $CaCl_2$ 0.050-1.0. The pH was 8.1-8.3 before addition of a small quantity of HCl to make the pH 7.4-7.8 at 23°C. For prolonged stimulation protocols, Ringers solution with glucose, oxygenation, and stronger pH buffering has been recommended (Ellis, 1952; Blinks and Koch-Weser, 1963, Mainwood and Lucieri, 1972; Mainwood and Worsley-Brown; 1975; Penefsky, 1982 personnel communication). In the latter 85% of the experiments, the composition was (in millimoles per liter): NaCl 93, KCl 3, $NaHCO_3$ 25, NaH_2PO_4 0.5, $MgCl_2$ 0.02, Glucose 5.5, and $CaCl_2$ 0.050-1.0. It was continuously gassed with 5% CO_2/95% O_2 gas at 22-23°C to obtain a pH of 7.25 $\pm$ 0.05 as predicted by Burton (1975).

In some experiments the composition of the Ringers was further modified, but solution tonicity was kept essentially constant. In low sodium experiments, equimolar (pH 7.3, Tris/Tris$^+Cl^-$) was substituted.

In high potassium experiments, sodium was lowered by an equimolar amount. The $CaCl_2$ concentration was varied from 0.050-1.0 millimolar without other adjustments. When 1 mM manganese chloride or nickel chloride was added, 1 milliliter aliquots of 1 M stock solutions were added without other adjustments. Higher manganese ion concentrations precipitated. Epinephrine (Parke-Davis), isoprotererol (Elkins-Sinn), and propranolol (Ayerst), purchased in 0.9% saline at 1 mg/ml concentration, were added to the stock Ringers just prior to need till the desired concentration was attained.

C. Electrical Measurements

1. Transmembrane Potential Difference

Transmembrane potential (Vm) was measured with fine tipped (diameter less than 1 micron) Borosilicate #7740 glass micropipets containing a 3M KCl electrolyte solution (Adrian, 1956). The filled microelectrodes had a resistence of 8-20 megohms. The micropipettes were pulled from 2 millimeter (WPI-Quik-fil™) glass capillaries on a vertical position pipette puller (Narishe PE-2). Prolonged cell membrane potential recordings of more than 5 minutes were difficult to obtain due to the small size of frog ventricular muscle cells (average diameter about 5 microns; Page and Niedergerke, 1972). Microelectrode reimpalements were frequently necessary during the experiments. Several muscle strips of similar dimensions were obtained from the same region of a heart and were superfused at the same time with field stimulation. Essentially identical action potentials could be measured in all the strips of each experiment. In order to not disturb good impalements of the calcium microelectrode, transmembrane potential was usually recorded in a

separate muscle strip during the experiment.

2. Extracellular Calcium Ion Concentration

Calcium ion concentration was determined using 1.5-2.5 micron diameter tip single-barrel (Oehme et al., 1976), and 2-4 micron diameter tip double-barrel Ca^{++} ion selective microelectrodes. The end of the microelectrode tip is the $[Ca^{++}]$ sensor. The shaft of the microelectrode is an electrical insulator. These electrodes are fragile and can be used for only a day or two. The are constructed and calibrated just before the experiment. The potentiometric response of the Ca^{++} microelectrode to the free extracellular $[Ca^{++}]$ obeys the Nerst equation which assumes that the electrode is purely selective for Ca^{++}. At 23°C the Nerst equation for a Ca^{++} electrode is:

Electrode Output (in millivolts) = Constant + 29.3 log $[Ca^{++}]$.

From the initial electrode potential, (E_1), the final electrode potential, (E_2), and the initial extracellular calcium ion concentration $[Ca_1^{++}]$, the final calcium ion concentration, $[Ca_2^{++}]$ is calculated as follows:

$$E_1 = \text{Constant} + 29.3 \log [Ca_1^{++}].$$

$$E_2 = \text{Constant} + 29.3 \log [Ca_2^{++}].$$

$$[Ca_2^{++}] = [Ca_1^{++}] \times EXP_{10} [(E_1 - E_2)/29.3]).$$

The change in $[Ca^{++}]$ is $[Ca_1^{++}] - [Ca_2^{++}]$.

Since it was known that the extracellular clefts in which the calcium microelectrode would be placed, would vary in free potassium ion concentration (Kline and Morad, 1978) and possibly in free sodium ion

concentration, the calcium ion selective microelectrodes were tested in calibration solutions varying in sodium and potassium concentration. The extracellular potassium during most experiments with frog ventricular strips never exceeded 10 millimolar (Kline and Morad, 1978) when the Ringers potassium ion concentration was 3 millimolar. Assuming the extracellular fluid remained isotonic, the extracellular $[K^+]$ would increase 7 mM while the $[Na^+]$ would decrease from 118.5 to 111.5 millimolar. In other calibration solutions sodium and potassium ion concentration were held constant while the calcium ion concentration was varied. The effect of 1 mM $NiCl_2$ or $MnCl_2$ addition to the 10 micromolar calcium ion calibration solution was also examined as were the effects of epinephrine, isoproterenol, and propranolol. Bicarbonate and phosphate ions were excluded from standard calibration solutions but complete Ringers solution were tested routinely for comparison. The following table lists the composition (in millimoles/liter) of the standard calibration solutions used to test the calcium microelectrodes before and after each experiment:

	$CaCl_2$	NaCl	KCl	$MgCl_2$	$MnCl_2$	$NiCl_2$
A)	1.0	118	3	0.02		
B)	0.10	118	3	0.02		
C)	0.010	118	3	0.02		
D)	0.010	101	20	0.02		
E)	0.010	118	3	0.02	1	
F)	0.010	118	3	0.02		1
G)	0.0050*	118	3	-		

*The 0.005 mM Ca^{++} Calibration solution was made using 5.0 mM $CaCl_2$ buffered by 10 mM HEDTA (at pH 7.03 buffered by 10 mM Imidazole). $MgCl_2$ was not present due to its high affinity for HEDTA (Martell and Smith, 1974). All other solutions used during experiments were tested with the calcium microelectrode in the experimental bath and were compared to the control Ringers solution.

The response of the calcium microelectrode to the $[Ca^{++}]$ in the presence of other cations is described by the formalism of the International Union of Pure and Applied Chemists (IUPAC). At 23°C this more complete Nerst equation (IUPAC, 1976) is:

$$E = \text{Constant} + 29.3 \text{ Log } [a_A + K^{Pot}_{A,B}(a_B)^{2/z_B} + K^{Pot}_{A,C}(a_C)^{2/z_C} + \ldots K^{Pot}_{A,N}(a_N)^{2/z_N}].$$

Where: a_A is the calcium ion activity, and a_B, a_C, $\ldots a_N$ are the activities of other cations present. The $K^{Pot}_{A,B}$, $K^{Pot}_{A,C}$, $\ldots$ $K^{Pot}_{A,N}$ are the selectivity coefficients of interfering ions (B, C,.. N) on an electrode selective for ion A. The valences of the interfering ions are z_B, z_C, .. z_N.

Lee, et al. (1980) reported:

$$K^{Pot}_{Ca++,Na+} = 10^{-4.1} - 10^{-5},$$
$$K^{Pot}_{Ca++,K+} = 10^{-5.2} - 10^{-6},$$
$$K^{Pot}_{Ca++,Mg++} = 10^{-6.3} - 10^{-7.3},$$

for single barrel, 1 micron tip diameter calcium ion selective microelectrodes using Simon et al.'s (1978) neutral carrier calcium ion exchange resin. Similar selectivity coefficients were obtained by Sheu and Fozzard (1982). The background interfering ions: 118 Na^+, 3 K^+, 0.02 Mg^{++} (in millimoles per liter) generate a calcium electrode output equivalent in the worst case to a 0.7 micromolar calcium ion solution. The solution of 101 Na^+, 20 K^+, 0.02 Mg^{++} is equivalent to a 0.4 micromolar calcium solution. The Ca^{++} microelectrode is 10 times more sensitive to Na^+ than K^+ interference. In the presence of 10 micromolar calcium (see standard calibration solutions C versus D) the change in interfering Na^+ concentration (from 118 to 101 mM while the $[K^+]$ changed from 3 to 20 mM) was equivalent to changing the Ca^{++} concentration from 10.7 to 10.4 micromolar. This 3% $[Ca^{++}]$ decrease should cause a small -0.4 mV potential change. In frog ventricular extracellular clefts $[Na^+]$ fluctuations are probably less than 10 mM (less than 118 to 108m). Therefore, less than a 0.3 mV Ca^{++} electrode error in 10 micromolar Ca^{++}Ringers, and less than a 0.03 mV error in 100 micromolar Ca^{++} Ringers solutions is expected. Calcium electrode measurements in 10 micromolar $[Ca^{++}]$ calibration solutions (C versus D, table 1) confirmed this prediction. The negative shift at steady state averaged less than 1 millivolt (see figure 1). In summary, the neutral carrier calcium ion selective microelectrode is a selective and sensitive instrument for the detection of small changes in the calcium ion concentration in the extracellular clefts of frog ventricle.

3. Construction of Calcium Ion Selective Microelectrodes

Three kinds of ion selective microelectrodes were used: single-barrel

Figure 1: Graph shows the response of the calcium ion selective microelectrode versus calcium ion concentration. Test solutions composition are listed in methods. The dashed line has a slope of 29 millivolts per ten fold calcium concentration increase and represents the Nerst slope for an electrode with ideal selectivity to calcium ions at 23°C. The actual response of constructed Ca^{++} ion selective electrodes ($n \geq 100$) is Nerstian between $10^{-5.3}$ - 10^{-3} molar, the range employed in the experiments described. The responses seen at 10^{-8}, 10^{-7}, and 10^{-6} molar free calcium ion concentration are the results of only a few electrodes. EGTA-calcium buffers were used to make these three solutions according to Lee et al. (1980) following suggested corrections by Tsien and Rink (1980).

Bottom record is the calibration of a Ca^{++} ion selective microelectrode in the calibration solutions and 0.20 and 0.050mM Ca^{++} Ringers solutions.

It can be seen that the electrode attains a steady potential in 1 to 2 seconds. The 0.20 and 0.050 mM Ca^{++} solutions were Ringers containing phosphate and bicarbonate. It appears that the Ca^{++} was not so significantly complexed with these anions to require a correction.

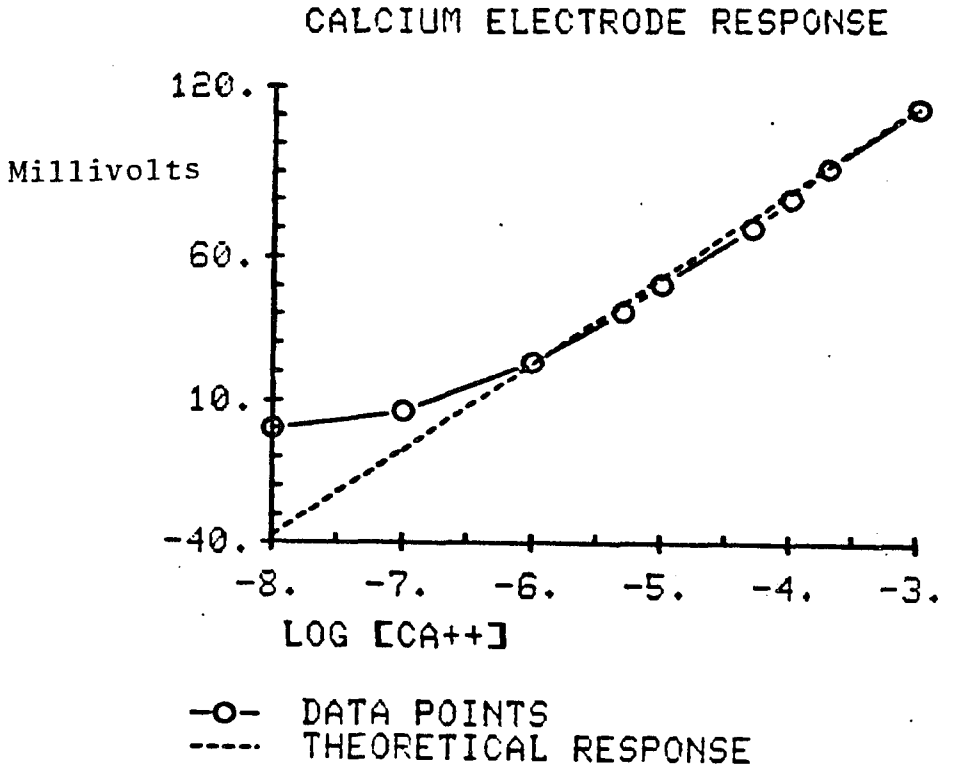

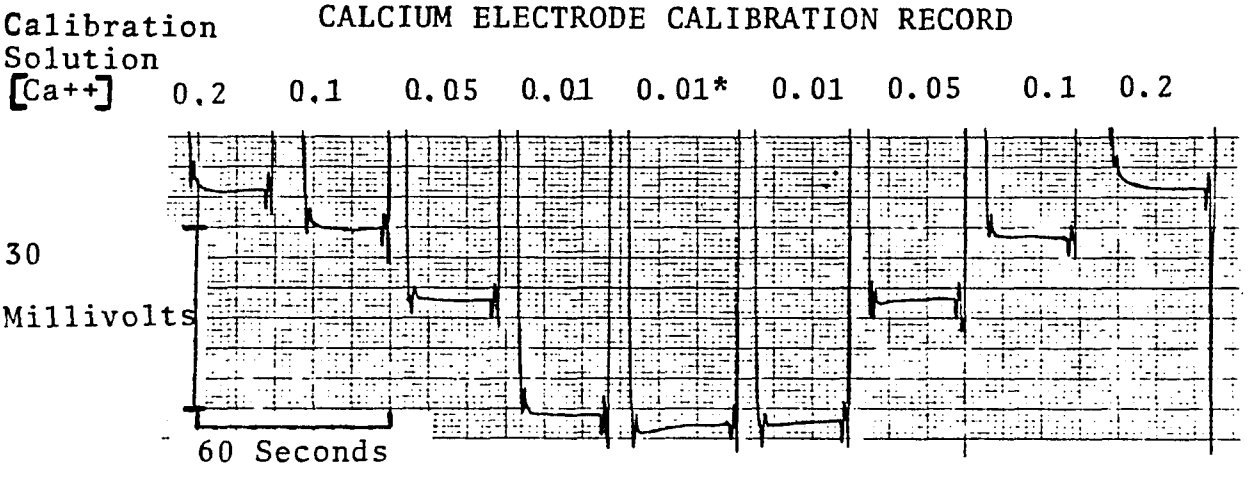

* The [Na+] = 101 mM, and the [K+] = 20 mM.

Ca^{++} microelectrodes, double-barrel Ca^{++} microelectrodes, and triple-barrel Ca^{++}/K^{+} microelectrodes. Most of the latter experiments were performed with single barrel Ca^{++} electrodes. For measurements of slow extracellular $[Ca^{++}]$ changes these electrodes were preferable due to their stability, small tips, and ease of construction.

Single-barrel Ca^{++} microelectrodes were made from aluminosilicate capillary glass (1 millimeter diameter, 10% wall: diameter ratio, Victor Palumbo, Glass Co. of America, N.J.). This capillary glass was cleaned twice by boiling in distilled water. The ends of the capillaries were fire-polished. Micropipettes which slowly tapered at the tip were created using a Narishige PE-2 vertical pipette puller. Batches of 10 to 20 two inch long micropipettes were pulled for each experiment. Under a microscope (400x magnification) their tips were carefully broken by a silver wire to between 1.5 and 2.5 microns. At the same time the tip diameter was determined by a calibrated grid in the microscope objective. Micropipettes were then placed in a silanized pyrex petri dish and baked at 120-160°C for at least one hour to remove all moisture. Then the temperature was reduced to 110 $\pm$ 10°C and several small drops of chlorotrimethylsilane liquid (Pierce Chem. Co., B.Pt. = 57°C) were added by syringe to the closed petri dish thru a small hole. After several hours the dish was vented at 115°C for about 1 hour. The dish was then covered again till the next step, typically the next day. Next, a micropipette was removed from the dish, cooled, and then filled with a 100 mM $CaCl_2$ solution to the tip. Using the vacuum generated by a 50 cc plastic syringe, Simon's neutral carrier Ca^{++} ion selective resin (Fluka Chemical Co., L.I., N.Y.), was drawn 500-2000 microns up the tip of the silanized aluminosilicate micropipette.

Double-barrel Ca^{++} microelectrodes were made from #7740 Borosilicate theta-style double-barrel capillaries (Glass Co. of America). After cleaning, firepolishing, and fabrication into micropipettes, one of two silanization procedures was used: the "dip" method or the "gas" method.

After filling one barrel with distilled water to the tip, the "dip" method of silanization involved dipping the double-barrel tip into a solution of 2.3% Dow Corning 200 fluid (viscosity 100 centistokes) and 97.7% Xylene, (v/v) until 300-500 microns of silanizing liquid had run up the empty barrel tip (Kline, 1975). The pipette was then allowed to dry overnight. By microliter syringe a small amount of Simon's Ca^{++} resin was placed inside the tapering tip of the silanized barrel. Once Simon's Ca^{++} resin had settled in the micropipette tip the barrel was backfilled with 100 mM $CaCl_2$ solution. The other barrel, containing the distilled water at this point, was then filled with 100 mM NaCl or a Ringers solution.

When double-barrel micropipettes were to be silanized by the "gas" method, one barrel was blocked quickly with some distilled water, while the other barrel was exposed to chlorotrimethylsilane gas at 22°C. To do this the butt of the double-barrel electrode was held for several seconds inside the neck of a 10 ml glass volumetric flask containing several milliliters of trimethylchorosilane liquid, removed, and then allowed to dry for several minutes to hours. The silanized barrel tip of the double barrel pipette was filled with Simon's Ca^{++} resin and backfilled with 100 mM $CaCl_2$. The reference side was filled with 100 mM NaCl or a Ringers solution.

Triple-barrel Ca^{++}/K^{+} microelectrodes were made from #7740 borosi-

licate glass theta-style triple-barrel capillaries (three barrels in a line; Glass Co. of America). The outer two barrels were made into a Ca^{++} and a K^{+} electrode, while the central barrel was filled with 100 mM NaCl or a Ringers solution. Although triple barrel Ca^{++}/K^{+} ion selective microelectrodes were more difficult to make, the principles followed during the construction of double-barrel Ca^{++} microelectrodes, were applicable to the construction of the triple-barrel Ca^{++}/K^{+} microelectrodes. The K^{+} electrode tip was filled with potassium liquid ion exchanger (Corning #477317). Its performance in measuring extracellular potassium ion concentration fluctuations has been described by Kline (1975), and Kline and Morad (1976, 1978) in detail.

Single-barrel, double-barrel, and triple barrel ion selective microelectrodes were equilibrated tip down in Ringers solution for about an hour to allow them to stabilize. Then they were tested in the calibration solutions.

4. Electronics

The tissue bath potential was defined by placing one end of a 2M KCl - 1.5% Agar bridge (in 2 millimeter polyethylene tubing) in the back of the bath, and the other end in a 2M KCl solution. A large coiled Ag-AgCl wire electrode in the 2M KCl solution was grounded to all the equipment. The bath ground system was relatively insensitive to the bath level, $[Cl^{-}]$ variations in the bath, and provided a stable reference potential.

The transmembrane potential (or intracellular) microelectrode was connected via a Ag-AgCl electrode to a unity gain electrometer (10^{11} ohms input impedance, 100 khz frequency response, Model M-707, W-P Instruments). The electrometer output was recorded on storage oscillo-

scope (Tektronics Model 5115) or on a paper chart recorder (Gould Model 2400).

The ion selective microelectrodes were connected via Ag-AgCl wire electrodes to preamplifiers with adjustable capacitance neutralization (input impedance 10^{14} ohms, Bloom Associates). The preamplifier output was connected to a differential amplifier (Design by Kline, Bloom Associates). Local extracellular potential was recorded by the reference barrel of double and triple barrel ion selective electrodes and was subtracted at the differential amplifier stage from the ion selective barrel(s). The differential amplifier output was recorded by the storage oscilloscope and chart paper recorder.

A wave generator (ATO Model F30) was used to test the electrical response time of the ion selective electrode. Output of the wave generator (a triangle wave function, period 5-20 seconds) was connected to the braid of a short segment of coaxial cable. This capacitively injected a square wave pulse on the wire linking the Ag-AgCl wire of the ion selective microelectrode to the preamplifier input, (Neher and Lux, 1973; Kline, 1975). The response of the ion selective electrode in the bath or muscle extracellular space, to the capacitatively produced square pulse was recorded alongside the triangle wave on the paper chart recorder, to measure the electrode's electrical time constant.

To miminize noise several precautions were taken. To reduce mechanical noise, a solid marble table supported the recording apparatus. The superfusion bath, electrode-positioning micromanipulators (Narishige), and ion selective preamplifier stands were mounted on a heavy steel plate cushioned by a partially-inflated bicycle tire laying on the marble table top. Exogenous high frequency electrical noise (i.e.

60 cycle A.C.) was reduced by enveloping all sides of the recording apparatus within a Faraday cage (small mesh copper screen). All apparatus were grounded to the Faraday cage including the bath suction outflow. Circuit loop diameters within the Faraday cage were minimized to reduce induced electrical noise. The gassing Ringers solution reservoirs, wave generator, differential amplifier, transmembrane potential electrometer, oscilloscope, field stimulator, and paper chart recorder were kept outside the Faraday Cage (See figure 2; Electronics schematic).

The response of the ion selective microelectrode to different Ringers solutions used in the experiment was examined with the microelectrode in the bath. In addition, before the experiment was begun, while the strip was equilibrating to low Ca^{++} Ringers in the bath, the prospective ion selective microelectrodes were calibrated in a separate system. Dishes of varying calcium, sodium, and potassium ion concentration Ringers were placed in a steel box serving as a second Faraday cage. The tip of the microelectrode and a Ag-AgCl ground wire were dipped into the dishes of calibration solutions. The output of the ion selective microelectrode was connected via a Ag-AgCl wire to an amplifier with adjustable capacitance neutralization, 10^{14} ohms input impedance, and x 50 gain (Metametrics). The amplifier output was fed to a paper chart recorder (Gould Model 220) located outside the steel box.

It should be noted that the methods employed to measure extracellular calcium ion concentration fluctuations and membrane potential in beating frog ventricular muscle were adapted from the methods reported by Kline (1975) and Kline and Morad (1976, 1978) for the measurement of extracellular potassium ion concentration fluctuations and membrane

Figure 2: This is a schematic diagram of the experimental equipment. Muscle strips (M) are field stimulated by stimulus isolation unit(S). Intracellular microelectrode membrane potential (Vm) is amplified by VA. IA amplifies ion selective electrode outputs (VCa + Vo, Vo). If Vo is not measured (as in the case of single barrel calcium microelectrodes) then the Vo input of the differential amplifier (DA) is grounded. The Ramp wave generator (R) is capacitatively coupled to output of ion selective microelectrode barrel to test the square pulse response of ion selective microelectrode. This equipment design was developed by Kline (1975).

Ground electrode (G) is a AgAgCl wire in 2M KCl connected to the bath (B) via a 2m KCl-1.5% Agar bridge. Data (Vm, Vo, VCa) are viewed on the storage oscilloscope and plotted on up to four channels of a paper chart recorder (not shown in figure)

When a triple barrel Ca^{++}/K^{+} ion selective microelectrode was used, an additional IA amplifier was used.

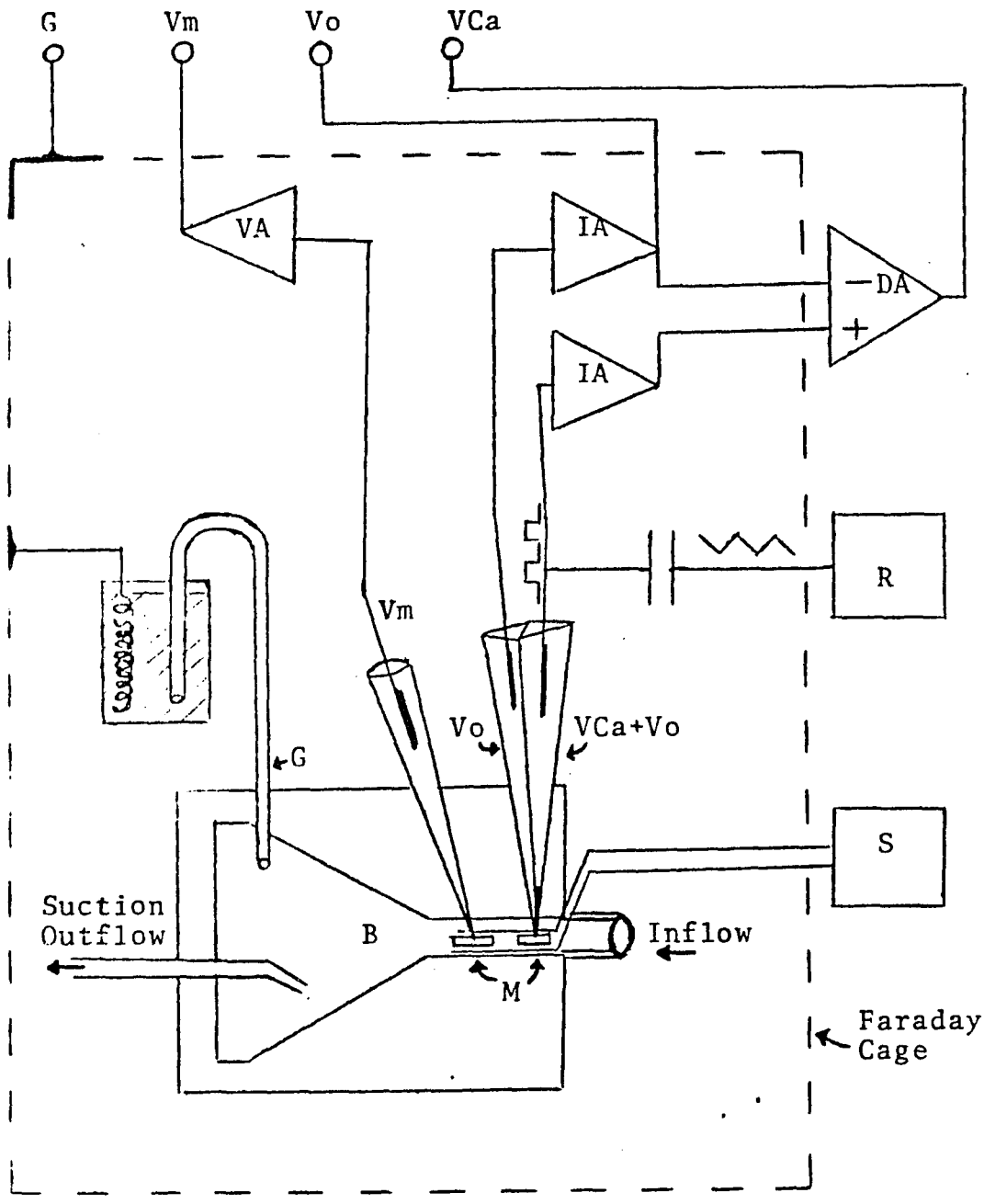
G
Vm
Vo
VCa
VA
IA
DA
IA
R
Vm
Vo
VCa+Vo
G
S
Suction
Outflow
B
Inflow
M
Faraday
Cage

Figure 3: Top record shows the output of a calcium ion selective microelectrode (tip in bath figure 2) during a doubling of the bath Ca^{++} concentration for 16 seconds starting at the arrow ( ) and reversing at the next arrow ( ). This shows that solution changes can be performed in this bath in 2-4 seconds. Noise was caused when the experimentor's hand entered the Faraday cage to operate the solution change valve.

Bottom panel, top record is the triangle wave used to generate a square pulse on the calcium ion selective microelectrode.

Bottom record is the response of the calcium ion selective microelectrode to a square pulse. The response of both single and double barrel calcium ion selective microelectrodes was not monoexponential. About 80% full response occurred in one second. Data from other experiments indicates that the approximate electrical response time constant ranged between 300-600 milliseconds. Therefore, Ca^{++} electrode responses possibly underestimate the actual magnitude of the beat to beat extracellular calcium ion depletion and Vo by about 20%.

RATE OF BATH [Ca++] CHANGE

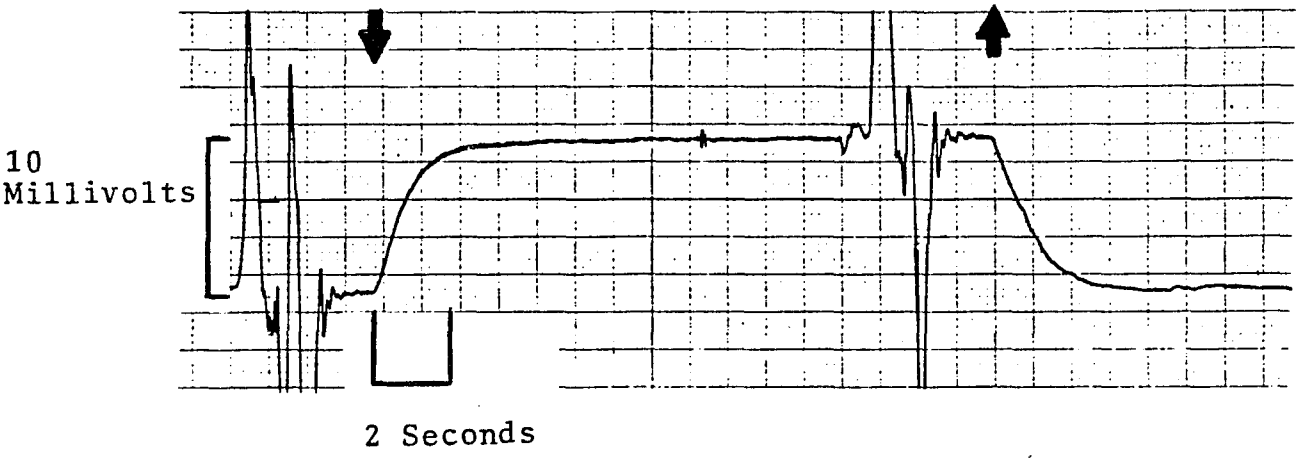

CALCIUM ELECTRODE ELECTRICAL RESPONSE TIME

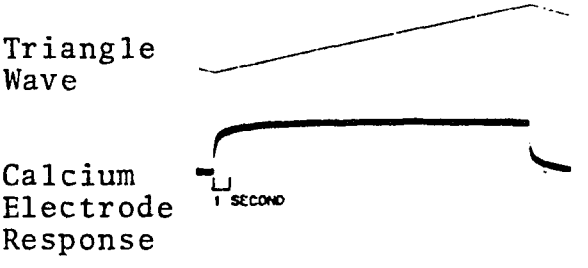

potential in this preparation.

5. Ion Selective Microelectrode Artifacts and Precautions

Possible mechanical and electrical artifacts had to be considered: 1) During the frog ventricular action potential twitch tension linearly increases over time peaking at repolarization. Tension then decays slightly more rapidly than it developed (Brown and Orkand, 1968). This tension can alter the extracellular position of the electrode tip.
2) Field stimulation can polarize the microelectrodes if the stimulation intensity or duration is excessive.
3) The evoked ventricular action potential has a detectable extracellular signal (V_o; Kline, 1975) of 0 to 10 mV amplitude which must be accurately subtracted from the ion selective barrel output.

Mechanical artifacts were reduced in several ways: 1) The majority of the experiments were performed with weakly contracting (hypodynamic) frog ventricular muscle strips. The hypodynamic state was produced by prolonged exposure of the muscle to subnormal Ca^{++}Ringers concentrations. One millimolar Ca^{++}Ringers is normal (Niedergerke, 1956). In 0.050-0.20 mM [Ca^{++}] twitch tension is 5-20% that caused by 1 mM Ca^{++}Ringers. 2) Evidence of a tension artifact can be seen occasionaly in both the ion selective and reference barrel outputs. The artifact is a fast, short-lived (less than 500 millisecond duration) negative-going spike at the end of the action potential. Sometimes its magnitude increases during repetitive stimulation. The tension artifact could be the result of a transient cell impalement, a transient increase in the extracellular resistence, or due to a bending of the microelectrode tip. This artifact was avoided by selecting microelectrode

impalements carefully. Data was screened for this artifact.

Artifacts due to field stimulation appeared at the onset of the action potential and had a variable amplitude and duration. Field stimulation electrodes were used as close as possible to the sides of the muscle. This decreased the required duration and current intensity of the stimulus. The polarity of field stimulation was reversed routinely during repetitive stimulation, when the ion selective microelectrode tip was in the bath, to be sure that the electrode did not polarize. When the microelectrode tip was in the muscle's extracellular space, its polarizability was tested with sub-threshold field stimulation. Extracellular $[Ca^{++}]$ depletion only occurred when action potentials were elicited.

Due to the high resistence of the trabecular endothelial sheath, some of the extracellular spaces within frog ventricular trabecula, exhibit a 1-10 millivolt extracellular action potential (V_o artifact during the intracellular action potential (Kline, 1975). It has the duration of the regular action potential. V_o is detected by the reference and ion selective barrels of a double-barrel Ca^{++} ion selective microelectrode. The reference barrel V_o is subtracted from the ion selective barrel V_o to obtain V_{Ca++} the calcium electrode signal at the differential amplifier stage. Due to the higher resistence of the ion selective barrel (10-1000x higher than the reference barrel) the two barrels do not detect V_o identically. Therefore, the V_o is not subtracted accurately from the Ca^{++} ion sensitive barrel. This is most evident when the V_o is large. Extracellular impalements of the microelectrode were selected to keep V_o small or absent. In addition, efforts were made to lower the resistence of the ion selective barrel.

The tip diameter was increased. The high resistence element is Simon's Ca^{++} resin. The height of this resin column was minimized. However, it was evident that the ion selective barrel resistence could not be lowered sufficiently without making the tip too large. Also, Ca^{++} ion selective electrodes with less than 500 micron long resin columns had short life times. In view of these difficulties, it was realized that only qualitative beat to beat extracellular [Ca++] measurements can be obtained with state of the art Ca^{++} ion selective microelectrodes. The $[Ca^{++}]$ depletions were quantitatively studied in the extrabecular spaces where V_o was absent (Kline, 1975). Thus, in the latter experiments of the present study, the $[Ca^{++}]$ depletion in the ETS was studied with single barrel Ca++ ion selective microelectrodes since the reference barrel was not necessary.

Following the guidelines developed by Kline (1975) and Kline and Morad (1976, 1978), certain criteria were observed during the measurement of the extracellular calcium ion concentration in beating frog ventricular strips.

1. At the beginning of each experiment, the calcium microelectrode output was monitered with the electrode tip in the bath while the preparation was stimulated. Electrode noise, drift, polarizability, and the effects of experimental solutions were determined. The bath Ringers $[Ca^{++}]$ potential was determined, and used as a reference point.
2. Calcium ion selective microelectrodes were slowly inserted into the muscle strip under the constant observation through a dissecting microscope to minimize dimpling the tissue, to minimize bending the microelectrode tip, and to estimate the electrode tip's radial depth in the strip.

3. After an extracellular space impalement in the muscle strip, up to 5-10 minutes time was given for the Ca^{++} electrode potential to return back to the potential observed in the bath. At the same time small adjustments in the depth of the electrode tip were made to minimize V_o, tension artifacts, and foster the return of the electrode's potential to the potential previously observed in the bath.

4. Short trains of repetitive action potentials were used to assess the impalement's stability. The magnitude of the $[Ca^{++}]_o$ depletion was used to confirm the visually estimated radial depth of the Ca^{++} ion selective microelectrode tip in the muscle strip.

5. Five to twenty minutes were required for $[Ca^{++}]_o$ equilibrium after a period of repetitive stimulation. The potential of the Ca^{++} ion selective microelectrode in the bath was used as a reference point. If this potential was not reattained during quiescence following repetitive stimulation, then there was a problem. The Ca^{++} microelectrode tip was withdrawn to the bath. This determined whether the electrode impalement was blocking the diffusion path from the microelectrode tip to the bath or whether the Ca^{++} electrode's potential had drifted. The Ca^{++} microelectrode bath potential drifted from +0.6 to +3 millivolts per hour on the average. Poor extracellular impalements caused a negative potential drift as cells were continuously injured, reducing the $[Ca^{++}]_o$ surrounding the electrode tip.

6. The extracellular Ca^{++} signal had to respond quanitatively and at an appropriate rate to changes in the bath Ca^{++} concentration. (See figure 4.)

7. Twenty to thirty minutes after an experiment, the electrode tip was withdrawn to the bath to test that the extracellular space and the bath

gave the same calcium ion Nerst potentials (within a millivolt or two).

8. By using 100 mM $CaCl_2$ instead of Ringers solution as the calcium electrode backfill, there was always an overriding electrochemical potential (about $^{-}80$ mV in a 0.2 mM Ca^{++}Ringers bath) which was monitored during the experiment. Large positive shifts in this potential signaled sudden damage or decay of the Ca^{++} microelectrode. When the tip diameter exceeded 3 microns or had an irregular tip, the Ca^{++} microelectrode was replaced.

9. Single-barred Ca^{++} ion selective microelectrodes were used in the latter experiments instead of double-barrel. The single barrel Ca^{++} microelectrodes were easier to make and laster longer. The tips could be made smaller. Qualitative measurements of beat to beat $[Ca^{++}]$ depletion inside the trabecula (in the SES and IFS) were made. Quantitative measurements of ETS $[Ca^{++}]$ depletion were made.

D. Twitch Tension Measurements

In the laboratory of Dr. Zia Penefsky, frog ventricular strip isometric tension was measured in several experiments using the apparatus described by Penefsky et al., (1981). A moving light beam transducer was used to detect isometric tension. The transducers output was recorded on a storage oscilloscope (Tektronix Model 564) and on a paper chart recorder (Gould Model 220). A 1 to 2 millimeter diameter muscle strip was tied via fine silk thread loops, to the transducer moment arm and to a hook anchored in the bath. The muscle strip was stretched approximately 150% of its resting length.

E. Data Analysis

Paper chart records and polaroid photographs from the storage oscilloscope were gathered during experiments and later analyzed. Data tables were made using the NIH-Prophet computer system. Derived table columns were used to calculate the extracellular ion concentration versus time. Data was then presented graphically or analyzed further. The prophet computor ExpFit program was used to fit multiexponential functions to the digitized data points. This program included a statistical evaluation of the fit. The accepted significance level of all curve fits was p less than 0.001.

F. Experimental Groups

1. Fluctuations of the extracellular calcium ion concentration occuring during each frog ventricular action potential were measured. The variables studied were the action potential duration, superfusate calcium ion concentration, amplitude of the accompanying extracellular action potential. The position of calcium microelectrode tip (interfibrillar space, subendothelial space, or extratrabecular space) was estimated from the time constants of the decay of the depletion following the action potential. Additionally effects of catecholamines, propanolol, manganese, and nickel ions on beat to beat $[Ca^{++}]_o$ depletions were examined.

2. Slow depletions of the extracellular calcium ion concentration with or without beat to beat calcium depletions were studied during 1 to 4 minute periods of repetitive stimulation. The variables studied were the

heart rate, action potential duration, the % time depolarized, superfusate calcium ion concentration, amplitude of the accompanying extracellular action potential, and the radial depth of the calcium microelectrode in the muscle strip. Also, slow extracellular calcium depletions were studied in low sodium Ringer, in high potassium/low sodium Ringer, and in Ringer containing manganese, nickel, or catecholamines. The cellular [Ca++] accumulation per action potential was estimated from the slow extracellular [Ca^{++}] depletions.

3. During prolonged repetitive stimulation lasting from 4 to 30 minutes, the extracellular [Ca^{++}] was measured. Evidence of a slowly activating Ca^{++} extrusion process was found. The effect of this Ca^{++} extrusion process on extracellular [Ca^{++}] depletion was studied. The time course of activation and deactivation of the Ca^{++} extrusion process and the Na^{+}/K^{+} pump were compared by simultaneously measuring the extracellular [K^{+}] and [Ca^{++}]. Isometric twitch tension staircase in 1.0 and 0.20mM Ca^{++} Ringers was studied at several heart rates. The time course of the early negative twitch tension staircase was compared to the time course of extracellular [Ca^{++}] depletion.

III RESULTS

A. Extracellular Ca^{++} Electrode Response in Frog Ventricular Muscle

The $[Ca^{++}]$ in the extracellular space of a frog ventricular strip is believed to be the same as the Ringers $[Ca^{++}]$ bathing the strip. To test this assumption, the tip of a Ca^{++} ion selective microelectrode was inserted into relaxed frog ventricular muscle strips. Initially the microelectrode appeared to cause some cellular damage. This was evident from the negative deflection of the Ca^{++} microelectrode potential indicating a fall in the $[Ca^{++}]$ at the microelectrode tip. After 5 to 10 minutes, the microelectrode potential slowly returned back to the value obtained when the microelectrode tip was in the Ringers.

When the bath Ringers $[Ca^{++}]$ was increased from 0.050 to 0.20 millimolar, the extracellular $[Ca^{++}]$ slowly increased, attaining equilibrium in 20 minutes. The time course of the extracellular $[Ca^{++}]$ increase from 0.050 to 0.20 mM is shown in figure 4. The subsequent reduction of the bath Ringers $[Ca^{++}]$ from 0.20 to 0.050 mM caused the extracellular $[Ca^{++}]$ to slowly return to 0.050 from 0.20 mM. The changes in the extracellular $[Ca^{++}]$ were inferred from the change in the Ca^{++} microelectrode potential which had also been observed when the electrode was tested in 0.050 and 0.20 mM Ca^{++} Ringers. These control experiments indicate that the extracellular space around the Ca^{++} microelectrode is in diffusion equilibrium with the bath and that the quantitative measurement of the extracellular $[Ca^{++}]$ is possible provided that reasonable care is taken.

Figure 4: Plot shows the extracellular calcium ion concentration measured over time by a calcium ion selective microelectrode tip in quiescent frog ventricular muscle strip. At time 0, superfusate [Ca^{++}] was increased from 0.05 to 0.20 mM. Between 20-60 minutes time the superfusate [Ca^{++}] was 0.050 mM. The calcium ion selective microelectrode response in muscle was the same as obtained in calibration solutions (figure 2).

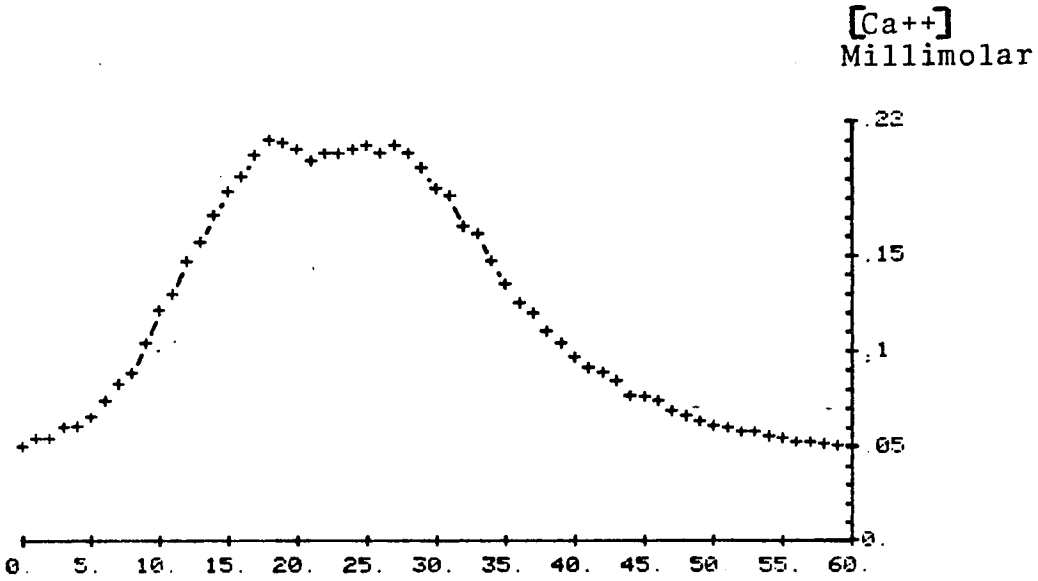
[Ca++]
Millimolar
.22
.15
.1
.05
0.
0. 5. 10. 15. 20. 25. 30. 35. 40. 45. 50. 55. 60.

B. Depletion of Extracellular Calcium Associated with a Single Heart Beat

The twitch tension of isolated frog ventricular strips bathed in 1 mM Ca^{++} Ringers was readily observed during electric field stimulation at a rate of 3 to 12 per minute. After one hour of superfusion with 0.05 or 0.2 millimolar calcium Ringers solution, twitch tension could not be visually detected using a 3x magnification dissecting microscope. However, intracellular glass microelectrodes indicated that similar action potentials were elicited in 0.050 - 1.0 mM Ca^{++} Ringers. A typical frog ventricular action potential is shown in the top panel of figure 5. The resting membrane potential varied from -75 to -85 millivolts. The amplitude of the action potential ranged between 100 and 120 millivolts. The duration of the frog ventricular action potential varied between 800 and 1000 milliseconds at a heart rate of 3 per minute.

In several experiments the isometric twitch tension of frog ventricular strips was measured in the laboratory of Dr. Zia Penefsky. When the Ringers [Ca^{++}] was lowered from 1 to 0.2 millimolar, the peak twitch tension was diminished 5 fold. The time to peak twitch tension was not changed but the rate of twitch tension development and relaxation was proportionately slower in the 0.2 millimolar calcium Ringer as shown in the lowest panel of figure 5. The field stimulus artifact can be seen as a fast vertical spike at the beginning of the tension record. Twitch tension development lagged about 100 to 200 milliseconds behind the upstroke of the frog ventricular action potential. Thereafter, tension development proceeded linearly over time in low calcium and quasi-linearly over time in high calcium Ringer. The onset of twitch tension relaxation in frog ventricle (superfused with normal Ringers solution) at the time of

rapid action potential repolarization is well known (Niedergerke, 1956). The rate of twitch tension relaxation was slightly more rapid than the rate of twitch tension development.

During continuous observation under a 3x magnification dissection microscope, the tip of a single-barrel Ca^{++} selective microelectrode was slowly inserted into a weakly contracting frog ventricular muscle strip and allowed to equilibrate as described. For some locations of the calcium electrode tip, a reproducible beat to beat voltage fluctuation was measured. An average magnitude calcium microelectrode voltage fluctuation is shown in the middle panel of figure 5. The initial rapid spike is the field stimulus artifact. This artifact may be used to indicate the onset of the frog ventricular action potential. The duration of the plateau phase of the evoked action potential is similar to the duration of the period of decrease in the output of the Ca^{++} electrode. In the midpanel record of figure 5, this deflection has a vertical magnitude of -3.6 mV. Background noise was 0.2 mV. The free $[Ca^{++}]_o$ at the tip of the extracellular microelectrode decreased from 0.20 to 0.15 mM during the frog ventricular action potential. The problems with using the beat to beat $[Ca^{++}]_o$ depletions for quantitative estimates of current flux will be discussed later. The measurement of beat to beat $[Ca^{++}]_o$ depletions was probably underestimated by 20% (See figure 3) due to the slow response time of the Ca^{++} ion selective microelectrode.

Following repolarization of the action potential the beat to beat $[Ca^{++}]_o$ stopped falling and began to increase. The minimum $[Ca^{++}]_o$ never occurred before rapid repolarization was initiated (n = 40 experiments). After repolarization, the extracellular $[Ca^{++}]$ changed in two phases: a rapid $[Ca^{++}]_o$ increase was followed by a slower

$[Ca^{++}]_o$ increase. When action potentials occurred at heart rates less than one per minute, the $[Ca^{++}]_o$ returned to baseline before the next beat. Initially at higher heart rates, the $[Ca^{++}]_o$ did not have to subside before the next beat.

The time constant of the slow phase of reversal of beat to beat calcium depletion varied between 1 to 5 seconds. This is similar to the time constant of equilibrium of calcium ions across the subendothelial sheath estimated by electron micrographs (uncorrected time constant = 3.3 $\pm$ 1.2 seconds; Page and Niedergerke, 1972). This suggests that the calcium microelectrode tip (for figure 5, middle record) was measuring either the subendothelial or the interfibrillar space calcium ion concentration. In section E of the analysis section, the beat to beat $[Ca^{++}]$ in the subendothelial space was estimated to be 0.184 mM at the end of the action potential. The corresponding interfibrillar space $[Ca^{++}]$ (for the center of the IFS) was estimated to be 0.120 mM. The beat to beat $[Ca^{++}]_o$ depletion shown in figure 5 was probably measured somewhere in the interfibrillar space. This conclusion is supported by the presence of a rapid phase of $[Ca^{++}]_o$ increase following membrane repolarization since two distinct phases of $[Ca^{++}]_o$ increase are expected in the IFS but not in the SES. The Ca^{++} electrode response is too slow to separate its response time constant from the time constant of the rapid $[Ca^{++}]_o$ change (Tau about 0.2 to 0.4 seconds). However, the Ca^{++} electrode response is faster than the expected SES time constant.

C. Cumulative Depletion of Extracellular Calcium during a Repetitive Train of Action Potentials

As the field stimulus rate is increased from 1 per minute to higher

Figure 5: Top panel shows output of an intracellular microelectrode in during a single action potential.

Middle panel shows output of a single barrel calcium ion selective microelectrode placed in the beat to beat extracellular space of a frog ventricular muscle strip during a single action potential (same experiment as top panel). Similar magnitude beat to beat $[Ca^{++}]_o$ depletions were obtained with double-barrel Ca^{++} ion selective microelectrodes.

Bottom panel shows superimposed isometric twitch tension records obtained every few minutes during a switch of the superfusate $[Ca^{++}]$ from 1.0 to 0.20 mM. The time scale is expanded compared to the upper two panels. During the frog ventricular action potential, twitch tension development and beat to beat $[Ca^{++}]_o$ depletion appear causally related. As the membrane repolarizes, twitch tension is maximal, and the extracellular $[Ca^{++}]$ is at its minimum.

FROG VENTRICLE ACTION POTENTIAL
AND EXTRACELLULAR [Ca++] DEPLETION

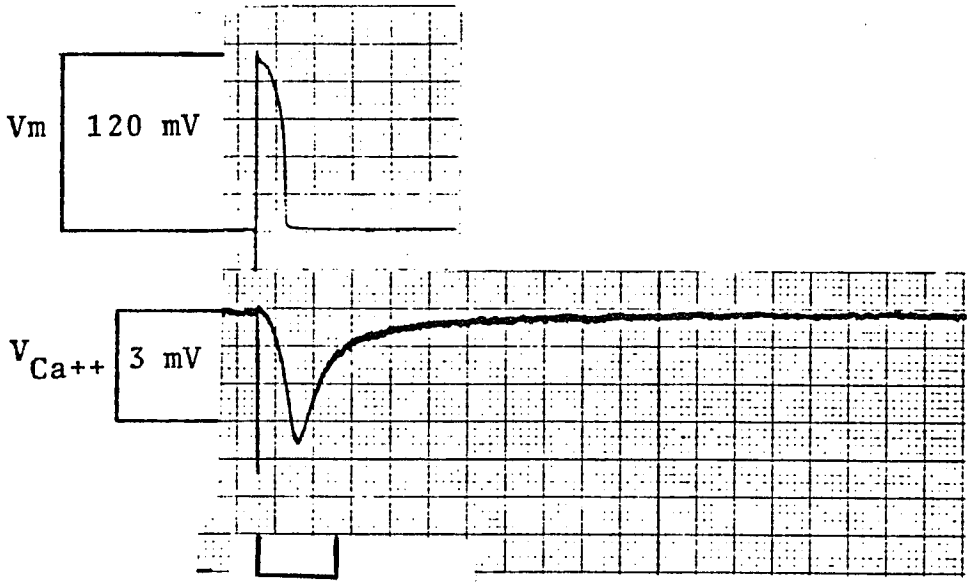

FROG VENTRICULAR TWITCH TENSION

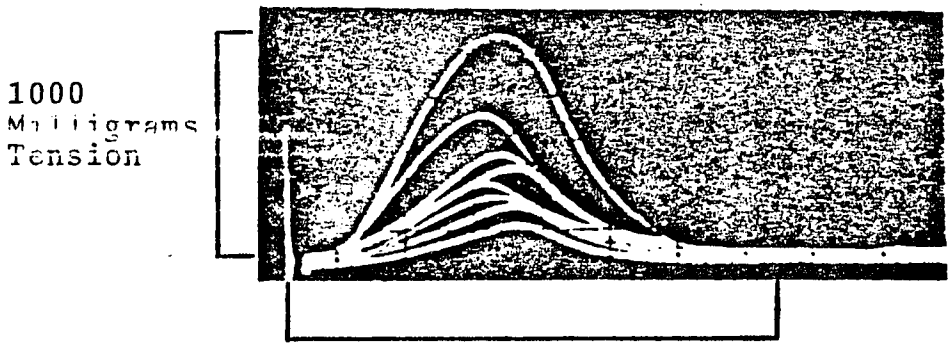

rates, the recovery of the beat to beat calcium depletion (during diastole) is interrupted by the next beat. As a result the next beat begins with a lower extracellular calcium ion concentration. Over several beats this results in cumulative $[Ca^{++}]_o$ depletion (see figure 6). When these beats were followed by a period of quiesence, the extracellular calcium ion concentration stopped falling but the depletion persisted for a time longer than necessary for the subendothelial space to equilibrate with the extratrabecular space.

When the depletion was caused by a train of repetitive action potentials lasting several minutes, (see figure 6B) the average cumulative $[Ca^{++}]_o$ depletion time course was exponential (time constant = 60 seconds in a one millimeter diameter muscle strip). The extracellular calcium ion concentration reached a minimum value in several minutes. After stimulation, return of the extracellular $[Ca^{++}]$ to the basal level had a time constant similar to the depletion phase when the magnitude of the $[Ca^{++}]_o$ depletion was a small percentage of the total extracellular $[Ca^{++}]$. Since slow $[Ca^{++}]_o$ depletions (during repetitive stimulation) were seen with and without accompanying beat to beat $[Ca^{++}]_o$ depletion but had similar slow time constants, the slow phase of extracellular calcium depletion must occur both inside and outside the trabecula as expected (Cohen & Kline, 1982).

D. Calcium Depletion in 1 millimolar Ca^{++} Ringers

Twitch tension of frog ventricular strips superfused in 1 millimolar calcium Ringers was five times larger than in 0.2 millimolar calcium Ringer. A few measurements of extracellular calcium concentration were successful in 1 millimolar calcium Ringer despite the large twitch tension.

Figure 6: Top trace (Vm) is the membrane potential measured by a conventional intracellular microelectrode. The single barrel Ca-ISE output is displayed in the second trace (Vca). The extracellular $[Ca^{++}]$, decays from 0.20 to 0.14 mM during the first action potential. Minimum $[Ca^{++}]_o$ at repolarization of last AP in the train of 5 beats is 0.12 mM. Negative going spikes at the start of each AP for both traces are stimulus artifacts.

Third trace (Vm) is membrane potential measured simultaneously with a single barrel Ca-ISE (Vca) shown in fourth trace. Vm depolarization during this train is consistent with previous findings of extracellular potassium accumulation (Kline and Morad, 1978). Fourth trace (Vca) is the Ca-ISE output. It shows the effect of an abrupt and more sustained change in heart rate from 3 to 30 (per minute for 2 minutes).The slow envelope of the $[Ca^{++}]_o$ depletion is seen. $[Ca^{++}]_o$ decreased from a bath level of 50 to 30 micromolar.

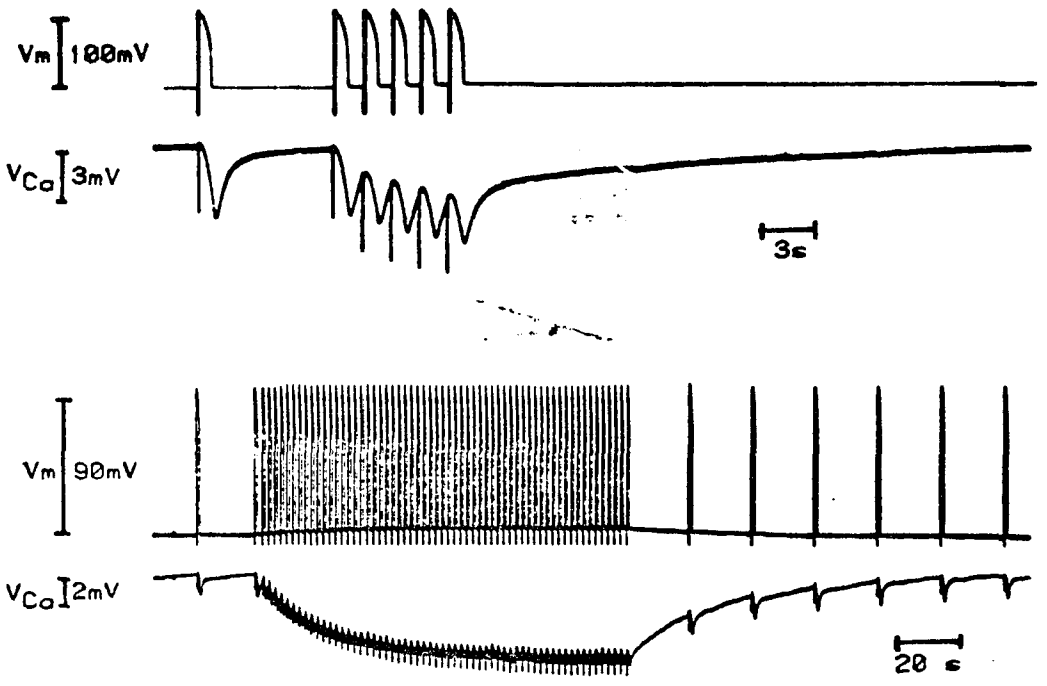
Vm 100mV
VCa 3mV
3s
Vm 90mV
VCa 2mV
20 s

Figure 7 is a record of the effect of an acute increase of heart rate from 1.3 to 12/minute for 2.3 minutes. In 2.3 minutes the extracellular calcium concentration fell by 32% from 1 to 0.68 millimolar. Upon return to 1.3 beats per minute the extracellular calcium concentration slowly increased up to the bath level. These results show that extracellular depletion occurs at physiological [Ca^{++}]. The absolute magnitude of depletion in 1 millimolar calcium Ringers is much larger than in 0.20 millimolar calcium Ringers. The magnitude of extracellular calcium depletion for any given protocol increased with increasing initial extracellular calcium concentration. Thus, the cellular uptake of calcium and twitch tension increase as the extracellular calcium concentration is increased.

E. Slow Depletions of Calcium versus Slow Accumulations of Potassium

Triple barrel Ca^{++}/K^{+} ion selective electrodes were used to compare the well-known time course of the extracellular potassium ion accumulation (Kline, 1975; Martin and Morad, 1982) with the time course of extracellular calcium ion depletion. The electrode tip was placed in the extratrabecular space according to criteria developed by Kline (1975) and Cohen and Kline (1982). When heart rate was increased from 12 to 24 per minute for 2.3 minutes, the extracellular potassium ion concentration increased from 3.0 to 4.0 millimolar in 60 to 90 seconds and then began to decrease during stimulation (figure 8). At the same time the extracellular calcium ion concentration fell from 0.20 to 0.13 millimolar, but steady state had not been reached. Upon return to a heart rate of 12 per minute, the potassium accumulation dissappeared in about 50 seconds while the calcium depletion recovered much more slowly.

Figure 7: Record of the calcium ion selective microelectrode output during repetitive stimulation is shown. The electrode was in a muscle strip bathed in 1 mM Ca^{++} Ringers. When heart rate was increased from 1.3 to 12 per minute for 2.3 minutes, the extracellular calcium ion concentration slowly fell from 1.0 to 0.68 mM (a 32% depletion). Upon return to the prior rate several minutes were required before the extracellular calcium ion concentration returned to 1mM.

EXTRACELLULAR [Ca++] DEPLETION IN 1.0 mM Ca++RINGER

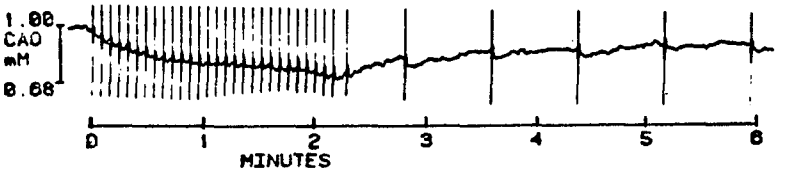

Figure 8: Top record is the output of the calcium ion selective barrel of a triple barrel Ca^{++}/K^{+} ion selective microelectrode. The bottom record is the output of the potassium ion selective barrel of this electrode. As heart rate was increased from 12 to 24 per minute, the slow accumulation of extracellular $[K^{+}]$ approached steady state sooner than the coincident slow depletion of the extracellular $[Ca^{++}]$.

SIMULTANEOUS MEASUREMENT OF THE EXTRACELLULAR [Ca++] AND [K+]

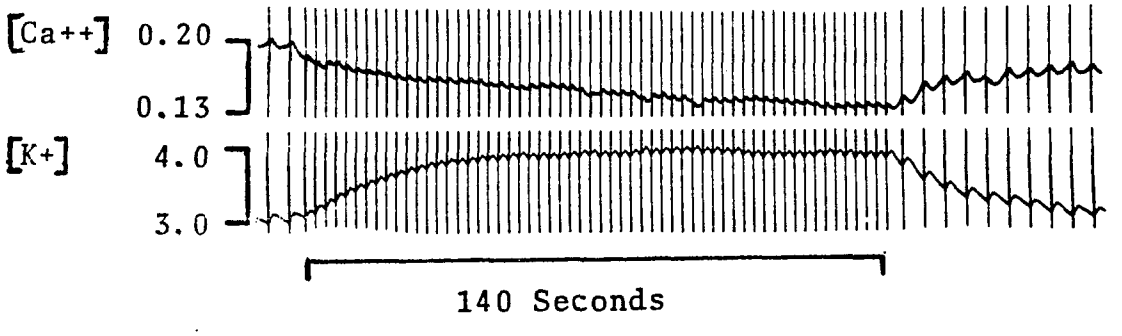

F. Effect of Heart Rate on Cumulative Calcium Depletion

Muscle strips were equilibriated in 0.050 or 0.20 millimolar Ca^{++} Ringer. At a low heart rate, (0.9 per minute), beat to beat calcium depletion in some trabecula did not last more than one minute (figure 9, top record). In this record the magnitude of the beat to beat $[Ca^{++}]_o$ depletion was about 14% of the total calcium concentration (beat to beat Vca = -1.8 mV). As heart rate was increased the beat to beat $[Ca^{++}]_o$ fluctuations remained around this value of about -1.5-2 mV until the heart rate exceeded 24 per minute. Thereafter, the beat to beat $[Ca^{++}]_o$ fluctuations decreased in magnitude.

As heart rate was increased from 0.9 to 1.5, 3, 6, 12, 24, and 48 beats per minute for 3 minutes, (see figure 9), the extracellular calcium ion concentration fell from 50 to 48, 41, 34, 25, 21, and 9 micromolar, respectively. The final $[Ca^{++}]_o$ depletion increased in magnitude at higher heart rates and the time constant of equilibration became smaller (see Analysis Section C). Five to fifteen minutes of quiescence was necessary between experimental runs, and the sequence of heart rates in these protocols was varied. In all frog ventricular strip preparations tested this general pheneomena of stimulus rate upon beat to beat and slow $[Ca^{++}]_o$ depletion was seen (n = 30).

Data from five complete experimental data sets was plotted as a function of heart rate. The Ringers calcium concentration and the radial depth of the calcium microelectrode tip in the muscle strip were varied. The extracellular calcium concentration versus heart rate after 2 minutes was plotted in figure 10. The magnitude of calcium depletion in 0.20 mM was 4x larger than in 0.050 millimolar calcium superfusate. This was determined from the magnitude of the steady state $[Ca^{++}]_o$ depletion.

Figure 9: Records of calcium ion selective output (VCa) are shown. A frog ventricular muscle strip (1 millimeter diameter) was repetitively stimulated (from top to bottom) at heart rates 0.9, 1.5, 3, 6, 12, 24, and 48 per minute for 3 minutes. The records show the extracellular calcium ion depletion which occurred at the center of the muscle strip. Strip was bathed in 0.050 millimolar Ca^{++}Ringers. Noise level = 0.2 mV.

HEART RATE DEPENDENCE OF EXTRACELLULAR [Ca++] DEPLETION

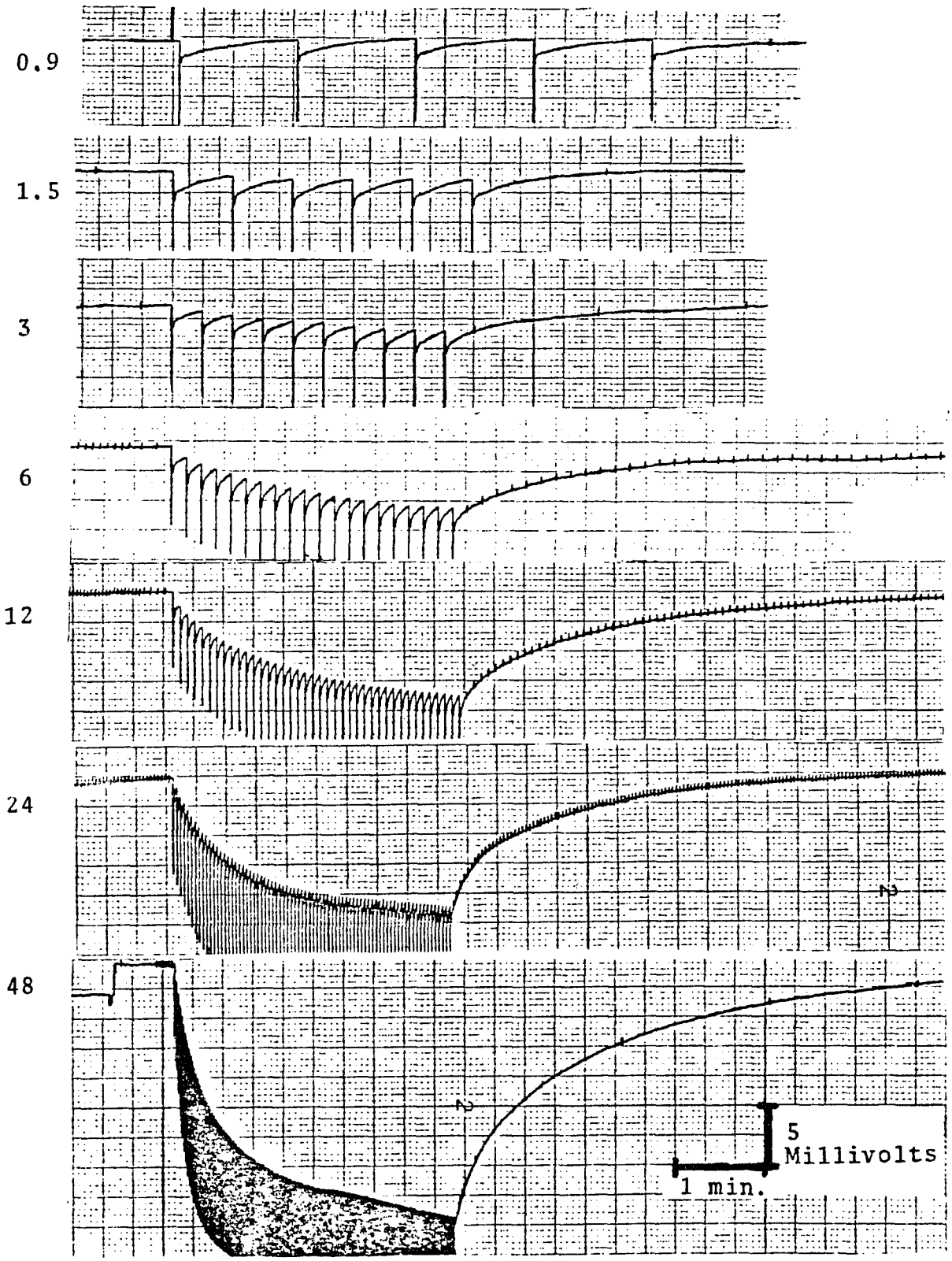

Calcium depletion was greater at deeper radial positions of the Ca^{++} microelectrode tip (see figure 10; compare circles to diamonds). The depth of the electrode tip was estimated from knowledge of the length of calcium neutral carrier resin in the ion selective barrel. The % of the resin column buried in the muscle was estimated using a calibrated grid in the eyepiece of the dissecting microscope during the impalement. The electrode tip depth was checked again before pulling the electrode tip out of the muscle and into the bath at the end of the experiment.

For small increases in heart rate (from low heart rates) the change in extracellular calcium concentration was proportional to the change in heart rate. However, as heart rate was increased beyond 30 per minute, the change in the extracellular calcium ion concentration after two minutes of beating approached a maximum change. The maximum % change in the extracellular calcium concentration after 2 minutes of beating was -80% (in 0.050 mM Bath Ca^{++}), and -75% (in 0.20 mM Bath Ca^{++}). This % change increased by the third minute of beating to -81% and -78%, respectively, indicating that the extracellular calcium ion concentration recorded after 2 minutes of beating in a 1 millimeter diameter muscle strip, had attained nearly steady state diffusional equilibrium. Equilibrium was attained after 3-5 minutes of beating.

An examination of the change in action potential duration as a function of heart rate after 1-2 minutes revealed two important points. 1) The change in action potential duration (caused by an increase in stimulus frequency) was largely complete within the first few beats. Thereafter, shortening or sometimes lengthening of the action potential duration took place slowly, amounting to usually less than 10% of the total action potential duration change. Thus, the percentage of the

Figure 10: Plot shows the extracellular calcium ion concentration in 1 millimeter diameter frog ventricular muscle attained after 2 minutes of repetitive stimulation at heart rates 1-60 per minute. (X) represents the mean of 3 or 4 trials with the same calcium microelectrode impalement (in center of the muscle strip) superfused with 0.20 mM Ca^{++} Ringer. (O) and (◆) represent the pooled data of two preprations. In each preparation data was obtained at the center of the muscle strip and at one-half the muscle strip's radial depth. Strips were superfused with 0.050 mM Ca^{++}Ringers.

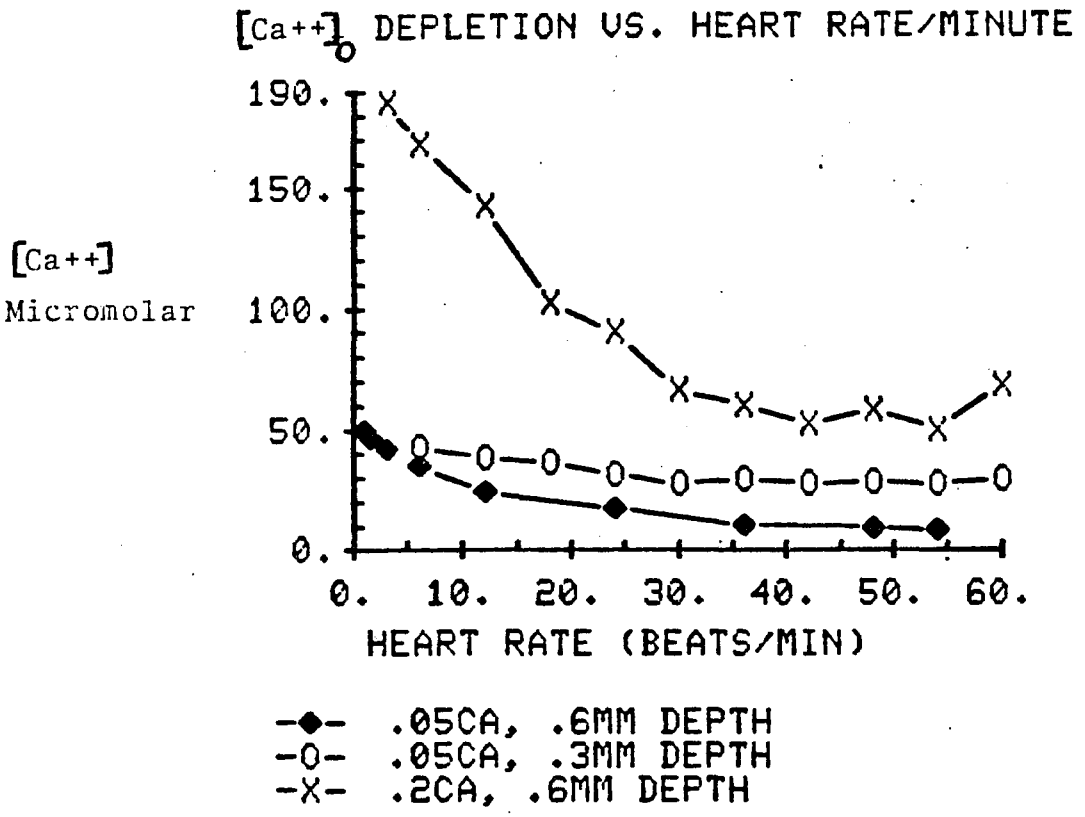
[Ca++]o DEPLETION VS. HEART RATE/MINUTE
[Ca++]
Micromolar
190.
150.
100.
50.
0.
0. 10. 20. 30. 40. 50. 60.
HEART RATE (BEATS/MIN)
-◆- .05CA, .6MM DEPTH
-O- .05CA, .3MM DEPTH
-X- .2CA, .6MM DEPTH

stimulus interval that the membrane was depolarized (% time depolarized) was approximately constant during two minutes of beating at a new rate (with exception for the first 5 beats at heart rates greater than 30 per minute). This observation has been reported by Kline (1975) and Kline and Morad (1978). 2) In 0.050-0.20 millimolar Ca^{++} Ringers, at heart rates 3-30 per minute, action potential duration averaged 940 $\pm$ 40 milliseconds. Thus at heart rates 3-30 per minute, the % time depolarized increased in direct proportion with heart rate (figure 11). At higher heart rates the action potential duration shortened. For example, at heart rates 36, 42, 48, 54, and 60 per minute, action potential duration shortened typically to to 850, 840, 760, 750, and 670 milliseconds respectively. A similar trend was reported by Kline (1975) and Kline and Morad (1978).

Membrane permeability to calcium ions is increased during the entire plateau of the frog ventricular action potential (figure 5). Therefore, extracellular calcium depletion should be correlated better with the % time membrane depolarization than to the heart rate. This was not necessary for heart rates 3-30 per minute where heart rate and % time depolarized were linearly related (figure 11, top panel). However, at higher heart rates where action potential duration shortened, the change in extracellular calcium ion concentration ought to be more linearly related to the % time depolarized than to the heart rate. A comparison of figure 10 versus figure 11 (bottom panel) indicates that % time depolarized was an improvement over heart rate as the independent variable in 0.20 mM Ca^{++} Ringers since the plot became more linear. However, the data in 0.050 mM Ca^{++} Ringers was not improved. The graph points for 0-20% time depolarized suggest a trend which extrapolated for longer %

time membrane depolarization, would have the extracellular calcium ion concentration fall to zero after 2 minutes at 40-60% time depolarized (see figure 11, bottom panel). Total depletion was unlikely to occur because calcium ions can diffuse in from the bath. Also, as the extracellular calcium ion concentration approached zero, the transmembrane calcium gradient would fall. This would reduce the net rate of calcium ion uptake by the muscle cells. This second possibility was tested by examining the time course of the calcium depletions at different % time depolarized (for the same impalement and bath Ca^{++} concentration).

The data from figure 9 plus 3 minute trains at 36 and 54 per minute were converted to extracellular calcium ion concentration as a function of time and plotted together on the same graph, shown in figure 12 (top panel). In this plot the time course of extracellular calcium ion depletion for % times: 47, 61, and 68%, superimposed. This graph was then transformed to the plot below it (middle panel, figure 12) by first converting the extracellular calcium ion concentration change to percent maximum change. Then (100% minus % change in the extracellular calcium ion concentration) was plotted as a function of time. This plot allowed the time courses of the extracellular calcium ion concentration depletions driven by different % time membrane depolarization, to be compared.

Normalized $[Ca^{++}]_o$ depletion time courses ought to superimpose if the net rate of cellular calcium uptake per second of membrane depolarization was only a function of drive rate and during the train was constant. Also, the time course should be exponential since the steady state calcium concentration in the compartment measured by the calcium microelectrode tip represents a balance between efflux into the cytoplasmic compartment and influx by diffusion from an adjoining

Figure 11: Top panel shows a plot of % time membrane depolarized (per cardiac cycle) as a function of heart rate per minute. If the action potential duration (APD) is constant at all heart rate (HR) and equals 950 milliseconds, the dashed line is obtained.

$$\% \text{ Time membrane depolarized (per cardiac cycle)} = \frac{(APD \times HR) \times 100\%}{60}$$

Bottom Panel shows a plot of extracellular calcium ion concentration after 2 minutes of repetitive stimulation as a function of the % membrane time depolarized. This plot is based upon data from figure 9 where the X axis (heart rate) was transformed to % time depolarized using data from the top panel of this figure.

% TIME DEPOLARIZED VS. HEART RATE/MIN

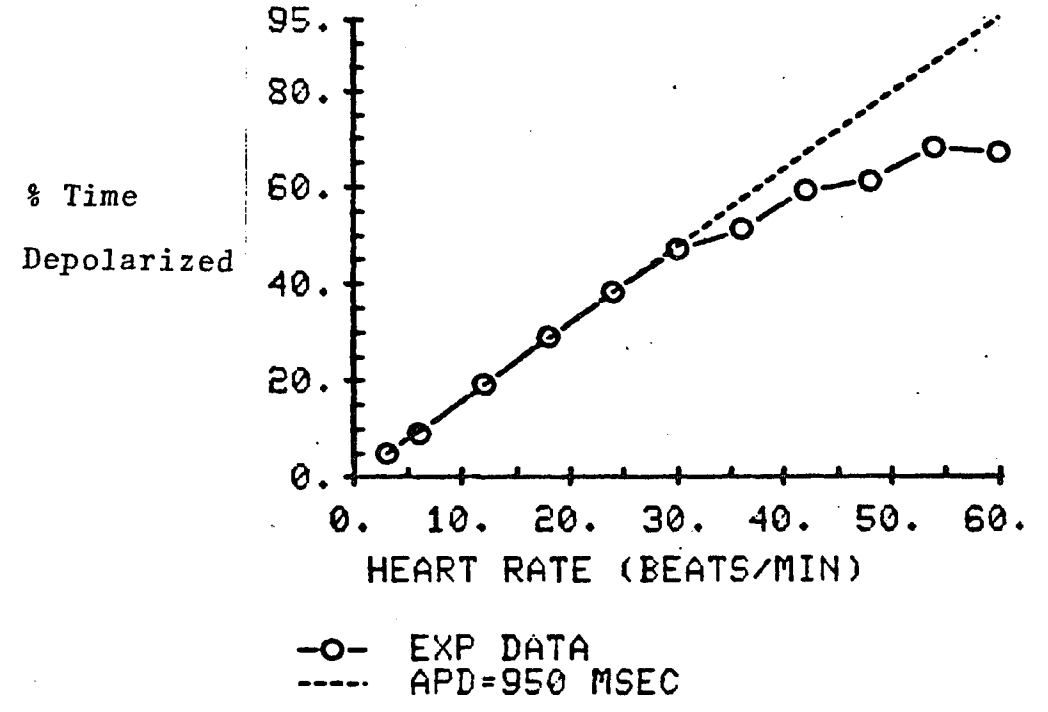

$[Ca++]_o$ DEPLETION VS. % TIME MEMBRANE DEPOLARIZATION

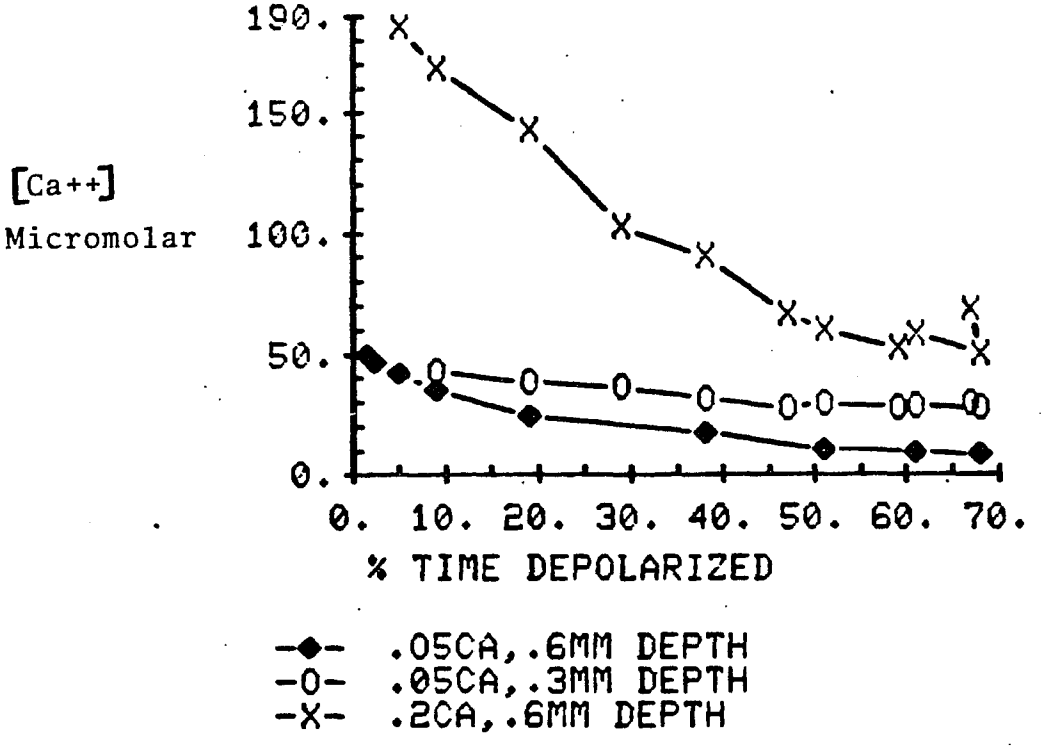

extracellular compartment of higher calcium ion concentration.

Since the normalized extracellular [Ca^{++}] depletion time courses of figure 12 (middle panel) did not superimpose, the rate of equilibration of the extracellular [Ca^{++}] was not constant for all heart rates during 2 minutes of beating. At higher % time depolarized (or higher heart rate) the time to apparent steady state decreased. On a semilog plot (bottom panel, figure 12) the exponentiality of the time course of the extracellular calcium depletions of figure 11 (middle panel) can be seen. In general the first 80% of the extracellular calcium depletion proceeds with an approximately monoexponential time course having a time constant ranging between 10-60 seconds. Sufficient extracellular calcium ion concentration depletion lowers the transmembrane calcium ion gradient enough to cause a decrease in the net cellular Ca^{++} influx. At higher heart rates (or high % time depolarized), the rate at which cellular Ca^{++} influx approaches steady state is accelerated. Thus the extracellular calcium ion concentration attains steady state sooner and with less final depletion than would have occurred for constant influx. This observation helps to explain the curvilinear plots of figure 11 (bottom panel). These results were observed in five preparations (three in 0.050 mM, and two in 0.20 mM Ca^{++}Ringers).

G. Slow Activation of a Cell Membrane Ca^{++} Extrusion Process During Sustained Cellular Uptake of Calcium Caused by Prolonged Repetitive Stimulation

The repetitive stimulation of frog ventricular muscle bathed in 0.050-1.0 millimolar calcium Ringers causes extracellular calcium ion concentration depletion and net cytoplasmic calcium ion accumulation.

Figure 12: Top panel shows a plot of the time course of the extracellular calcium ion concentration measured continuously by a calcium ion selective microelectrode as the heart was driven at rates 0.9, 1.5, 3, 6, 12, 24, 36, 48, and 54 per minute for 180 seconds. This data was obtained from the same source as figure 8. Data for heart rates 36, 48, and 54 per minute superimposed.

Middle panel shows a transformation of upper panel data to (100% - % extracellular calcium concentration change) during 3 minutes at heart rates 3, 6, 12, 24, 36, and 48 per minute. The time scale is the same as upper panel.

Bottom panel shows a semilog plot of the middle panel plot for 90-98% of the extracellular calcium change which occurred. Note that the time scale (x-axis) is expanded slightly compared to the other panels. See the Analysis section for an interpretation of the cause of the decrease in time constants of this plot for higher heart rates and greater Ca^{++} depletions.

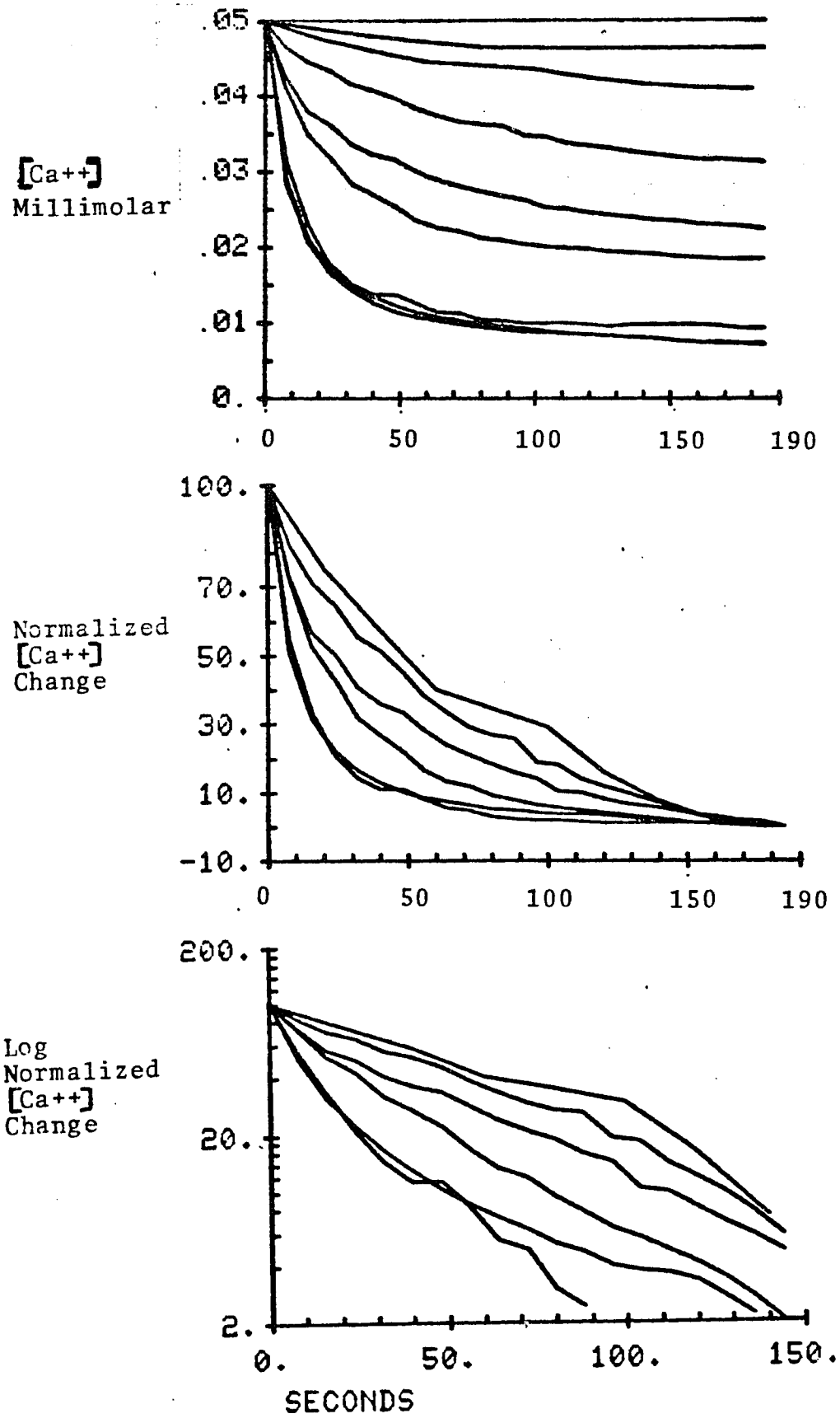
[Ca++]
Millimolar
.05
.04
.03
.02
.01
0.
0
50
100
150
190
Normalized
[Ca++]
Change
100.
70.
50.
30.
10.
-10.
0
50
100
150
190
Log
Normalized
[Ca++]
Change
200.
20.
2.
0.
50.
100.
150.
SECONDS

During two to five minutes of repetitive stimulation the extracellular calcium ion concentration in ventricular muscle strips falls to a minimum value (figures 6, 7, 8, 9, and 12). When stimulation is prolonged for times longer than 3-4 minutes, evidence of activation of a cell calcium extrusion process (flux outward) is apparent (figure 13, top panel). When stimulation is stopped, the level of extracellular calcium ions returns to the superfusate Ca^{++} level and then proceeds to increase above it. This extracellular calcium ion concentration overshoot may be prolonged for 10-30 minutes (figure 13, bottom panel). The minimum duration of stimulation required to observe the $[Ca^{++}]_o$ overshoot is also indicated by a slight reversal of the extracellular $[Ca^{++}]$ depletion minima, seen at 4-5 minutes time. The minimum extracellular Ca^{++} level attained during repetitive stimulation at a high rate (from a low basal stimulation rate of 0-3 per minute) represents an equilibrium. A slowly activating Ca^{++} efflux will shift the equilibrium extracellular $[Ca^{++}]$ to higher and higher extracellular calcium ion concentrations as the Ca^{++} efflux increases in magnitude (see figure 13 lower panel). Prolonged stimulation resulted in a slow return of the extracellular $[Ca^{++}]$ to the superfusate $[Ca^{++}]$. After about 16 minutes of repetitive stimulation the return was 2/3rds complete (figure 13, lower panel). The subsequent $[Ca^{++}]_o$ overshoot reached 0.066 millimolar (an overshoot of 0.016 millimolar after 16 minutes of stimulation). A smaller $[Ca^{++}]_o$ overshoot of 0.060 millimolar occurred after 4 minutes of stimulation. Thus prolonged repetitive stimulation activates a Ca^{++} extrusion process (signified by a higher $[Ca^{++}]_o$ overshoot, and less extracellular Ca^{++} depletion at the time stimulation is stopped). It is important to emphasize that sustained extratrabecular space $[Ca^{++}]$ depletion indicates on going net

Figure 13: Top panel is a plot of an experiment measuring the effect of stimulation duration on extracellular calcium ion concentration. The stimulus durations were 1, 2, and 4 minutes. The heart rate was 48 per minute.

Bottom panel is a plot of the extracellular calcium ion concentration during 16 minutes of repetitive stimulation at 48 per minute followed by a 25 minute rest period. Note that the initial $[Ca^{++}]_o$ level is high since the experiment was started before the $[Ca^{++}]_o$ overshoot from the 4 minute train (top panel) had dissipated.

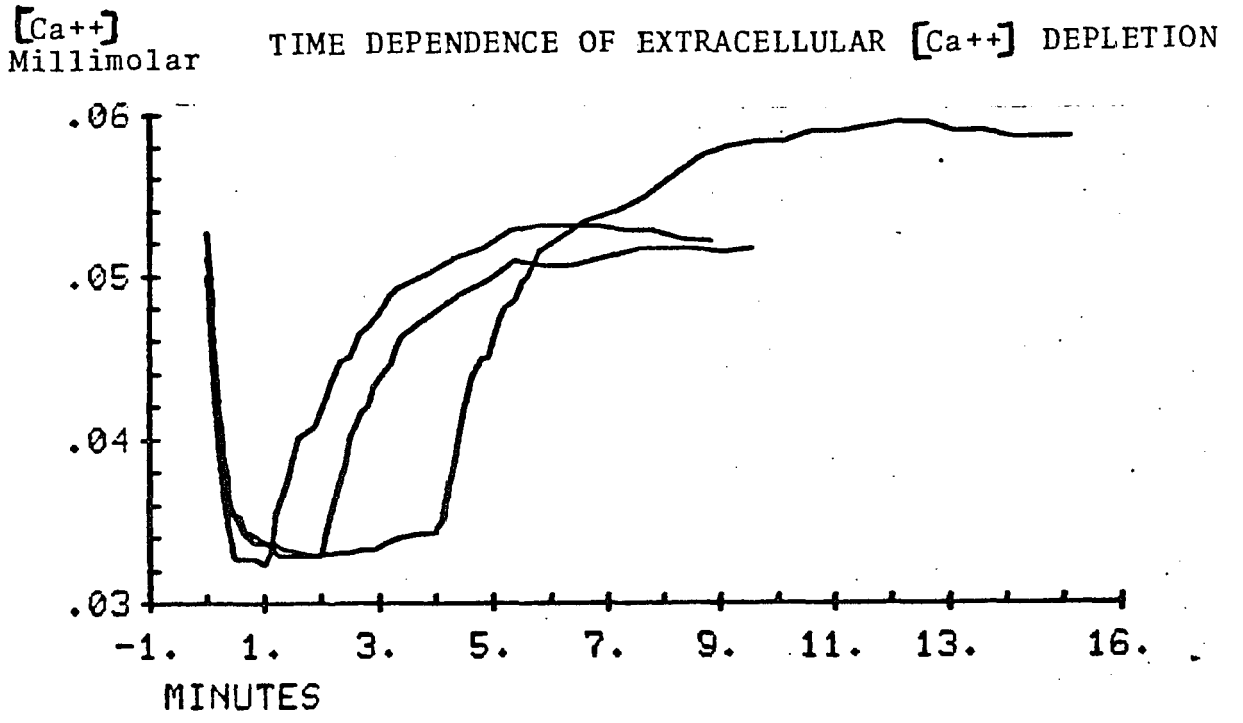
[Ca++]
Millimolar
TIME DEPENDENCE OF EXTRACELLULAR [Ca++] DEPLETION
.06
.05
.04
.03
-1.
1.
3.
5.
7.
9.
11.
13.
16.
MINUTES

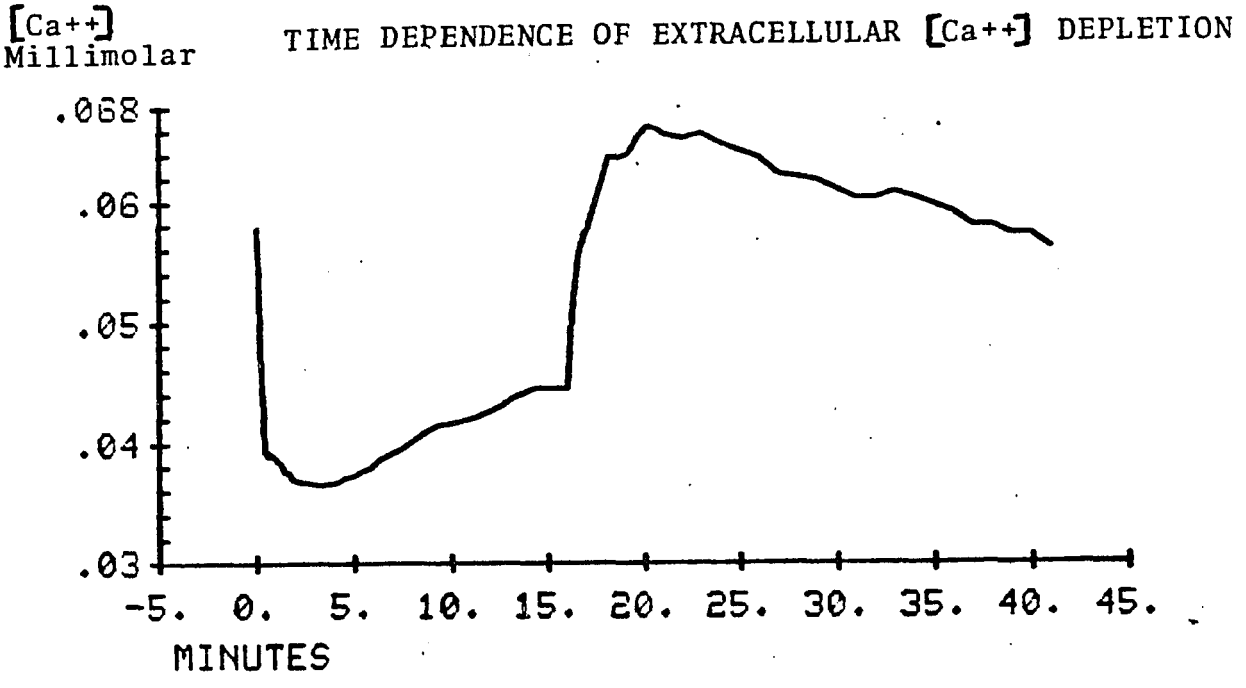
[Ca++]
Millimolar
TIME DEPENDENCE OF EXTRACELLULAR [Ca++] DEPLETION
.068
.06
.05
.04
.03
-5.
0.
5.
10.
15.
20.
25.
30.
35.
40.
45.
MINUTES

cellular Ca^{++} accumulation.

The capacity of cardiac cells to store calcium ions must be finite. Therefore, at steady state cellular calcium ion homeostasis implies the net transmembrane flux of calcium ions per cardiac cycle is zero. Prolonged stimulation must lead to a steady state and eventually to zero cumulative extracellular depletion of calcium. In figure 14, prolonged repetitive stimulation for 25-30 minutes resulted in gradual disappearance of the extracellular $[Ca^{++}]$ depletion.

Calcium depletion did not primarily reverse because the ventricular cells became filled up with Ca^{++} such that the undirectional influx was decreased. Rather as indicated by the subsequent $[Ca^{++}]_o$ overshoot, the unidirectional Ca^{++} efflux from cells was increased till it was equal to the unidirectional cellular Ca^{++} influx. This is supported by the fact that the maximum depletion at about 4 minutes time (0.050 to 0.032 mM; - 0.018mM) is similar to the maximum $[Ca^{++}]_o$ overshoot (accumulation) at 40 minutes time (0.052 to 0.076 mM; 0.024 mM) seen in figure 14. For further details see section B of Discussion.

Similar results were obtained using a triple barrel Ca^{++}/K^{+} ion selective microelectrode in a ventricular strip bathed in 0.20 millimolar Ca^{++}, 3 millimolar K^{+}Ringers (figure 15). After increasing the heart rate from 6 to 24 per minute the extracellular $[K^{+}]$ increased to a maximum in 60 to 90 seconds and then proceeded to decrease, as shown in figure 15. The extracellular $[Ca^{++}]$ depletion fell almost to minimum in 3-5 minutes, and slowly decreased for another 6 minutes. The $[Ca^{++}]_o$ began to increase after 11 minutes and one-third of the $[Ca^{++}]_o$ depletion had reversed at 24 minutes. The $[K^{+}]_o$ accumulation was two-thirds reversed at 24 minutes. When the heart rate was slowed from 24 to

Figure 14: Plot is of the extracellular calcium ion concentration versus time. Repetitive stimulation occurred from 0 to 33 minutes at 18 per minute. In the subsequent quiesent period an extracellular [Ca^{++}] overshoot occurred. Data was not from the same preparation as used for figure 12. Note that some Ca^{++} microelectrode drift of about 4 micromolar per hour (or 1 mV/hour) is present.

[Ca++] Millimolar TIME DEPENDENCE OF EXTRACELLULAR [Ca++] DEPLETION

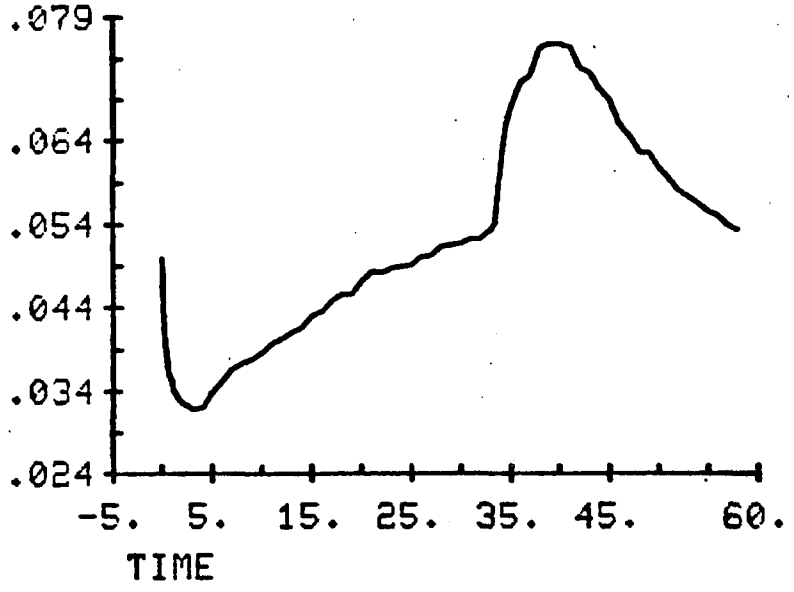

Figure 15: Top panel plots show extracellular Ca^{++} concentration (thick line) and K^+ concentration (thin line) of a frog ventricular muscle strip during an increase in the rate of stimulation from 6 to 24 per minute for 24 minutes. Basal rate was 6 per minute. Ca^{++} Ringers was 0.20mM. After 1 minute of stimulation, $[K^+]_o$ increased to a maximum of 5.9mM. After 11 minutes $[Ca^{++}]_o$ fell to minimum of 0.093mM. After 24 minutes $[K^+]_o$ was 3.9mM and $[Ca^{++}]_o$ was 0.14mM. Data was obtained with triple barrel Ca^{++}/K^+ ion selective microelectrode.

Bottom panel plots show the effect of decreasing the stimulus rate from 24 back to 6 per minute. $[K^+]_o$ falls from 3.9 to 2.9 mM in 2 minutes. $[Ca^{++}]_o$ increases more slowly over 6 minutes from 0.14 to 0.28mM. After 45 minutes $[K^+]_o$ has returned to 3.2mM and $[Ca^{++}]_o$ is 0.20mM. Following a change in stimulus rate, $[K^+]_o$ equilibrium in extratrabecular spaces (ETS) is more rapid than $[Ca^{++}]_o$ equilibration in the ETS. This is probably in part due to the faster diffusion coefficient for K^+ versus Ca^{++} in free solution. $D_{K^+} = 2.5\ DCa^{++}$ (Wang, 1953, Friedman and Kennedy, 1955).

RESULTS FROM K^{+}/CA^{++} TRIPLE BARREL ION SELECTIVE MICROELECTRODE

FIGURE A

EXTRACELLULAR CALCIUM AND POTASSIUM FLUCTUATIONS DURING DRIVE

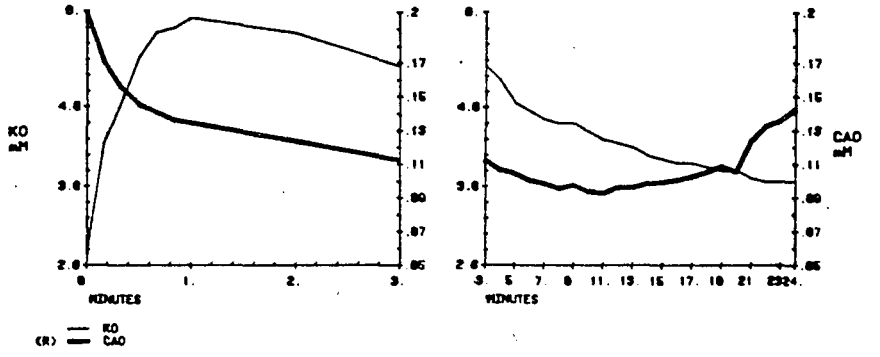

FIGURE B

CAO AND KO FLUCTUATIONS FOLLOWING RETURN TO PRIOR RATE

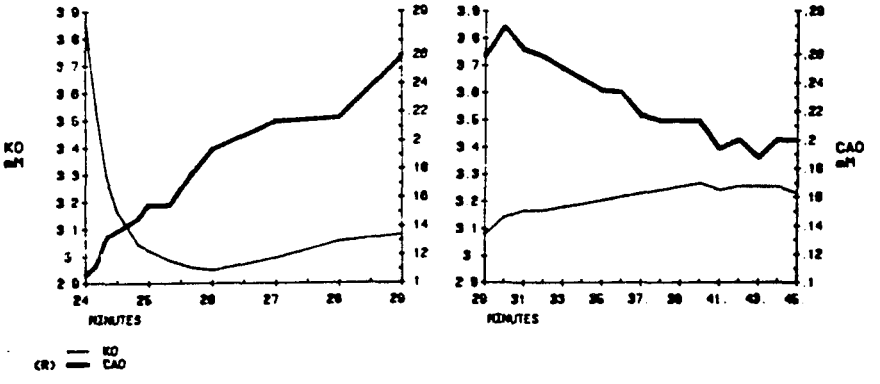

6 per minute at 24 minutes time the $[K^+]_o$ rapidly fell below 3mM while the $[Ca^{++}]_o$ increased above 0.20mM. The extracellular $[Ca^{++}]$ increased to a maximum level in 6 to 7 minutes while the $[K^+]_o$ fell to a minimum in 2 minutes. Twenty one minutes after the return to a slower heart rate the extracellular $[Ca^{++}]$ had returned to the bath $[Ca^{++}]$ while the $[K^+]_o$ was slightly elevated. The slightly elevated $[K^+]_o$ was an error due to electrode drift (see page 31). During long protocols some drift of ion-selective microelectrode potentials was inevitable.

To examine the consequences of calcium efflux activation on short trains of repetitive stimulation and the subsequent quiescent periods when the extracellular $[Ca^{++}]$ returned to the bath level, frog ventricular muscle strips were beat at 48 per minute for 1 minute followed by 1 minute of quiescence. This two minute cycle was repeated without interruption 11 times in a row. In a protocol of this design, the steady state unidirectional efflux should increase till it equals the net cellular Ca^{++} influx averaged over the period of the protocol's cycle (in this case the period was 2 minutes). At 48 beats per minute the % time depolarized was about 60% (figure 11, top panel). In a 2 minute cycle, the membrane would be depolarized on the average during 30% of the 2 minute cycle. This % time depolarized (30%) was equivalent to a period of continuous repetitive stimulation at 18 per minute (see figure 11, top panel). Thus Ca^{++} efflux activation should result in a steady state Ca^{++} efflux proportional to the cellular Ca^{++} influx caused by stimulation at 18 per minute. Since the cellular Ca^{++} uptake occurs due to membrane depolarization, primarily during the first half of the cycle, steady state extracellular calcium levels should oscillate slowly within each cycle.

Figure 16: Sequential records from the output of a single barrel calcium microelectrode are shown. First, a run of 48 per minute for 1 minute (control run) is shown. Next the same heart rate was performed for 30 seconds. Note the long time required for extracellular [Ca^{++}] return to the bath level (indicating a time constant of around 60 seconds).

Next 11 cycles of 48 beats per minute for 1 minute followed by a 1 minute rest were recorded. After a 24 minute rest period (20 minutes of it are shown), another control run was performed. Some drift (in upward direction) of about 1.5 mV occurred in the hour of this experiment but evidence of reversible Ca^{++} efflux activation is shown. The Ca^{++} extrusion process activation and deactivation are slower than extracellular diffusion equilibrium. (See figures 13 and 14.)

CALCIUM EFFLUX ACTIVATION - EFFECT ON $[Ca^{++}]_o$ DEPLETION

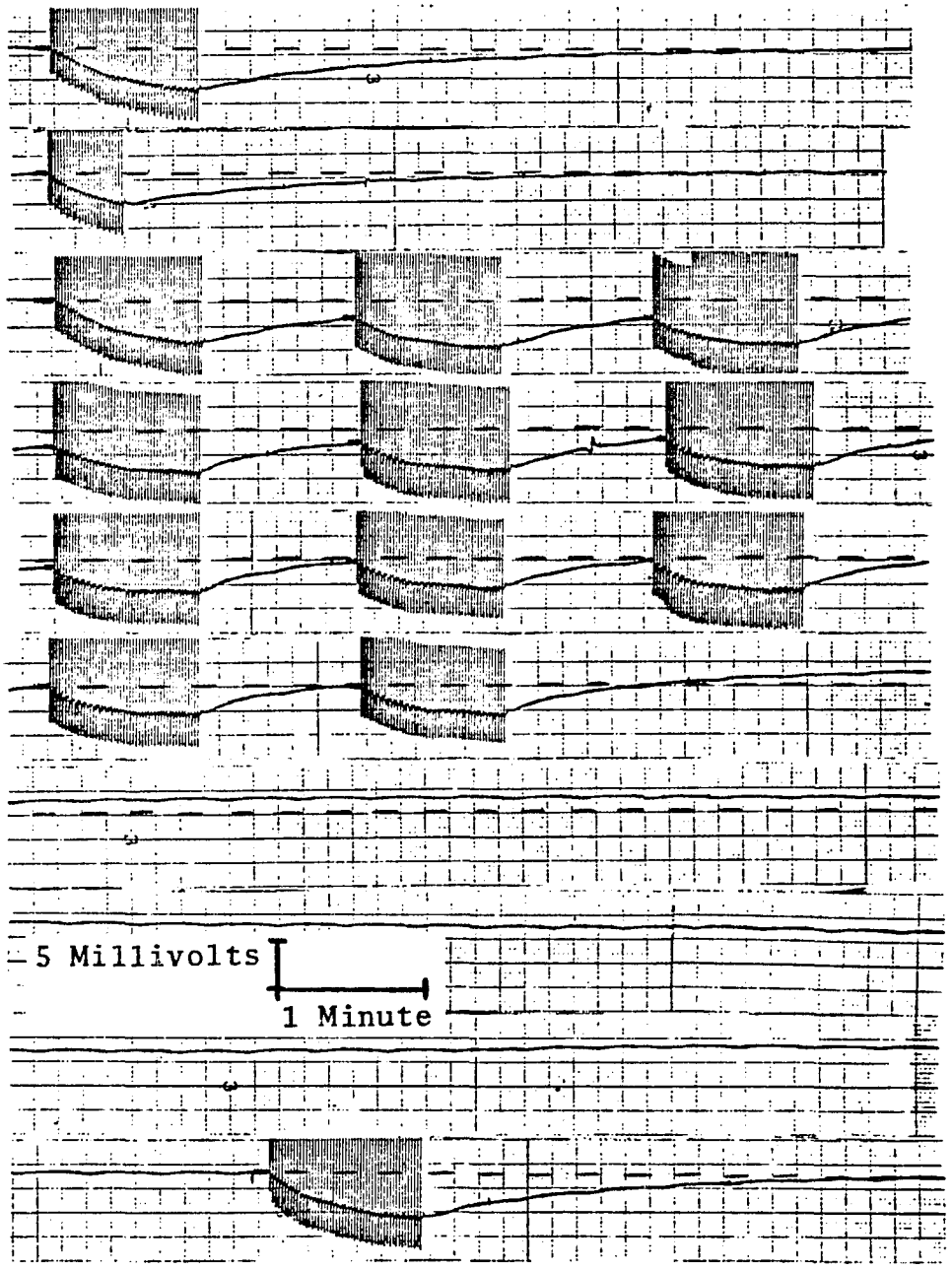

In figure 16, records of the calcium microelectrode output during this protocol are shown. The 2 minute protocol was repeated 11 times. Initially, net depletion was seen at the end of each cycle. The net depletion per cycle soon became negative in value and the average extracellular $[Ca^{++}]$ slowly reversed, oscillating in each cycle although there was no net extracellular $[Ca^{++}]$ depletion per cycle. In the prolonged quiescence lasting 24 minutes which followed the 11th cycle, the extracellular calcium ion concentration overshot the Ringers $[Ca^{++}]$ level by about 8 micromolar (similar to the change in the magnitude of $[Ca^{++}]_o$ depletion seen after 1 minute in the 1st versus 11th cycles (20 versus 14 micromolar). A subsequent stimulation of 48 per minute for 1 minute (figure 16, lower most) indicated that calcium efflux activation had subsided with prolonged quiescence of the preparation.

A plot of the results of this 11 cycle protocol including the early postdrive $[Ca^{++}]_o$ overshoot is shown in figure 17. The 2nd and 3rd cycle $[Ca^{++}]_o$ depletions started from a lower initial $[Ca^{++}]_o$ and were smaller in magnitude than the 1st depletion. By the 11th cycle the magnitude of the $[Ca^{++}]_o$ depletions had increased although it was noticably smaller than that of the 1st cycle.

Several segments of this experiment were examined in greater detail. A control calcium depletion (top run of figure 16) was compared to the eleventh depletion of figure 16, (both having the same initial extracellular calcium level). Each depletion was fit with a single exponetial plus a constant. The rate of calcium ion depletion of the 11th run was slower due to concurrent antagonism by calcium efflux activation. The extracellular calcium ion concentration after the last run approached a constant level 150% faster than in the control run which depleted more.

Figure 17: Data from records of figure 16 (series of 11 cycles of $[Ca^{++}]_o$ depletion) is plotted. Open circles are the extracellular $[Ca^{++}]$ at the start of repetitive beating at 48 per minute. Solid circles indicate the extracellular $[Ca^{++}]$ after 1 minute of repetitive stimulation at 48 per minute. After 22 minutes the extracellular $[Ca^{++}]$ increased above the Ringers $[Ca^{++}]$. The last 14 minutes of the $[Ca^{++}]$ overshoot are not shown because upward calcium electrode drift obscured the falling phase of the $[Ca^{++}]_o$ overshoot.

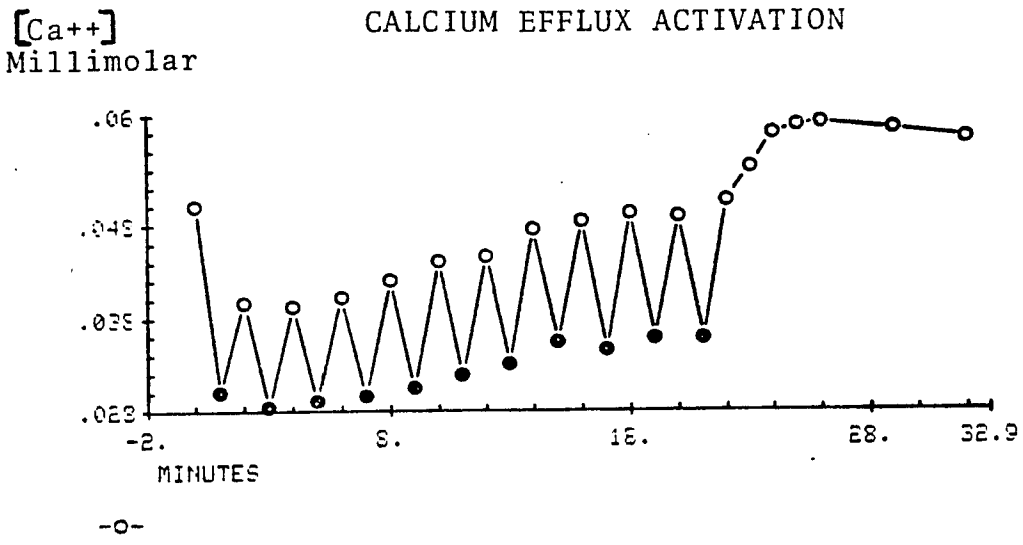
[Ca++]
Millimolar
CALCIUM EFFLUX ACTIVATION
.06
.049
.039
.029
-2.
8.
18.
28.
32.9
MINUTES
-o-

Figure 18: Top panel shows the time course of a depletion before and after Ca^{++} efflux activation (taken from data of figure 15). Control points are (+) while points of a calcium depletion in the presence of calcium efflux activation are (*). The solid lines are computor fits where X is in units of seconds. The control fit is:

$$[Ca^{++}]_{(+)} = ([0.021 \text{ EXP } (-0.044X)] + 0.027) \text{ mM } [Ca^{++}].$$

The calcium depletion (in presence of calcium efflux activation) was fit by the equation:

$$[Ca^{++}]_{(*)} = ([0.013 \text{ EXP } (-0.067X)] + 0.033) \text{ mM } [Ca^{++}].$$

Lower panel shows the time course of extracellular calcium during a rest period before and after calcium efflux activation. (+) are control points, while (*) are points of rest period with Ca^{++} efflux activated. The points were fit:

$$[Ca^{++}]_{(+)} = ([-0.013 \text{ EXP } (-0.011X)] + 0.048) \text{ mM } [Ca^{++}].$$

$$[Ca^{++}]_{(*)} = ([-0.022 \text{ EXP } (-0.015X)] + 0.055) \text{ mM } [Ca^{++}].$$

During 60 seconds of beating, 6 micromolar more $[Ca^{++}]_o$ depleted in the absence of Ca^{++} efflux activation. In the rest periods which followed (using data with the same $[Ca^{++}]_o$ level just after the stimulation) the extracellular $[Ca^{++}]$ was about 8 micromolar higher in the presence of Ca^{++} efflux activation.

EFFECT OF CALCIUM EFFLUX ACTIVATION
ON EXTRACELLULAR $[Ca^{++}]_o$ DEPLETION

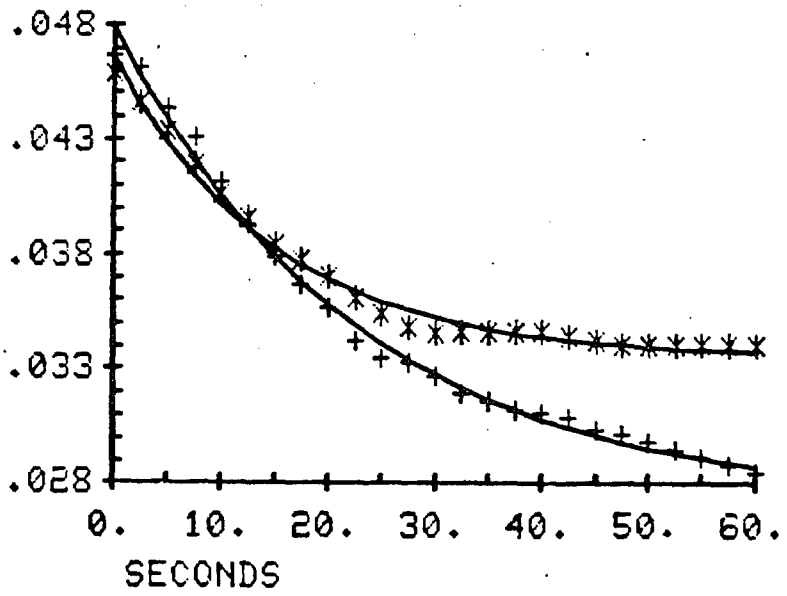

\+ CONTROL PTS.
—— CONTROL FIT
* Ca++ EFFLUX ACTIVATED PTS.
—— Ca++ EFFLUX ACTIVATED PTS. FIT

EFFECT OF CALCIUM EFFLUX ACTIVATION
ON POST-DRIVE DIFFUSIONAL EQUILIBRIUM

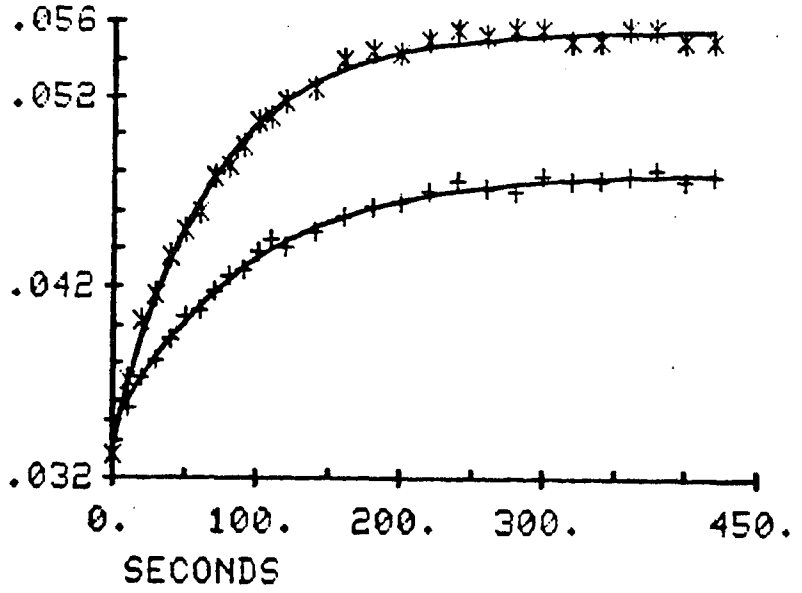

The magnitude of the eleventh run $[Ca^{++}]_o$ depletion was about two-thirds the controls. This is shown in figure 18, top panel, where the computer exponential fit is the solid line. In the lower panel of figure 18, the time course of the decay of the extracellular depletion is shown. Calcium efflux activation increased by 130%, the rate at which the extracellular calcium ion concentration during the post drive period approached a quasi-steady state level . The extracellular calcium level in the resting preparation of the last run was also higher due to concurrent calcium efflux activity versus its absence in the control.

These results show that the equilibrium of transmembrane calcium fluxes is mediated by activation of a membrane calcium extrusion process. Ca^{++} efflux activation permits higher undirectional cellular calcium uptake when the heart beats faster by preventing chronic calcium depletion. During the 20-30 minutes of transition, sustained extracellular calcium depletion occurs and is associated with a reduced net influx of calcium. Once the extracellular calcium ion concentration depletion is eliminated by enhanced calcium efflux, more calcium can be delivered to frog ventricular cells. (This is shown by measuring the magnitude of the extracellular calcium ion concentration depletion of the 2nd cycle versus 11th cycle in figure 17.)

H. Effect of Low Na^+ Ringers on Extracellular $[Ca^{++}]$ Depletions

Low Na^+ Ringers potentiates contractility (Ringer, 1883; Brown & Orkand, 1968) in frog ventricle and should therefore potentiate extracellular $[Ca^{++}]$ depletion. The Ringers sodium concentration was lowered to 50 and 25% of the normal concentration. The sodium substitute was equimolar pH 7.3 Tris/Tris+Cl-. When the preparation was quiescent in

0.050 mM Ca^{++} Ringers, the low Na^{+} solutions caused a slow and small depletion of the extracellular $[Ca^{++}]$ (data not shown). After allowing 30-60 minutes for the preparation to equilibriate in a low Na^{+} solution, the muscle was repetitively stimulated at 24 beats per minute for 12 minutes. The 50% Na^{+} Ringers decreased action potential duration at 24 per minute from 1000 $\pm$ 40 to 430 $\pm$ 10 milliseconds (a 57% decrease). The magnitude of the steady state $[Ca^{++}]_o$ depletion is dependent upon the % time membrane depolarization (figure 11) in normal Na^{+} Ringers. Since the % time membrane depolarization is decreased from 40% to 17% by 50% Na^{+} Ringers, the magnitude of $[Ca^{++}]_o$ might have proportionately decreased. However, the normal Na^{+} Ringers and 50% Na^{+} Ringers $[Ca^{++}]_o$ depletions (figure 19) were similar during the first 50 seconds of the run. Thereafter, the control depletion reached a minimum of 7 micromolar (bath $[Ca^{++}]$ was 50 micromolar) while the 50% Na^{+} Ringers caused depletion to 12 micromolar (figure 19). In spite of a 57% decrease in the % time membrane depolarization, the $[Ca^{++}]_o$ depletion in 50% Na^{+} Ringers was similar in time course and magnitude to that in normal Na^{+} Ringers.

In 25% Na^{+} Ringers the action potential duration was shortened to 90 $\pm$ 10 milliseconds (9% as large as that observed in normal Na^{+} Ringers). The normal Na^{+} Ringers depletion was 43 micromolar (50 to 7 uM). The 25% Na^{+} Ringers was expected on the basis of the % membrane time depolarization to cause a 4 micromolar $[Ca^{++}]_o$ depletion (50 to 46 uM). However, in 25% Na^{+} Ringers the $[Ca^{++}]_o$ depletion was 22 micromolar (50 to 28 uM) only half as large as the depletion in normal Na^{+} Ringers.

The normal Na^{+} Ringers was tested again (post-control). Action

Figure 19: The extracellular calcium ion concentration versus time was plotted during repetitive stimulation (24 per minute for 12 minutes) in a muscle strip superfused in 100%, 50%, and 25% Na^+ Ringers. The ventricular strip diameter was 2 millimeters and the calcium ion selective microelectrode tip depth in the strip was about 1 millimeter. The symbols key for the curves is listed below the graph. Extracellular calcium ion depletion in low Na^+ Ringers was greater than expected after correcting for the fact that low Na^+ Ringers significantly shortened the action potential duration.

EFFECT OF THE EXTRACELLULAR [Na+] ON THE MAGNITUDE OF EXTRACELLULAR CALCIUM DEPLETION DURING A LONG TRAIN.

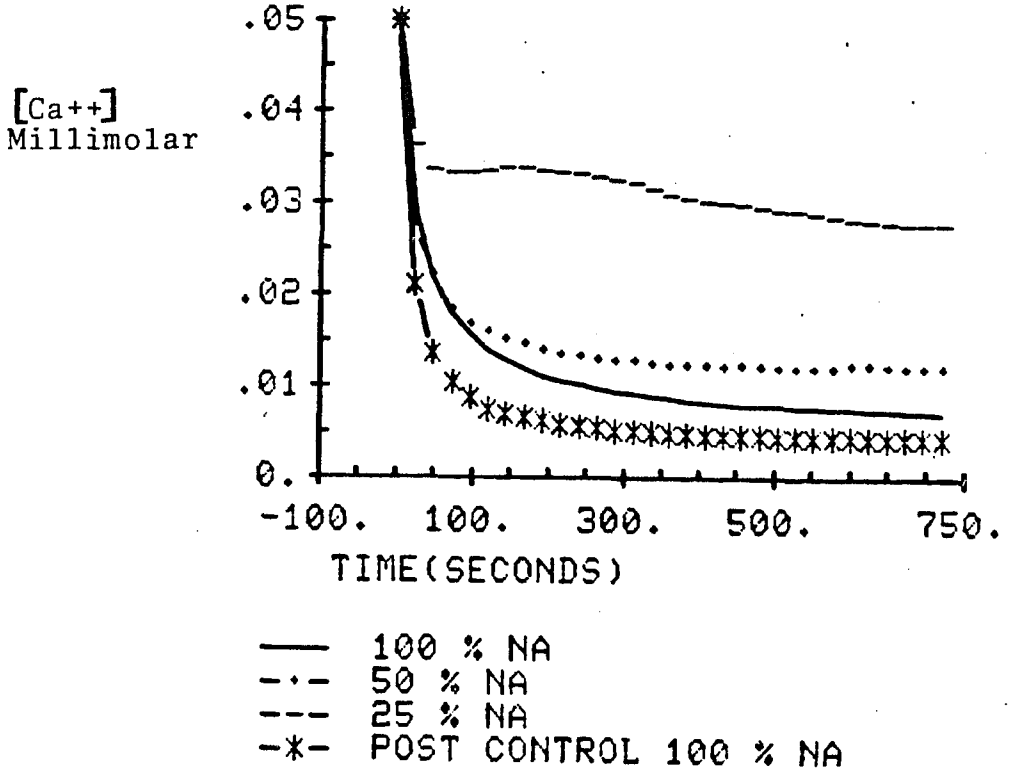

potential duration increased from 90 ± 10 milliseconds to 920 ± 80 milliseconds. The extracellular calcium level fell by 46 micromolar in the post-control versus 43 micromolar in the initial control. Thus the results were not due to a change in the location of the microelectrode tip.

These experiments in low Na^+ Ringers indicate that lowering the $[Na^+]_o$ which shortens the action potential duration, does not reduce the magnitude of the $[Ca^{++}]_o$ depletion as expected on the basis of the % time membrane depolarization. The low Na^+ Ringers appears to increases the $[Ca^{++}]_o$ depletion for a given % time membrane depolarization. (See section D of Discussion.) Alternatively, the majority of the cellular uptake of Ca_o^{++} may occur in the beginning 20% of the action potential. (See section D of Analysis.) Further testing of this hypothesis was not attempted since the Ca^{++} microelectrode response time was too slow (see figure 3).

I. Effect of Prolonged Membrane Depolarization upon Extracellular Calcium Depletion

The rate and magnitude of extracellular calcium ion depletion (or cellular calcium ion uptake) in ventricular muscle strips bathed in Ringers solution has been shown to be a function of the percent time membrane depolarization (for 0-70% time membrane depolarization caused by trains of action potentials). After each ventricular action potential the cell membrane potential repolarized. Most prevailing models of calcium channel behavior propose that prolonged depolarization causes inactivation of most or all of the calcium current (Scheuer and Kass, 1983). This model was tested by exposing the muscle strip to high potassium Ringers to

cause prolonged membrane depolarization. The extracellular [K^+] was increased from 3 to 63 mM. Assuming the intracellular [K^+] is 120 mM (Walker, 1971), the membrane potential would be -16 mV in 63mM [K^+] Ringers for a membrane principally permeable to K^+ (Adrian, 1956). To keep the Ringers tonicity and ionic strength constant, the Ringers sodium ion concentration was lowered as the potassium ion concentration was elevated. To control for the effects of the low [Na^+] in the Ringers, the muscle strip was tested in a low Na^+ Ringers. The sodium substitute was equimolar pH 7.3 Tris/$Tris^+Cl^-$.

The low Na^+ Ringers caused a small and variable extracellular calcium depletion at resting membrane potential. The low Na^+/$Tris^+$ Ringers and low Na^+/high K^+ Ringers were alternatively run thru the bath with the calcium microelectrode tip in the bath as a control. The low Na^+ Ringers consistently caused a positive voltage artifact of 1-2 millivolts. The low Na^+/high K^+ Ringers caused a negative voltage artifact of 6-8 millivolts.

The calcium microelectrode tip was placed in an extracellular cleft in a ventricular muscle strip. This was confirmed by induction of $[Ca^{++}]_o$ depletion during repetitive stimulation. Superfusion with the low Na^+/high K^+ Ringers caused the Ca^{++} microelectrode signal to shift positive to +2 mV for about 2 minutes (minutes 3 to 5 on figure 20) followed then by a negative shift to -16 mV (at time 7 minutes, figure 20). The maximum artifactual potential was -6 to -8 mV. Therefore, a conservative estimate of the calcium depletion would be -8 mV (the equivalent molar $[Ca^{++}]$ change would be 0.20 to 0.11 mM). After 30 minutes exposure time to the low Na^+/high K^+ Ringers, the calcium electrode potential was only about -6 mV. This -6 mV was probably the

Figure 20: Top panel shows calcium microelectrode output versus time. At 2 minutes time, the superfusate was changed from normal (3mM K^+, 118mM Na^+) Ringers to (63mM K^+, 58mM Na^+) Ringers till time 32 minutes, when the superfusate was changed back to normal Ringers. The calcium electrode output rather than calcium ion concentration was shown since there was some uncertainty concerning the time course of the extracellular equilibration of the low Na^+/high K^+ Ringers. A correction in this time course for the -6 to -8 mV artifact caused by the low Na^+/high K^+ Ringers could not be simply determinted.

Solid line is plot of the slow change in extracellular calcium concentration during repetitive stimulation at 36 per minute for 4 minutes. At 15 minutes time, the abrupt shift in the measured calcium ion concentration was caused by removal of the calcium microelectrode tip from the extracellular location in the tissue and its placement in the superfusate.

HIGH K/LOW NA CONTRACTURE
MILLIVOLT RESPONSE OF CA ELECTRODE

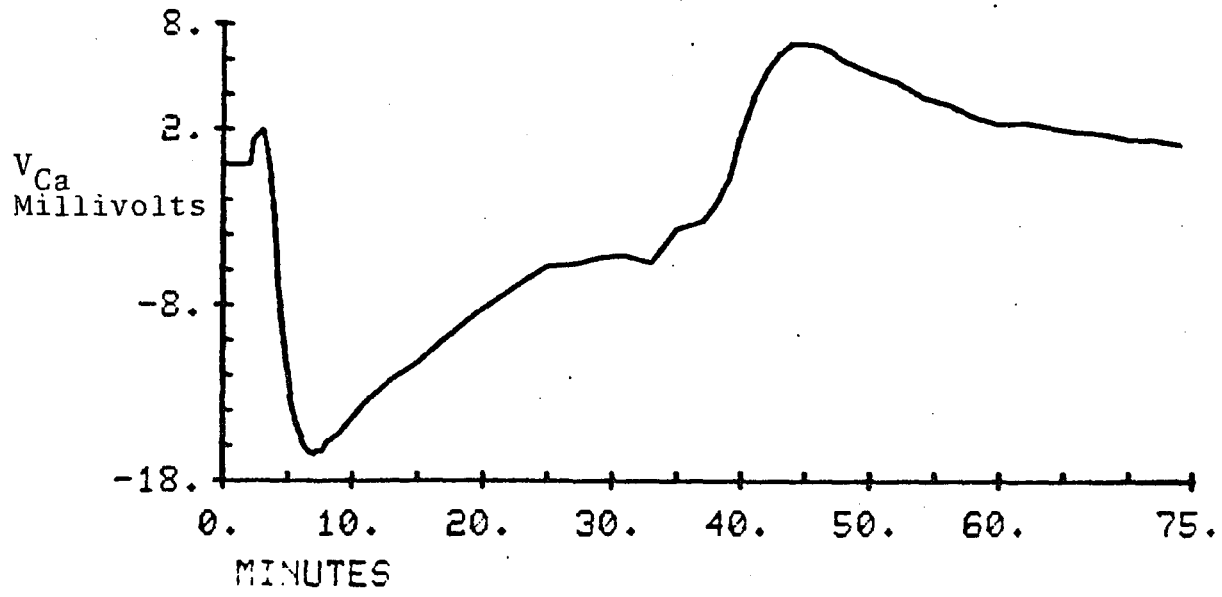

DEPLETION FOLLOWING CONTRACTURE

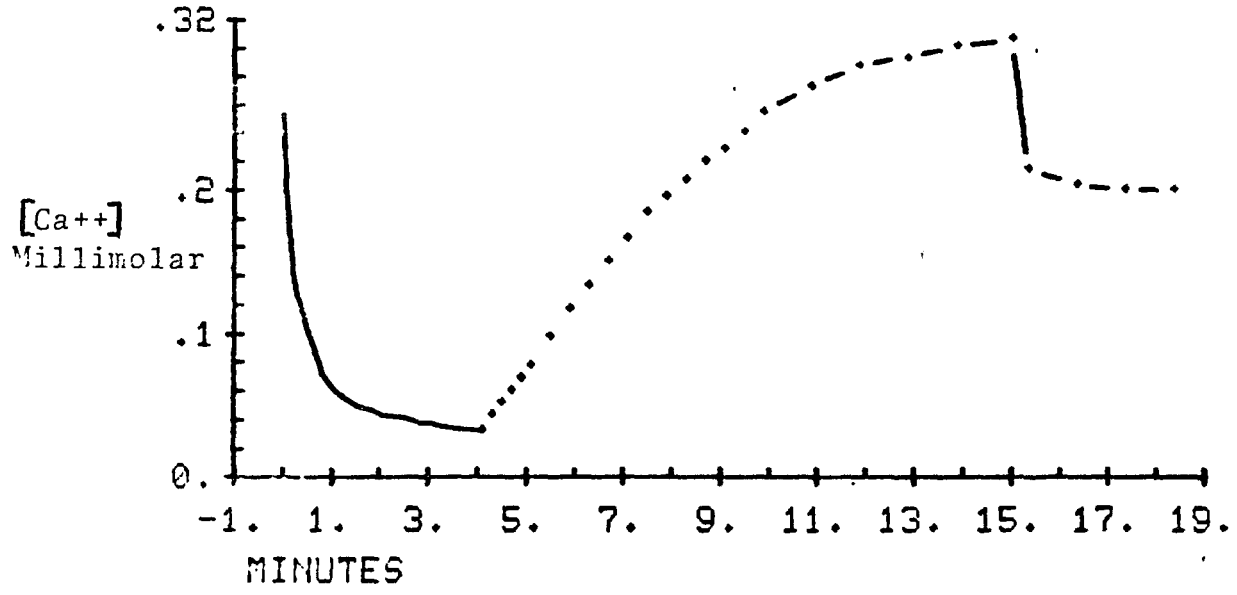

forementioned low Na^+/high K^+ Ringers solution artifact. Hence after 30 minutes time, the extracellular $[Ca^{++}]$ at the microelectrode tip was presumably the same as the bath $[Ca^{++}]$ while the cell membrane was depolarized to -16 mV. Upon switching back to normal Ringers, there was an extracellular $[Ca^{++}]$ overshoot of about +7 mV (0.20 to 0.35 mM). This $[Ca^{++}]_o$ overshoot lasted about 35 minutes. Thus, the steady state extracellular $[Ca^{++}]$ during prolonged continuous membrane depolarization was controlled by a slowly activating calcium extrusion process.

After the low Na^+/high K^+ Ringers experiment with the same Ca^{++} microelectrode impalement, the muscle strip was repetitively stimulated at 36 per minute for 4 minutes. The repetitive stimulation was initiated before the $[Ca^{++}]_o$ overshoot from the prior experiment had dissappeared. During the stimulation the extracellular calcium ion concentration fell from 0.25 to 0.040 millimolar in two minutes (figure 20, lower panel). The large magnitude of this $[Ca^{++}]_o$ depletion indicates that the electrode tip impalement was near the center of the preparation. It also enables us to quantitatively compare the depletions caused by stimulation versus those due to prolonged high K^+ induced depolarization. The post stimulation extracellular $[Ca^{++}]$ increased beyond the bath $[Ca^{++}]$. This $[Ca^{++}]_o$ overshoot was not electrical drift. When the calcium micro- electrode was pulled into the bath, the calcium microelectrode signal fell from 0.31 mM at time 15 minutes to bath Ca^{++} level of 0.20 mM (see figure 20, bottom panel).

J. Effect of Manganese Ion upon Slow Extracellular $[Ca^{++}]$ Depletion

Manganese ions are thought to block calcium channels and sodium dependent calcium exchange. Manganese ions should then block extracellular

calcium ion depletion in frog ventricle. The control protocol was to repetitively stimulate the preparation for 2 minutes at 30 per minute. The extracellular [Ca^{++}] fell from 0.20 to 0.115 millimolar (an 85 micromolar depletion). Figure 21, top panel shows a typical record. The magnitude of these control runs was plotted in the lowest panel of figure 21 at times 0 to 60 minutes. Five control runs were performed to establish reproducibility. After about a 30 minute exposure to 1 millimolar manganese, the action potential duration (at 30 beats per minute) was reduced from 930 $\pm$ 70 to 790 $\pm$ 50 milliseconds (n = 4). The plateau of the action potential was lowered. While action potential duration was reduced by 14 $\pm$ 2%, the magnitude of the extracellular [Ca^{++}] depletion was reduced by 56 $\pm$ 9% (n = 5). This is shown in figure 21. Twenty minutes following manganese ion washout the rate and magnitude of the $[Ca^{++}]_o$ depletions had increased nearly back to control (figure 20, third vs. first panels). In the lowest panel of figure 21 the diamond points indicate the magnitude of extracellular [Ca^{++}] depletion caused by a 2 minute train of action potentials. The points under the black bar indicate the period of manganese exposure. The action of manganese was not tested at higher manganese concentrations due to the precipitation of the higher manganese concentrations with bicarbonate.

K. Effect of Catecholamines on Extracellular [Ca^{++}] Depletions

Catecholamines should increase extracellular calcium ion concentration depletion since catecholamines are known to increase twitch tension and the voltage-sensitive calcium current. In preliminary experiments in 0.2 mM Ca^{++} Ringers, 5 micromolar epinephrine markedly increased the force of contraction of the ventricular strips. Experiments had to be

Figure 21: Top, second, and third panels show calcium microelectrode output during repetitive stimulation at 30 per minute for 2 minutes (A) in control, (B) during manganese, and (C) in post-manganese periods respectively. Regular pattern of the vertical spikes is caused by the electrical field stimulus while the other spikes are artifacts due to the suction pipette method used to remove the superfusate from the bath. Vertical calibration mark is 5 millivolts and the horizontal calibration mark is 1 minute.

Bottom panel (D) plots the magnitude of the calcium depletions. There were 5 control depletions (at times 0-60 minutes), during manganese ion exposure (time interval covered by the blackbar, 4 depletions were performed), and after manganese washout there were 5 post control depletions (at time 150-210 minutes). Manganese ion (1.0 mM in presence of 0.20 millimolar Ca^{++}Ringers in this experiment reduced extracellular Ca^{++} depletion from 85 to about 35 micromolar (59% inhibition) while decreasing action potential duration by only 14%.

EFFECT OF MANGANESE ION ON $[Ca^{++}]_o$ DEPLETION

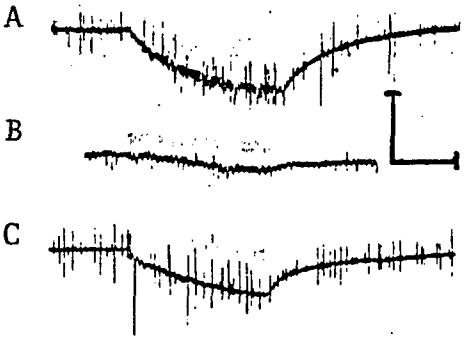

D

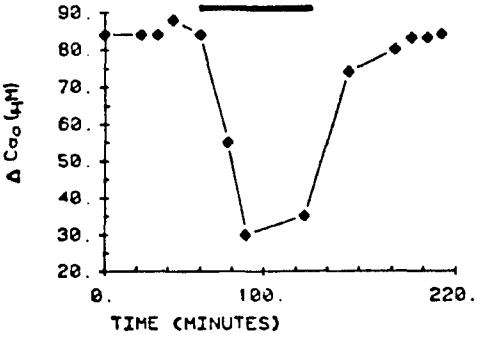

performed in 0.10 and 0.050 millimolar Ca^{++}Ringers to reduce the complication of tension artifacts.

Five micromolar epinephrine (Parke Davis) doubled the rate of extracellular calcium depletion in ventricular strips superfused with 0.10 mM Ca^{++}Ringers during short trains of repetitive stimulation at 12 and 24 beats per minute (figure 22, top panel). The rate was determined as the time necessary for the extracellular calcium concentration to fall from 0.10 to 0.070 millimolar. The drug was washed in for 30 minutes at a heart rate of 3 per minute before starting the experiment. During this time subtle increases in the magnitude of beat to beat depletion were seen and action potential duration was observed to increase from 850 to 1250 milliseconds.

The prolongation of action potential duration was examined and correlated with the superfusate epinephrine concentration. Data from 23 frogs (at epinephrine doses 0.1 to 120 micromolar) was pooled to generate an epinephrine log dose-response curve for the % action potential duration prolongation. Frog ventricular strips were bathed in 0.050 mM Ca^{++} Ringers and stimulated at a constant heart rate of 3-12 per minute (figure 22, bottom panel). The primary purpose of this D/R curve was to establish the suitable dose of epinephrine to effect a 50-90% response. Using the prophet computer "Logistics" program, data from 12 different epinephrine dose-response points were fit with a sigmoidal curve (see figure 22, lower panel). It was assumed that simple, reversible mass action between drug and receptor was involved. The curve fit K_D was 20 micromolar, with slope of 1.2, and a Vmax equal to 120% of the maximum observed response. The low affinity of the epinephrine receptor precluded the use of epinephrine doses much above 100 micromolar. A dose of 50 micromolar

Figure 22: Top panel shows that epinephrine increases the rate of extracellular $[Ca^{++}]$ depletion. In the control $[Ca^{++}]_o$ depleted from 0.10 to 0.070 mM in 4 minutes when heart rate was increased from 0 to 12 per minute (solid line). After 30 minutes exposure to 5 micromolar epinephrine, the rate of $[Ca^{++}]_o$ depletion at heart rate 12 per minute was doubled (solid triangles) relative to control (solid line). $[Ca^{++}]_o$ depleted from 0.10 to 0.70 mM in 70 seconds when heart rate was increased from 0 to 24 per minute (dashed line). Five micromolar epinephrine doubled the rate of $[Ca^{++}]_o$ depletions ($[Ca^{++}]_o$ fell from 0.10 to 0.070 mM in 35 seconds at heart rate 24 per minute, shown by solid squares).

Bottom panel plots the % change in the frog ventricular strip action potential duration as a function of the logarithim of the concentration of superfusate epinephrine concentration (Parke-Davis). The points are each the mean of 1 to 12 experiments. Where applicable standard deviation bars were used. The solid line is the prophet computer "Logistics" fit to the points. The estimated K_D = 20 micromolar (slope = 1.2 and Vmax = 120%). Bath Ca^{++} concentration was 0.050 mM.

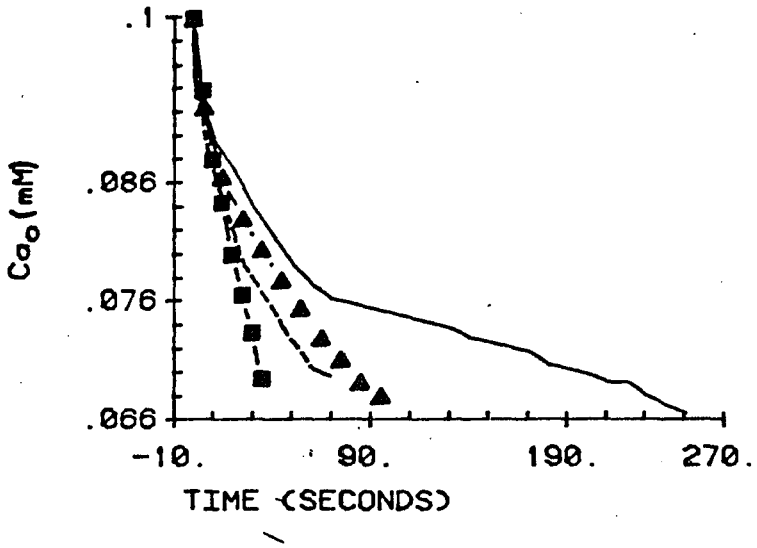
.1
.086
.076
.066
Ca_o (mM)
-10.
90.
190.
270.
TIME (SECONDS)

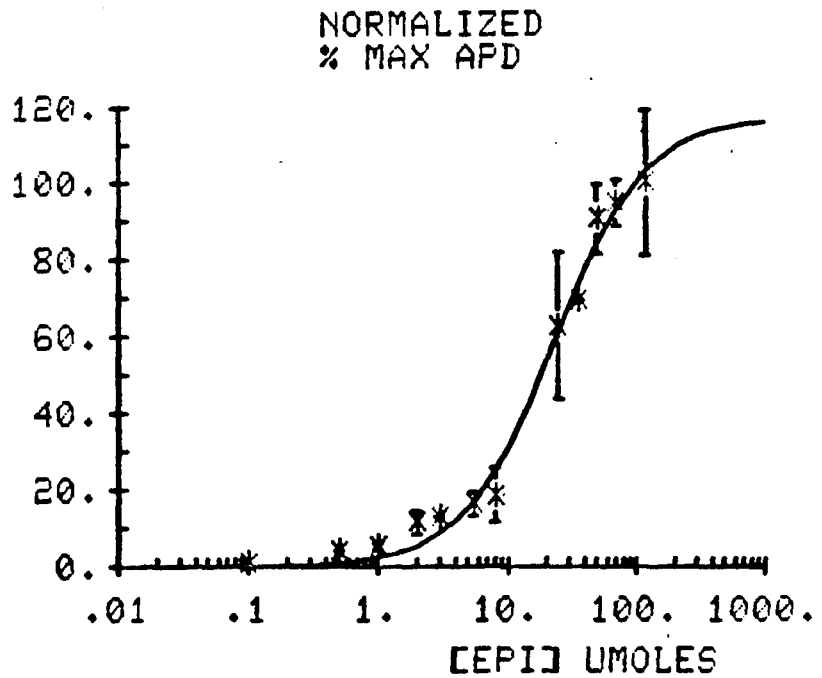
NORMALIZED
% MAX APD
120.
100.
80.
60.
40.
20.
0.
.01
.1
1.
10.
100.
1000.
[EPI] UMOLES

epinephrine was selected to be used in the subsequent experiments.

When 50 micromolar epinephrine was washed into a slowly beating (3 per minute) ventricular muscle strip superfused with 0.050 millimolar Ca^{++} Ringers, action potential duration and action potential plateau height significantly increased. At the same time the magnitude of the beat to beat $[Ca^{++}]_o$ depletions increased. Ten to thirty minutes were needed to reach steady state (see figure 23, top 2 panels). Compared to control, beat to beat $[Ca^{++}]_o$ depletions during epinephrine increased 3-fold in rate and the magnitude of the beat to beat $[Ca^{++}]_o$ depletions increased 5-fold (see figure 23, lower panels and figure 24, top panel). The magnitude of these extracellular $[Ca^{++}]$ depletions was increased from about 5 micromolar to about 25 micromolar in some instances. The magnitude of the response did not change much with repeated epinephrine exposures provided that sufficient time was given for the attainment of extracellular diffusion equilibrium of the superfused drug. Since the rate of the calcium microelectrode response to a change in calcium ion concentration was similar to the actual rate of extracellular $[Ca^{++}]$ depletion, these observations will be considered qualitative.

The magnitude and rate of beat to beat extracellular $[Ca^{++}]$ depletions were plotted in figure 24 (top panel) as a function of the action potential duration during the washin and washout of a 50 micromolar epinephrine dose. The magnitude of $[Ca^{++}]_o$ depletion during the first second of the action potential was used to determine the average instantaneous rate of $[Ca^{++}]_o$ depletion. As the action potential duration increased from 850 to about 1600 milliseconds, the rate and magnitude of $[Ca^{++}]_o$ depletion increased by the same proportion. The average epinephrine-dependent action potential duration was 2300 milliseconds, at

Figure 23: Top 2 panels show the effect of 50 micromolar epinephrine upon the magnitude and rate of beat to beat $[Ca^{++}]_o$ depletion shown as VCa (heart rate was 3 per minute) as this drug diffuses into a frog ventricular strip. A slow cummulative $[Ca^{++}]_o$ depletion develops while a large increase in the magnitude and rate of the extracellular beat to beat $[Ca^{++}]_o$ depletions occurs.

Bottom panel shows the calcium microelectrode output (VCa) recording (at a higher chart speed and gain) of single beat to beat $[Ca^{++}]_o$ depletions (heart rate 3 per minute) and the following diastolic period of recovery from the $[Ca^{++}]_o$ depletion. In the first record, the response to 50 micromolar epinephrine is shown. The second record is the post-Epi washout control. The third record is the effect of the second exposure to 50 micromolar epinephrine. The fourth record is the subsequent post-Epi washout control. The fifth record is the effect of the third exposure to 50 micromolar epinephrine. These records indicate that epinephrine increases both the rate and magnitude of beat to beat extracellular $[Ca^{++}]$ depletion in a reversible, reproducible manner. The $[Ca^{++}]$ in the Ringers was 0.050 millimolar.

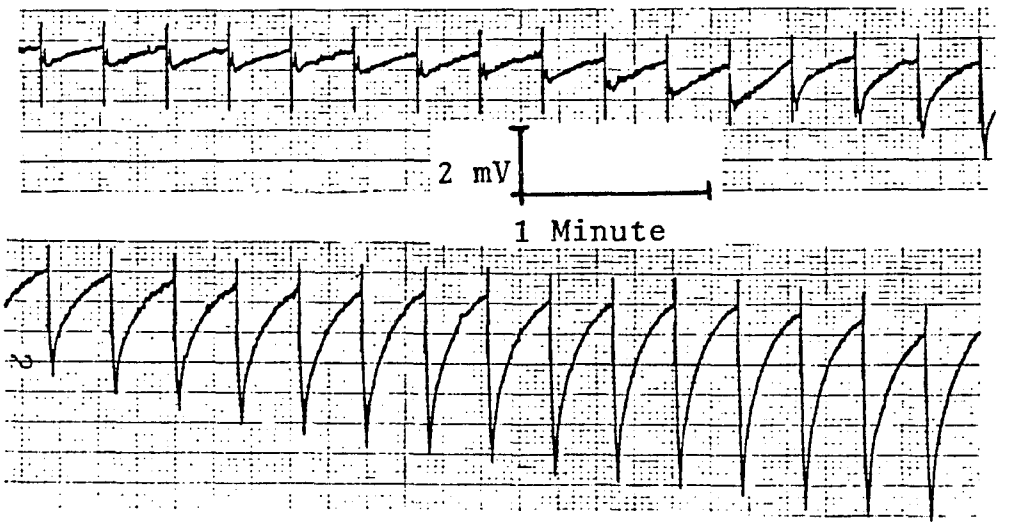
2 mV
1 Minute

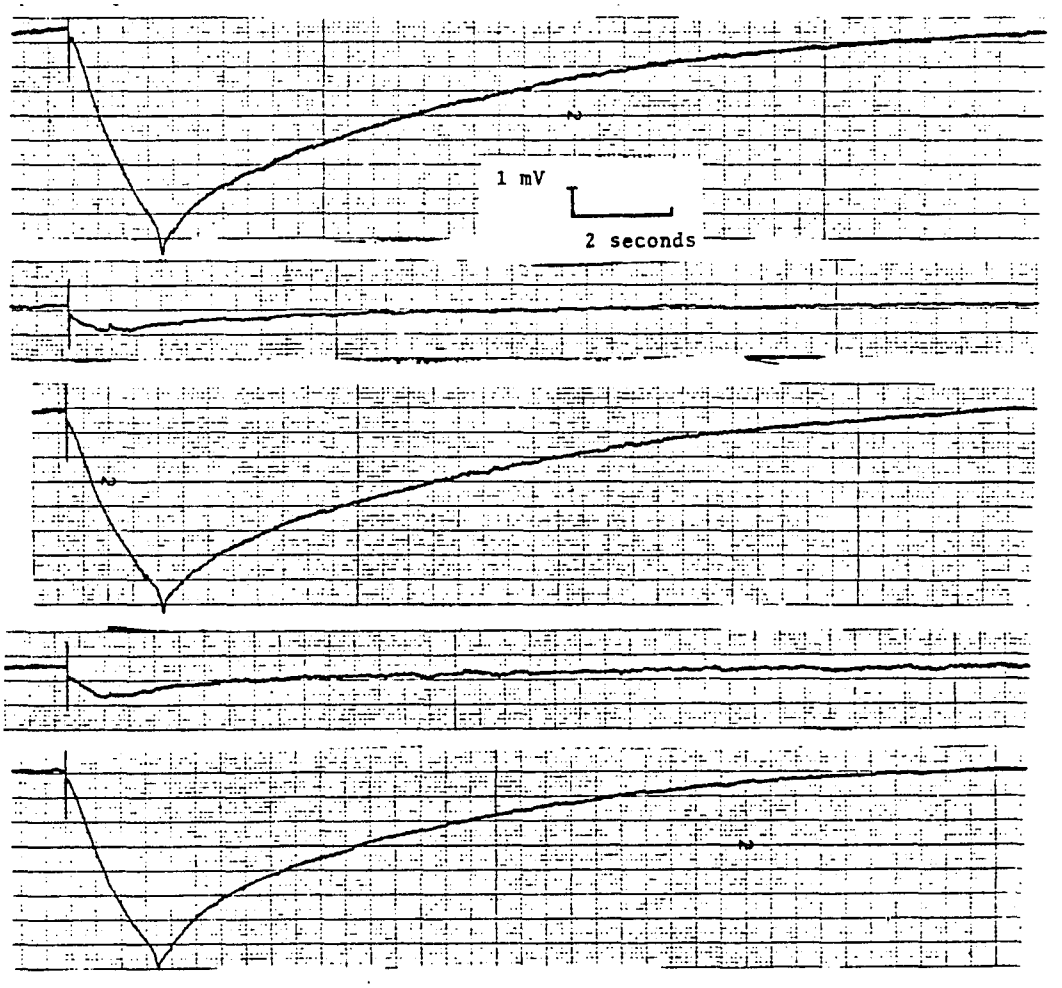
1 mV
2 seconds

Figure 24: Top panel plots the magnitude (solid line) and rate (dotted line) of beat to beat calcium depletion (micromolar) in frog ventricular muscle strips exposed to 50 micromolar epinephrine versus action potential duration. As this drug washed into the muscle strip the action potential duration increased. The lower respective curves of the hystersis loop were caused during epinephrine washin while the effect of drug washout follows the upper curves. The change in $[Ca^{++}]_o$ depletion magnitude and rate of $[Ca^{++}]_o$ depletion appear to lag behind the changes in the action potential duration. The $[Ca^{++}]$ of the Ringers was 0.050 millimolar.

Lower panel plots the magnitude of the beat to beat $[Ca^{++}]_o$ depletion versus action potential duration during washin of 50 micromolar epinephrine (open circles). Subsequently a mixture of 50 micromolar epinephrine plus 50 micromolar propranolol was washed in (solid diamonds). The beat to beat $[Ca^{++}]_o$ depletion and action potential duration potentiation due to epinephrine were blocked by propranolol. The $[Ca^{++}]$ in the Ringers was 0.050 millimolar and heart rate was 3 per minute.

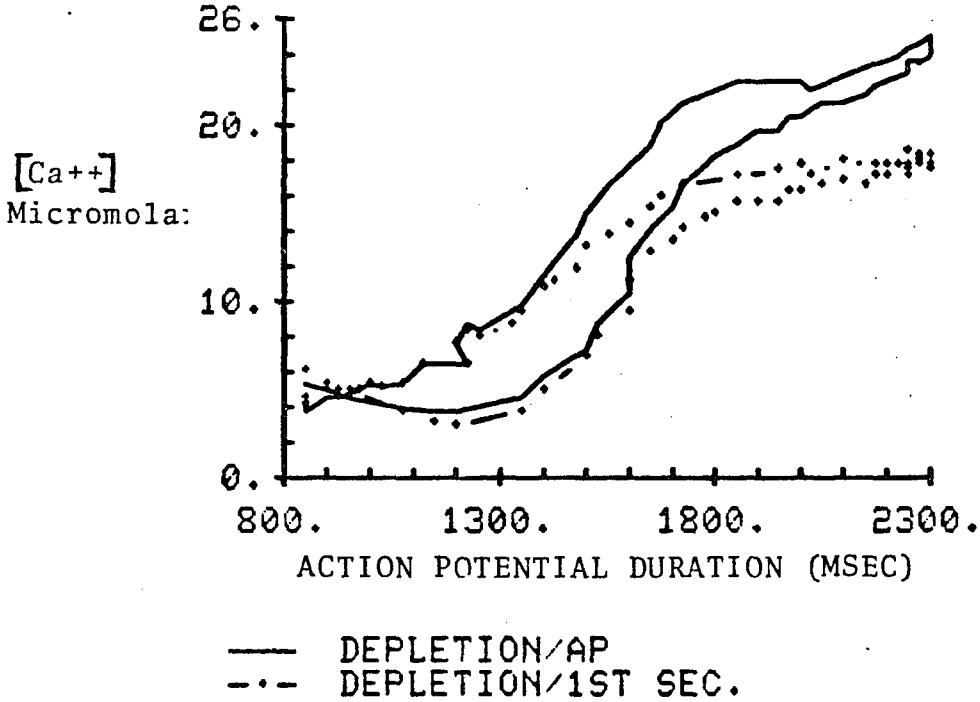
26.
20.
10.
0.
[Ca++]
Micromola:
800.
1300.
1800.
2300.
ACTION POTENTIAL DURATION (MSEC)
DEPLETION/AP
DEPLETION/1ST SEC.

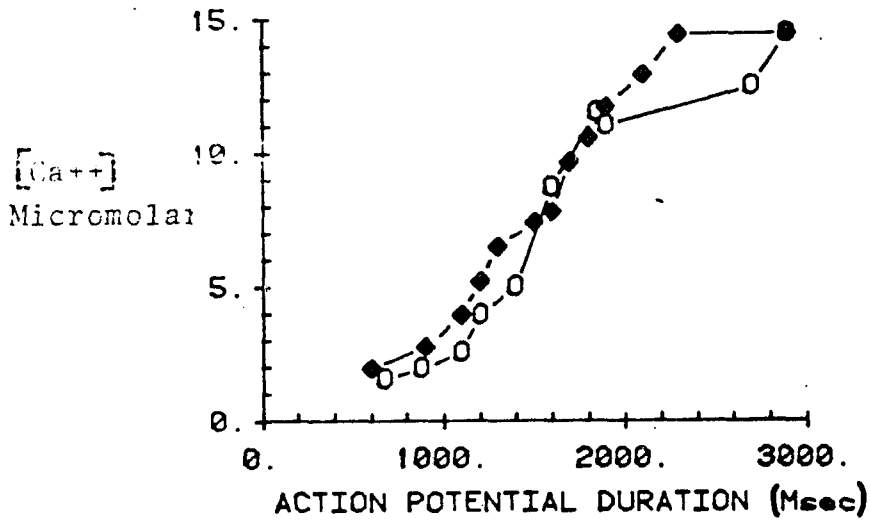
15.
10.
5.
0.
[Ca++]
Micromolar
0.
1000.
2000.
3000.
ACTION POTENTIAL DURATION (Msec)

heart rate 3/minute. A 270 $\pm$ 50% action potential duration increase was typical for this epinephrine dose. As the epinephrine was washed out, the rate and magnitude of the beat to beat $[Ca^{++}]_o$ depletion lagged behind the decrease in action potential duration. The washin and washout response showed hysteresis. Thus, epinephrine's action upon action potential duration seemed to occur and to dissappear more rapidly than epinephrine's action upon extracellular beat to beat $[Ca^{++}]_o$ depletion (see figure 24, upper panel). This hysteresis may have been due to asymmetry of extracellular drug diffusion in the muscle.

Since catecholamines are known to stimulate Beta adrenergic receptors, there must be a dose of Beta adrenergic receptor antagonist which can completely reverse the action of a dose of epinephrine. Since frog ventricle functionally lacks alpha adrenergec receptors (Morad et al., 1981), it is most likely that epinephrine acts at Beta adrenergic receptors. As shown in figure 24, bottom panel, propranolol (50 micromolar; Ayerst) completely reversed both responses of 50 micromolar epinephrine. Action potential duration prolongation and the increase in the magnitude of extracellular beat to beat $[Ca^{++}]_o$ depletion were restored to control values. Fifty micromolar propranolol was chosen since the K_A of propranolol (estimated from preliminary antagonist experiments) was between 0.1 and 1 micromolar. Hence, 50 micromolar propranolol was expected to cause between a 51 and 501 fold decrease in the apparent receptor affinity for epinephrine. With epinephrine plus propranolol the action potential duration decreased from 3000 to 600 milliseconds (lower panel, figure 24). The magnitude of the beat to beat extracellular calcium depletions decreased along the same curve generated by the effect of epinephrine alone. Since the effects of epinephrine were antagonized fully by an appropriate dose of Beta adrenergic receptor

antagonist, the stimulation of the rate of extracellular calcium ion concentration depletion by epinephrine, was ascribed to Beta adrenergic receptor stimulation.

The effects of nickel and manganese ions as antagonists of the epinephrine augmented beat to beat $[Ca^{++}]_o$ depletion were studied. A control depletion (heart rate 3 per minute) is shown in the upper panel of figure 25. The effect of 50 micromolar epinephrine is shown in the middle panel of figure 25. One millimolar manganese blocked 30% of the epinephrine stimulated beat to beat depletion and action potential duration. One millimolar nickel ion blocked the epinephrine induced beat to beat $[Ca^{++}]_o$ depletion by 70% while action potential duration was only slightly reduced. Unlike manganese ions, the action of nickel ions was slowly reversible, requiring up to 2 hours. One millimolar manganese or nickel ions caused about a 0.5 millivolt artifact (a 4% signal error) in the 10 micromolar Ca^{++} Ringers calibration solution. This did not alter the results.

Prolonged exposure (20-40 minutes) with catecholamine often resulted in an attenuated beat to beat calcium depletion response (most evident with the larger doses of catecholamine). Evidence of cumulative beat to beat extracellular calcium depletion due to catecholamines can be seen in figure 23 (top panel) and figure 26 (top panel). In figure 26 (top panel) the time course of effect of washing in 9 micromolar isoproterenol (a maximum dose) is shown. The beat to beat $[Ca^{++}]_o$ depletions were increased about six fold in magnitude after 10 minutes (figure 26). Heart rate was 3/minute. Thereafter, the cumulative $[Ca^{++}]_o$ depletion slowly decreased and was zero after 40 minutes of drug exposure. The magnitude of the beat to beat calcium depletion at 40 minutes was two

Figure 25: Top record shows a control calcium microelectrode output (heart rate 3 per minute, bath Ca^{++} = 0.050 mM).

Middle record shows the effect of 50 micromolar epinephrine on the $[Ca^{++}]_o$ depletion (beat to beat)

Bottom record shows the effect of subsequent washin of 1 millimolar nickel plus 50 micromolar epinephrine.

In all three records the initial spike marks the stimulus artifact. The second artifact (a little notch or bump) in the $[Ca^{++}]_o$ depletion phase of the record coincides with the end of the action potential duration. (It may be caused by a combination of extracellular action potential and mild tension artifacts). One millimolar nickel ion can substantially antagonize the beat to beat $[Ca^{++}]_o$ depletion while keeping the action potential duration constant, unlike manganese ion (data not shown). The action potential plateau is lowered by either Ni^{++} or Mn^{++}.

BLOCK OF EPINEPHRINE EFFECT BY NICKEL ION

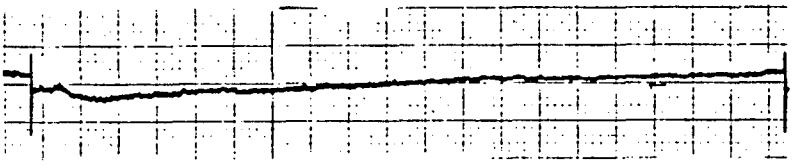

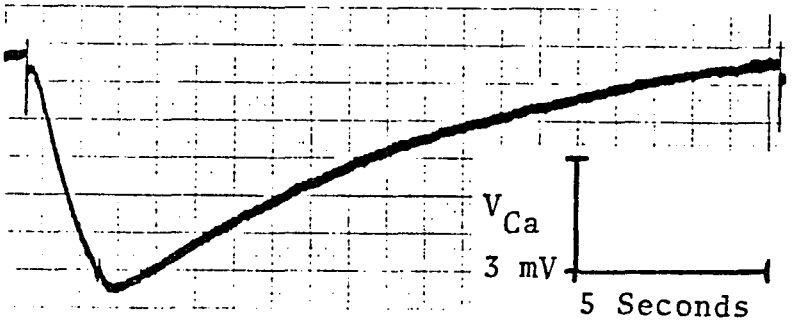

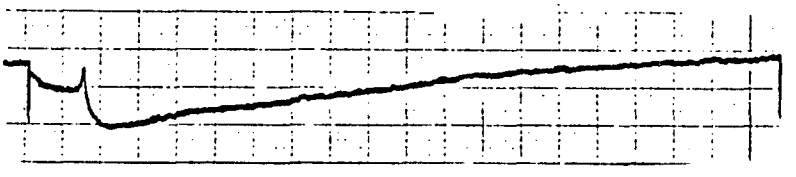

Figure 26: Top records of a calcium microelectrode shows the effect of 9 micromolar isoproterenol upon beat to beat $[Ca^{++}]_o$ depletion (Heart rate = 3/minute) . As in figure 22 (top panel) with epinephrine, isoproterenal causes a significant increase in the magnitude of beat to beat $[Ca^{++}]_o$ depletion and noticible slow cumulative $[Ca^{++}]_o$ depletion. After 40 minutes of drug exposure the small cumulative $[Ca^{++}]_o$ depletion was gone and the beat to beat $[Ca^{++}]_o$ depletions were smaller.

Bottom plots two curves. Solid line is the extracellular $[Ca^{++}]$ just before each beat versus time of exposure to 9 micromolar isoproterenol. Nine micromolar isoproterenol was added to the Ringers at time 0 minutes. The solid line also traces the "slow cumulative $[Ca^{++}]_o$ depletion". The dashed line plots the minimum extracellular $[Ca^{++}]$. Thus the difference ($[Ca^{++}]_o$ level at solid line minus $[Ca^{++}]_o$ level at dashed line) is the change in magnitude of the beat to beat $[Ca^{++}]_o$ depletions. Since a small $[Ca^{++}]_o$ overshoot occurred when the isoproterenol was washed out, the data suggests that some Ca^{++} efflux activation occurred. Hence the slow cumulative $[Ca^{++}]_o$ depletion over time observed for 30 to 40 minutes (solid line) may have been abolished by gradual $[Ca^{++}]_o$ efflux The net beat to beat $[Ca^{++}]_o$ depletion was also reduced (solid-dashed lines) over time. This is evident during the times 10 to 40 minutes as $[Ca^{++}]_o$ efflux eliminated the slow $[Ca^{++}]_o$ depletion.

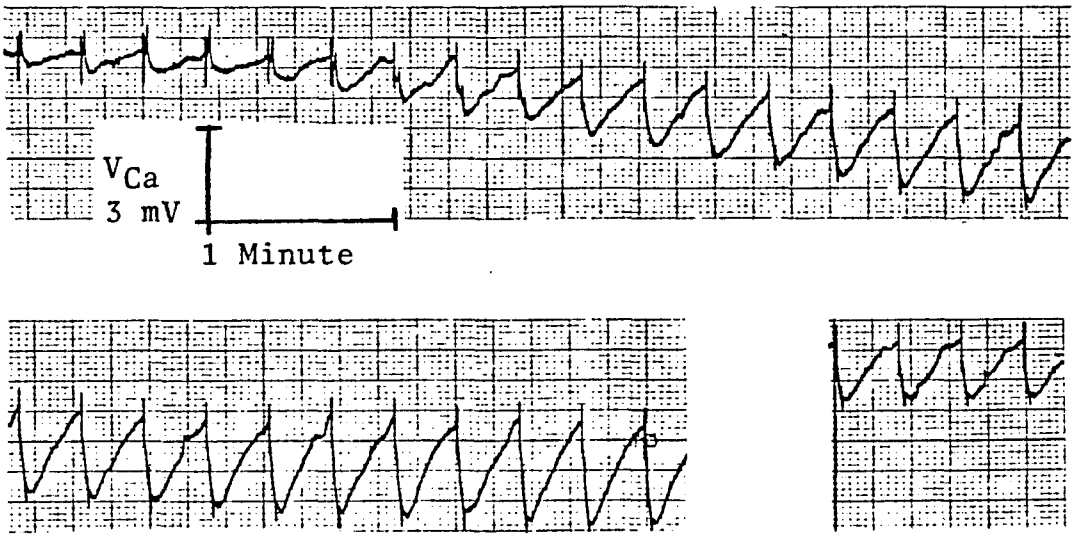

TIME COURSE OF CA0 DEPLETION IN FROG VENTRICLE BEATING (3/MIN) WITH 9 MICROMOLAR ISOPROTERENOL.

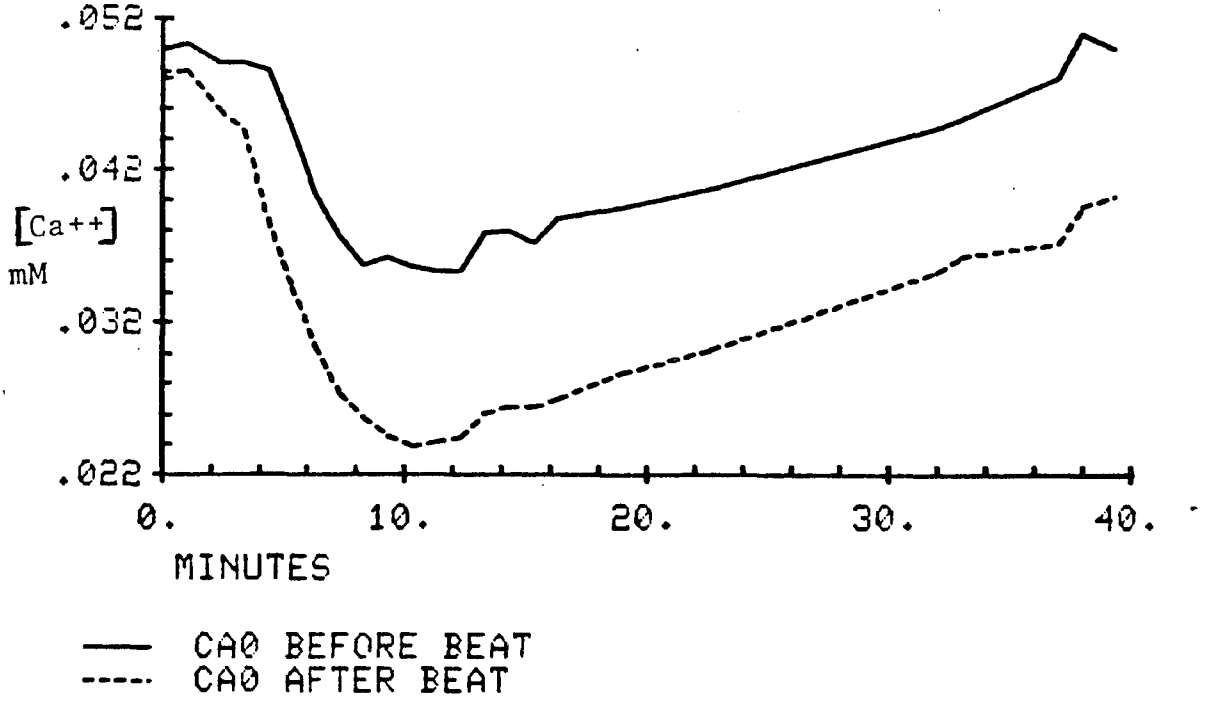

thirds as large as the beat to beat $[Ca^{++}]_o$ depletion at 10 minutes. This result indicates that prolonged catecholamine stimulation at a low heart rate caused intracellular calcium ion accumulation and Ca^{++} efflux. Evidence of Ca^{++} efflux was also indicated when the removal of the catecholamine evoked a small $[Ca^{++}]_o$ overshoot.

L. Isometric Twitch Tension during Repetitive Stimulation of 0.2 and 1.0mM Ca^{++} Ringers Superfused Frog Ventricular Muscle Strips

In 1 mM Ca^{++} Ringers a frog ventricular strip of diameter 1 millimeter was stretched 150% resting length. The muscle twitch generated about 1000 milligrams of isometric twitch tension at heart rate 6 per minute at steady state. When bath $[Ca^{++}]$ was lowered to 0.20 millimolar during beating at 6 per minute, twitch tension fell to approximately 200 milligrams in 30-60 minutes, as expected. At least 60 minutes time was required for a reproducible steady state tension response. Since the magnitude of the extracellular calcium depletion in 0.2 mM Ca^{++} Ringers varies between 0-75% after 2 minutes of acute rapid stimulation, it was important to investigate possible temporal correlations between extracellular $[Ca^{++}]$ depletion and the peak twitch tension during trains of action potentials (tension staircase).

When the heart rate was increased from 6 to 30 per minute (in 0.20 mM $[Ca^{++}]$ Ringers) a biphasic twitch tension staircase occurred (figure 27, top panel). The twitch tension fell by 30% in 15-30 seconds and thereafter slowly increased over the next 26.5 minutes to 2.8 times control twitch tension. At 2 minutes time twitch tension was similar to control.

The large increase in twitch tension observed in figure 27 (top panel) was reduced when the increment in heart rate was reduced. In figure 27

(middle panel), heart rate was increased from 6 to 12 per minute (rather than 30) for 27 minutes. At steady state, the twitch tension at 12 per minute was the same as observed at 6 per minute. There was a negative tension staircase for about 14 minutes. The maximum twitch tension depression was 20% and occurred in the first 20 seconds of the trial. After 27 minutes, the heart rate was returned to 6 per minute. In about 20 seconds, twitch tension was increased by 22% over the control twitch tension. The tension overshoot then decayed by 63% in about 7 minutes. Thus, at a low heart rate where the positive inotropic effect of repetitive stimulation was minor, the isometric twitch tension time course seemed to parallel the time course of extracellular calcium ion concentration depletion. The magnitude of the change in tension during its depression and overshoot (20, and 22%) were similar to each other and to the % change in the extracellular calcium ion concentration observed in this size ventricular muscle strip at heart rate 12 per minute (see figure 10). It should be noted that the action potential duration did not shorten in 0.20 mM Ca^{++} Ringers since heart rate was changed between 0-30 per minute. The presence of a frog ventricular muscle negative twitch tension staircase was first reported by Brown and Orkand (1968) for strips superfused in low Ca^{++} Ringers.

Figure 27: Top record is the isometric twitch tension of a frog ventricular muscle strip as the heart rate (at the arrow) was increased from 6 to 30 per minute. Strip is in 0.20 mM Ca^{++}Ringers. A biphasic twitch tension staircase is seen. Final twitch tension at 27 minutes was sketched in ink and was 2.8 times tension at 6 per minute. Maximum depression of twitch tension at 30 beats per minute was 30% and occurred in 15-30 seconds. Tension at 30 per minute was more negative than control only for the first 2 minutes of the high rate of stimulation.

Middle record is the isometric tension of the strip bathed in 0.20 mM Ca^{++}Ringers. When the muscle strip heart rate was increased from 6 to 12 per minute a negative tension staircase was seen. The minimum tension occurred at 20 seconds and maximum tension depression was 20%. Tension returned to control only after 14 minutes. Stimulation was maintained for 27 minutes, but tension never exceeded control.

Bottom records shows the effect of reversal of the rate of stimulation (from 12 to 6 per minute) after 27 minutes of beatings (follows middle record). Tension overshoots the steady state level by 22% about 20 seconds after the heart rate change. Tension was elevated for more 10 minutes. The tension overshoot had decayed by 63% in 7 minutes. In none of the isometric tension studies was there any depression or increase in baseline tension causally related to these changes in twitch tension. For all the records shown the muscle strip was equilibrated at about 150% of it resting length before the experiment.

FROG VENTRICULAR MUSCLE TWITCH TENSION

- EFFECT OF HEART RATE CHANGE -

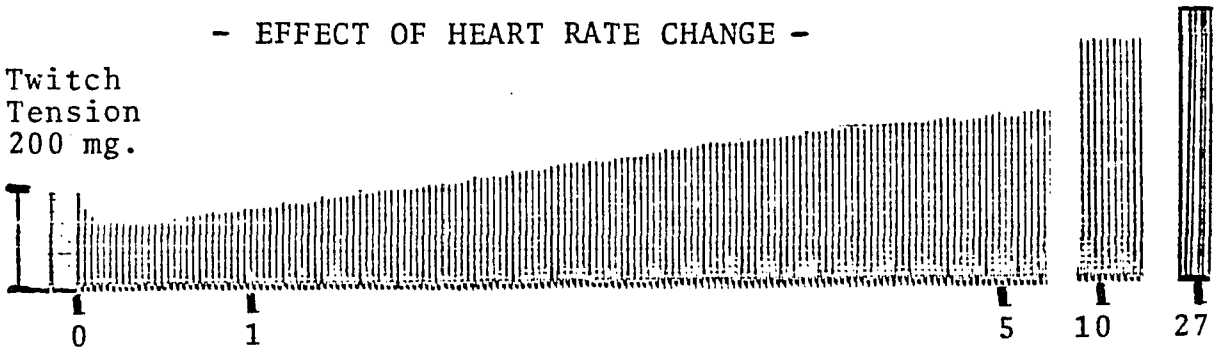

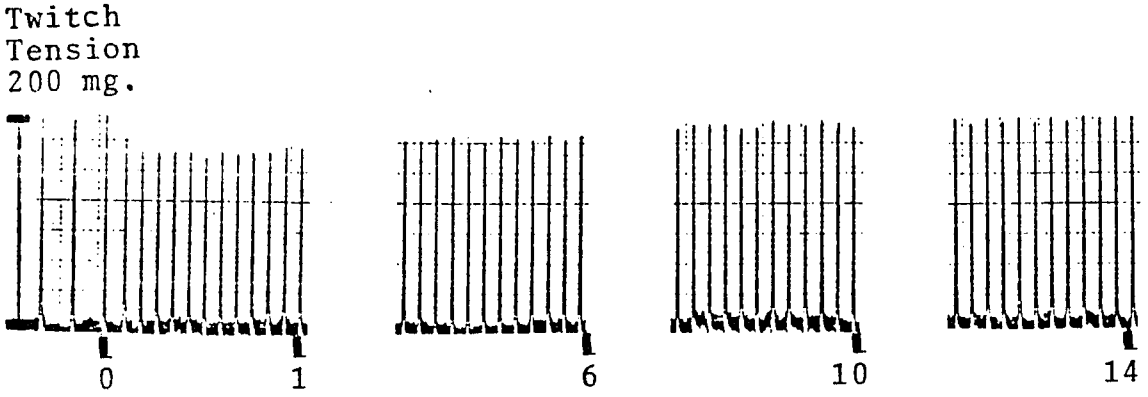

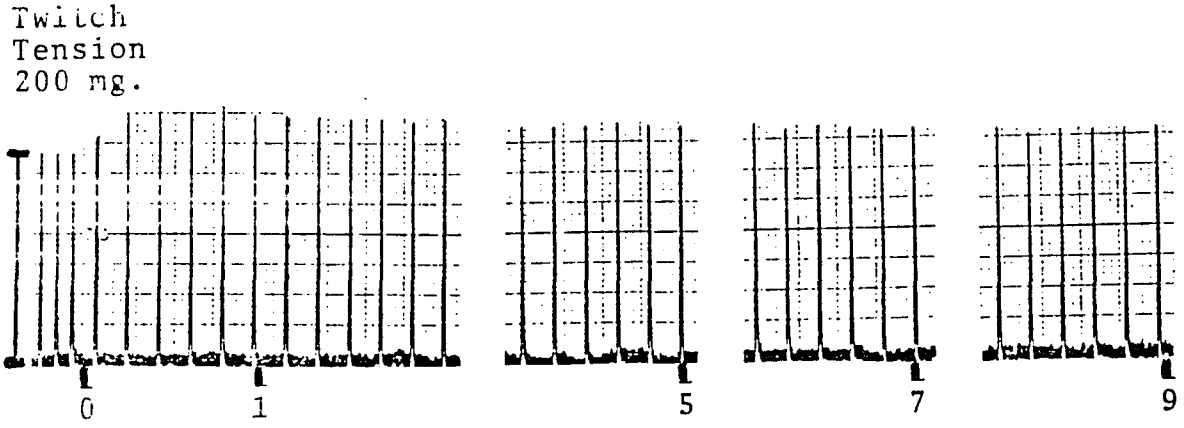

TIME (MINUTES) ⟶

IV ANALYSIS SECTION

Analysis of the experimental data was accomplished with equations developed with Dr. Richard Kline. Since the application of these equations to extracellular $[Ca^{++}]$ depletion in frog ventricle has not been reported, their derivation is described.

There are three distinct extracellular spaces in frog ventricle (see figure 28). The interfibrillar space (IFS) lies immediately external to the cardiac muscle cell membrane. Clusters of muscle cells are surrounded by a subendothelial space (SES). A step change in the SES $[Ca^{++}]_o$ equilibrates in the IFS with an estimated time constant (Ti) of 250 milliseconds. The SES is surrounded by a sheath of endothelial cells which are a diffusion barrier and delineate each ventricular muscle trabeculum. Muscle trabeculum are separated from each other by extratrabecular space (ETS). A step change in the ETS $[Ca^{++}]$ equilibrates in the SES with a time constant of several seconds. A step change in the bath $[Ca^{++}]$ equilibrates in the ETS of a 1 millimeter diameter muscle strip in about 20 minutes (see figure 4). For further details see section A of Discussion . This topic was also discussed by Cohen & Kline (1982) for extracellular $[K^{+}]$ equilibrium in frog ventricle.

A. Calculation of Subendothelial Space Vo Amplitude

It is important to know the amplitude of the extracellular action potential (Vo) in the subendothelial space (see figure 28). The absence or presence of a Vo helps to indicate the location of the Ca^{++} ion selective microelectrode tip.

The amplitude of the Vo is calculated as follows.

The terms are:

τs = Subendothelial space diffusion time constant (in seconds).
Vo = Extracellular action potential amplitude (in millivolts).
Vm = Action potential amplitude (in millivolts).
Rm = Total ventricular membrane resistence (in ohms).
Rsh = Trabecular endothelial sheath resistence (in ohms).
$D_{Ca^{++}}$ = Ca^{++} diffusion coefficient in free solution (Wang, 1953).
A = Total endothelial cleft area for diffusion.
S = Interendothelial cell cleft length for diffusion.
Vs = Subendothelial space volume.
p = Extracellular fluid resistivity (Chapman & Fry, 1978).
Z = Trabecular axial length.
D_T = Trabecular diameter (in microns).
R* = Ventricular membrane resistence x Membrane area.
$D_{T'}$ = Subendothelial muscle cell core diameter (in microns).
Am = Total cell membrane area.
Dc = Average frog ventricular cell diameter (in microns).
C_{SES} = $[Ca^{++}]$ in the subendothelial space.
C_{ETS} = $[Ca^{++}]$ in the extratrabecular space.
75 = % cellular tissue space (Page & Niedergerke, 1972).
85 = % trabecular space (Page & Niedergerke, 1972).

Assuming that the potential is distributed proportionally with the resistence of each segment in the path:

$$Vm/Rm = Vo/Rsh \text{ and thus } Vo = Vm \times Rsh/Rm.$$

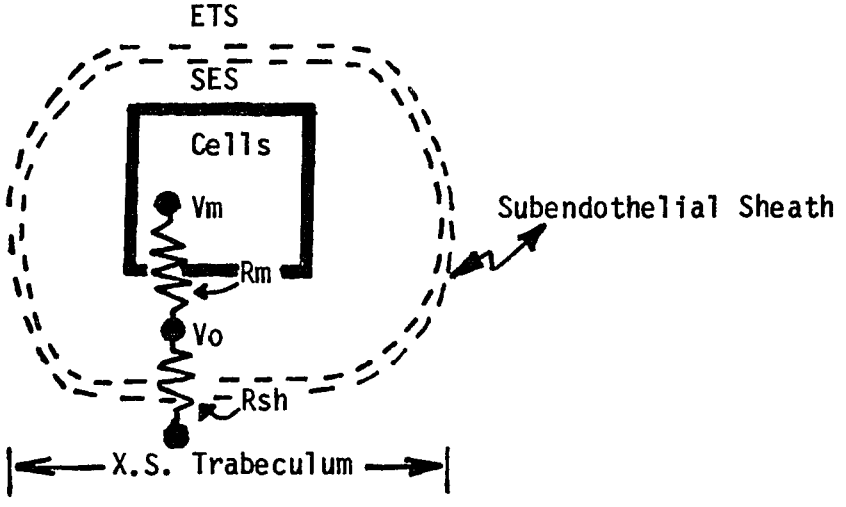

Since the diffusion time constant of the sheath (τ_s) is known, we use it to calculate Rsh.

$d(C_{SES})/dt = -(1/\tau_s) \times (C_{SES}-C_{ETS})$ and $\tau_s = S \times Vs/(D_{Ca^{++}} \times A)$, (Page & Niedergerke, 1972).

By applying Ohm's law to this three dimensional case:

$Rsh = S \times p/A$ and we see that Rsh and τ_s are related through the term S/A since $S/A = (\tau_s \times D_{Ca^{++}})/Vs = Rsh/p$.

Hence, $Rsh = \tau_s \times D_{Ca^{++}} \times p/Vs$.

All the variables in the equation above are known except Vs which is obtained from knowing that Vs = Trabecular volume - Cellular volume

$$= \pi \times Z \times [(D_T/2)^2 - (D_{T'}/2)^2].$$

Thus, $Rsh = \tau_s \times D_{Ca^{++}} \times p/\pi \times Z \times [1/4 (D_T2 - D_{T'}2)]$.

The calculation of Rm is based upon the following relations: $Rm = R^*/Am$, where Am = (surface area/cell of length Z) x (cells/trabeculum in cross section) and R^* = (membrane resistance). Frog ventricular cells are long and narrow with little membrane area abutting at the ends (Page & Niedergerke, 1972). It is a good approximation of the cell membrane area to treat the cells as cylinders with negligable area at the ends.

Hence, $Am = (\pi \times Z \times Dc) \times$ (cells/trabeculum in cross section).

The cells per trabeculum/cross section can be obtained from the following equivalent:

The $\frac{\text{(cellular cross-sectional area/trabeculum)}}{\text{(cross-sectional area/cell)}}$ = the cells per trabeculum, in cross-section where the cellular cross-sectional area/trabeculum is obtained from knowing that it is 75/85ths of the cross-sectional area of a trabeculum (Page & Niedergerke, 1972).

Thus, the $\frac{\%\text{ cellular tissue space}}{\%\text{trabecular tissue space}} \times \frac{\text{crossectional area}}{\text{trabeculum}}$

$$= 75/85 \times (\pi/4)\, D_T{}^2.$$

Since the single cell cross-sectional area = $(\pi/4)\, Dc^2$, then combining the last two equations one obtains the number of frog ventricular cells/trabecular cross section:

$$[(75/85) \times (\pi/4)\, D_T{}^2]/[(\pi/4)\, Dc^2]$$

$$= (75/85) \times (D_T/Dc)^2.$$

Multiplying the surface area per cell by the cells per trabecular cross-section one obtains Am as follows:

$$Am = (\pi \times Z \times Dc) \times (75/85) \times (D_T/Dc)^2$$

$$= \pi \times Z \times 75/85 \times (D_T)^2/Dc.$$

Since Rm equals R* divided by Am then one obtains that:

$$Rm = R^* \times (85/75) \times Dc/[\pi \times Z \times (D_T)^2].$$

Knowing now Rm and Rsh and (Vm; experimentally) one can calculate Vo from the following: Vo = Vm x Rsh/Rm

$$= \frac{Vm \times [\tau s \times D_{Ca}{}^{++} \times p/(\pi \times Z/4 \times (D_T 2 - D_T{}'2))]}{R^* \times 85/75 \times Dc/(\pi \times Z \times D_T 2)}$$

$$= (3.5 \times Vm \times \tau s \times D_{Ca}{}^{++} \times p \times (D_T)^2)/$$

$$(R^* \times Dc \times [(D_T)^2 - (D_T{}')^2]).$$

Now plugging in actual values for the variables allows an estimation of Vo:

Let.. Vm = 130 millivolts
$D_{Ca}{}^{++}$= 8×10^{-6} cm.^{2}/sec. (Wang, 1953).
p = 70 ohm-cm (Chapman & Fry, 1978).
D_T = 49 microns (Page & Niedergerke, 1972).
R* = 4000 ohm-cm^2 (Chapman & Fry, 1978).
Dc = 5×10^{-4} cm. (Page & Niedergerke, 1972).
$D_T{}'$ = 46 microns (Page & Niedergerke, 1972).
τs = 1.6 to 3.4 seconds (Page & Niedergerke, 1972), (see section E of Analysis).

Hence: $Vo = 3.5 \times 130 \times (8 \times 10^{-6}) \times 70 \times Ts \times (49)^2 /$

$(4000 \times (5 \times 10^{-4}) \times [(49)^2 - (46)^2])$

= 2 to 4 millivolts.

The Ca^{++} ion selective microelectrode attains 80% response to an electrical square pulse in one second. Therefore only 80% of the 2 to 4 millivolts Vo should be detected during a one second action potential. Less than a one millivolt Vo (the instanteous jump following the stimulus artifact) is evident in figure 5 and 6 (top panel). See section C-5 of Methods for precautions in the interpretation of the Vo magnitude. Kline (1975) has measured Vo magnitudes of 5 millivolts in the subendothelial space.

B. Magnitude of Interfibrillar Space $[Ca^{++}]$ Depletion per Beat

The Ca^{++} ion selective microelectrode response time is slow (time constant is 0.3 to 0.6 seconds). Thus we probably underestimate the magnitude of the subendothelial space and interfibrillar space beat to beat $[Ca^{++}]$ depletions. The data of figure 5 and 6 (top panel) suggest experimentally that beat to beat $[Ca^{++}]_o$ depletions of 50 to 60 micromolar occur. The expected magnitude of the interfibrillar space beat to beat $[Ca^{++}]$ depletions can also be calculated from the characteristics of the extratrabecular space $[Ca^{++}]$ depletion. These calculations support our experimental findings. We have measured the depletions in the extratrabecular space (ETS) and know from Page & Niedergerke (1972) the dimensional and membrane surface area to volume ratio of this space. From analogous solutions to the heat equation (Carslaw & Jaeger, 1959, page 204, equation 7.9.1) we can extrapolate to the depletions in any other extracellular space, from the geometry and

surface area to volume ratio of that space, in this case the interfibrillar space (IFS). Since we know that all the Ca^{++} flux leaving the ETS was first removed from the IFS, the rapid depletions of $[Ca^{++}]$ in the IFS should relate to the ETS depletions we measure as follows:

1) The Ca^{++} flux (M) per extracellular volume is proportional to the surface area to volume ratio of the space. At steady state the Ca^{++} flux per surface area $M_{IFS} \propto M_{ETS}$ where $M = \Delta [Ca^{++}]_o \times V$ and $\Delta [Ca^{++}]_{IFS} \times V_{IFS} \propto \Delta [Ca^{++}]_{ETS} \times V_{ETS}$, and hence $\Delta [Ca^{++}]_{IFS} \propto \Delta [Ca^{++}]_{ETS} \times (V_{ETS}/V_{IFS})$. $(V_{ETS}/V_{IFS}) = 26$ (Page & Niedergerke, 1972).

2) The magnitude of the final $[Ca^{++}]_o$ depletion is proportional to the time constant of the time course of the depletion. From the solution to the standard single compartment diffusion equation:
$\Delta [Ca^{++}]_{(t)} = J_T \tau (1-EXP(-t/\tau)$, (Page & Niedergerke, 1972).
$[Ca^{++}]_{(t=3\tau)} \cong J_T \tau$ and since $\tau \propto$ (compartmental radius)^2, (Carslaw & Jaeger, 1959, eqn. 7.9.1.) and $\tau \propto$ (the tortuosity)^2, (Nicholson, 1980).

$\Delta [Ca^{++}]_{(t=3\tau)} \propto [\text{radius} \times \text{(the tortuosity)}]^2$. The time constant of the ETS and IFS are Te and Ti respectively.

3) Although we assumed that the transmembrane Ca^{++} flux was continuous in our ETS model, in actuality it only occurs during the action potential. Thus to get the appropriate IFS Ca^{++} flux which causes depletion during a single action potential, we must multiply our time averaged ETS flux by the ratio of the stimulus interval (S.I.) to

the action potential duration (APD).

Thus, $M_{IFS}{}_{(t=3\tau_i)} \propto M_{ETS}{}_{(t=3\tau_e)} \times \frac{S.I.}{A.P.D.}$ since APD was constant in the range of % time deplorization (0-40%) employed in this calculation (see figure 11). The S.I. $\times \Delta [Ca^{++}]_{ETS}{}_{(t=3\tau_e)}$ = constant for % time deplorizations up to 40% (see figure 11).

Combining equations from steps 1, 2, and 3:

$$\Delta [Ca^{++}]_{IFS}{}_{(t=3\tau_i)} \propto \Delta [Ca^{++}]_{ETS}{}_{(t=3\tau_e)} \times \frac{V_{ETS}}{V_{IFS}} \text{ since } A_{IFS} = A_{ETS}$$

for compartmental flux exchange and since radius $_{IFS} \neq$ radius$_{ETS}$ and $@_{IFS} \neq @_{ETS}$, then

$$\Delta [Ca^{++}]_{IFS}{}_{(t=3\tau_i)} \propto \Delta [Ca^{++}]_{ETS}{}_{(t=3\tau_e)} \times \frac{V_{ETS}}{V_{IFS}} \times \left(\frac{r_{IFS} \times @_{IFS}}{r_{ETS} \times @_{ETS}}\right)^2 \text{ and}$$

Since the flux from the IFS into cells occurred only during the action potentials then;

$$\Delta [Ca^{++}]_{IFS}{}_{(t=3\tau_i)} = \Delta [Ca^{++}]_{ETS}{}_{(t=3\tau_e)} \times \frac{V_{ETS}}{V_{IFS}} \times \left(\frac{r_{IFS} \times @_{IFS}}{r_{ETS} \times @_{ETS}}\right)^2 \times \frac{S.I.}{A.P.D.}$$

Using this formula we estimated the average steady state $[Ca^{++}]$ depletion in the interfibrillar space from experimental data and the anatomical data of Page & Niedegerke (1972).

a.) In 0.050 mM Ca^{++}Ringer:

The change in the $[Ca^{++}]_{ETS}(t = 3\tau_e)$ = 9 micromolar.
Action potential duration = 950 milliseconds.
Stimulus interval = 20 seconds.
(Extracellular space volume/Interfibrillar space volume) = 26.
The radius of the interfibrillar space = 23 microns.
The radius of the extracellular space = 500 microns.
The tortuosity (@) of the extratrabecular space is 1.0.
The tortuosity (@) of the interfibrillar space is 1.5.

Thus, the IFS $[Ca^{++}]$ depletion = $9 \times (20/0.95) \times 26 \times (23 \times 1.5/500)^2$

= <u>23 micromolar</u>.

b.) In 0.20 mM Ca^{++}Ringers:

The change in $[Ca^{++}]_{ETS}(t = 3\tau e)$ = 23 micromolar.
The action potential duration = 900 milliseconds.
The stimulus interval = 20 seconds.
All other variable are the same as above in a.).

Thus, the IFS $[Ca^{++}]$ depletion = 22 x (20/0.90) x 26 x $(23 \times 1.5/500)^2$.

= 64 micromolar.

c.) In 1.0 mM Ca^{++}Ringers:

The change in $[Ca^{++}]_{ETS}(t = 3\tau e)$ = 320 micromolar.
The action potential duration = 800 milliseconds.
The stimulus interval = 5 seconds.
All other variables are the same as above in a.).

Thus, the IFS $[Ca^{++}]$ depletion = 320 x (5/0.80) x 26 x $(23 \times 1.5/500)^2$

= 250 micromolar.

Hence, in 0.20 mM Ca^{++}Ringers, after an ETS $[Ca^{++}]$ depletion of 75% (0.20 mM to 0.050 mM $[Ca^{++}]$) the beat to beat IFS $[Ca^{++}]$ depletion will have decreased from 64 to 23 micromolar. A decrease in the beat to beat $[Ca^{++}]_o$ depletion magnitude during large ETS $[Ca^{++}]$ depletions was experimentally observed.

There are two sources of error in the estimation of IFS $[Ca^{++}]$ depletion.

1.) If the tip of the Ca^{++} ion selective microelectrode was at 1/2 radius depth in the muscle strip instead of 1 radius depth as estimated during the experiment, then the IFS $[Ca^{++}]$ depletion is underestimated by 33%, (Carslaw & Jaeger, 1959, eqn. 7.9.1.).

2.) The maximum possible overestimation of the IFS depletion is when the tortuosity of the IFS is maximum and the tortuosity of the ETS is minimum. Letting the IFS = $\pi/2$ = 1.57 and the ETS = 1.0, then the maximal tortuosity factor is 246% of the minimum factor (Kline, 1975).

C. Change in the ETS $[Ca^{++}]$ Depletion Time Course Time Constant

The magnitude of the ETS $[Ca^{++}]$ depletion in ventricular muscle strips is not proportional to the % time membrane depolarization at high heart rates (see figure 11) however, final magnitudes of depletion appear to have saturated. The time constant of the time course of $[Ca^{++}]_o$ depletion also decreased at high heart rates (figure 12). Both results could be explained by proposing that the $[Ca^{++}]_o$ depletion causes a decrease in the transmembrane Ca^{++} influx during the rapid stimulation. This relationship will be derived below using a 3 compartment model (Attwell, Eisner, & Cohen; 1979).

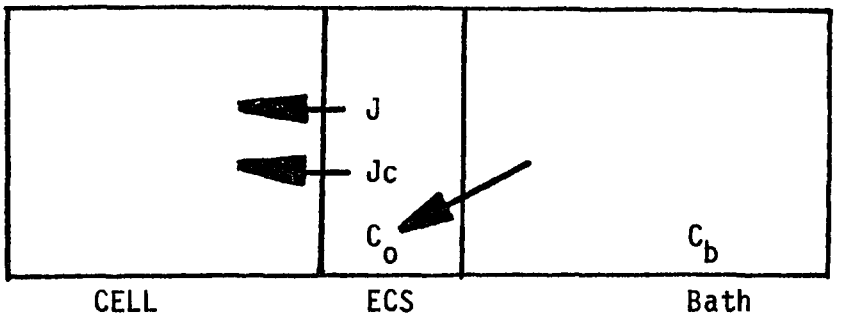

The cellular Ca^{++} influx will be assumed to depend upon two variables, the heart rate and the extracellular $[Ca^{++}]$. The free cytoplasmic $[Ca^{++}]$ is assumed essentially not changed since basal tension did not increase (see figure 27), thus there is always a lower $[Ca^{++}]$ inside the cell relative to outside.

The new terms are:

J = cellular Ca^{++} influx that varies with heart rate.
J_c = cellular Ca^{++} influx that varies with the extracellular $[Ca^{++}]$.
C_o = the extracellular $[Ca^{++}]$.
C_b = the bath $[Ca^{++}]$.
τe = time constant of ETS $[Ca^{++}]$ equilibrium.

This same case is treated in Carslaw & Jaeger (1959) for a cylinder and with the same qualitative conclusions (see page 405, equation 15.7.13). We will outline the one dimensional treatment below to show that the time constant and magnitude of the depletion change by the same amount. The rate of change of C_o depends on both the flux terms and diffusion.

Thus, $dC_o/dt = -1/\tau e\ (C_o - C_b) + J_c C_o + J.$

If $J_c = 0$ and then

$$dC_o/dt = -(1/\tau e)\ C_o + (J + C_b/\tau e).$$

The solution for this depletion is:

$$C_o(t) = C_b - J\tau e\ [1 - Exp\ (-t/\tau e)].$$

If j_c does not equal 0, then the equation becomes

$$dC_o/dt = [J_c - 1/\tau e]\ C_o + (J + C_b/\tau e).$$

This equation is analogous to the equation above it except that the coefficient multiplying C_o has been changed from $-1/\tau e$ to $[J_c - 1/\tau e]$ or $-[1/\tau e - J_c]$.

This then changes the solution to:

$$C_o(t) = C_b - [J/(1/\tau_e - J_c)] \times [1-EXP\ (-t[1/\tau_e - J_c])].$$

Thus, the new time constant is smaller by a factor of $[1/\tau_e]/[1/\tau_e - J_c]$. The final depletion is smaller by the same amount. In cylinderical coordinates, this is shown by Carslaw & Jaeger (1959) 15.7.13. .

D. The Instantaneous Rate of Cellular $[Ca^{++}]$ Accumulation in a Cylindrical Frog Ventricular Muscle Strip

The extracellular space of a frog ventricular strip can be modeled to approximate a long cylinder in which the muscle cells are homogeneously dispersed to occupy about 75% of the cylindrical volume. The cells, clustered as trabecula, increase the tortuosity of the extracellular space but do not alter the basic equation of diffusion in cylindrical coordinates. For simplicity the frog ventricular strip is modeled to have radial $[Ca^{++}]_o$ gradients but no azimuthal and no axial $[Ca^{++}]_o$ gradient. The cells throughout the cylinder are assumed to uniformly take up and release Ca^{++}. The $[Ca^{++}]_o$ at the surface of the cylinder is maintained at a constant concentration (Cb). The $[Ca^{++}]_o$ in the ETS at steady state is used in the model to reflect the $[Ca^{++}]_o$ of the extracellular space (a one compartment model) although the SES and IFS $[Ca^{++}]_o$ are always slightly lower during prolonged repetitive stimulation (see figure 29). In the model the $[Ca^{++}]_o$ in the cylinder equilibrates to have a steady state radial dependence. Maximal $[Ca^{++}]_o$ depletion occurs at the center axis of

the cylinder. The $[Ca^{++}]_o$ depletion at the surface of the cylinder is zero.

The diffusion equation for radial $[Ca^{++}]_o$ equilibrium in cylindrical coordinates at steady state is:

$$D_{Ca^{++}} \left(\frac{\partial^2 Co}{\partial r^2} + \frac{1}{r}\frac{\partial Co}{\partial r}\right) - J_T = 0$$

where J_T = instantaneous decrease in Co due to net Ca^{++} up take into the cells (Co = $[Ca^{++}]_o$ in the cylinder).
$D_{Ca^{++}}$ = diffusion coefficient of Ca^{++} in aqueous solution.
r = cylindrical radius.

The boundary conditions are that the $[Ca^{++}]_o$ at the surface of the cylinder is constantly maintained at Cb.

At steady state the equation for the Co in the cylinder is analogous to the equation for a model for constant heat generation in a long cylinder with zero, constant surface temperature (Carslaw & Jaeger, 1959, equation 7.2.17). This steady state heat equation is: $V = \frac{Ao}{K} \times \frac{a^2 - r^2}{4}$

where V = temperature (analogous to Cb - Co).
Ao = rate of heat generation (analogous to J_T).
K = thermal conductivity (analogous to $D_{Ca^{++}}$, Carslaw & Jaeger, 1959, page 28).
a = cylindrical radius.
r = radial position such that r=o at the center and r=a at the surface of the cylinder.

The analogous equation for extracellular $[Ca^{++}]$ diffusional equilibrium in a cylinder of frog ventricle during constant Ca^{++} uptake by the muscle cells is:

$$-(Cb - Co) = \frac{J_T}{D_{Ca^{++}}} \times \frac{(a^2 - r^2)}{4}$$ and at the center of the cylinder

where Co was measured at r=o, so that

$$-(Cb - Co) = \frac{J_T \times (a^2/4)}{D_{Ca^{++}}}.$$

The heat equation time dependent term is (Carslaw & Jaegar, 1959, equation 7.9.1):

$$-\frac{2\,Ao}{aK}\sum_{n=1}^{\infty}\left(\exp\left[(-K\alpha_n^2 t)\,\frac{J_o(r\alpha n)}{\alpha_n^3\,J_1(a\alpha n)}\right]\right)$$

where αn are the positive roots of $Jo\,(a\alpha) = 0$.
The initial and final surface temperature = 0 and $Co = C_b$ at $t = 0$.
The time constant of the major component (1st Bessel term) for r=0 is:

$= a^2/(K \times (2.4048)^2)$ hence $a^2/K = \tau \times (2.4048)^2$.

The analogous relationship for extracellular $[Ca^{++}]$ diffusion in the frog cylinder is: $\tau \times (2.4048)^2 = a^2/D_{Ca^{++}}$. The second term of the time-dependent heat equation was examined and it did not alter the results significantly.

$-(Cb - Co) \times 4/J_T = a^2/D_{Ca^{++}} = \tau \times (2.4048)^2$ hence

$$J_T = \frac{-(Cb - Co) \times 4}{\tau \times (2.4048)^2} = \frac{-(Cb - Co)}{\tau \times 1.45}$$

To obtain J_T/second, the time averaged ETS Ca^{++} flux is multiplied by the stimulus interval/action potential duration. Thus the average instantaneous extracellular space $[Ca^{++}]$ change per second during an action potential, induced by the influx is given by:

$$J_T = \frac{\text{The change in } [Ca^{++}] \text{ ETS} \times \text{S.I.}}{\text{Tau}_{obs} \times 1.45 \qquad \text{APD.}}$$

The terms are:

J_T = Extracellular rate of change of $[Ca^{++}]$.
$[Ca^{++}]$ = The extracellular Ca^{++} concentration.
Tau_{obs} = Observed time constant of depletion time course (τ).
1.45 = (The first root of the Bessel function.)^2/4
S.I. = Stimulus Interval.
APD = Action Potential Duration.
3 = The intracellular:extracellular volume ratio.

The extracellular [Ca^{++}] depletion is assumed to result from Ca^{++} ion entry into cells. Thus, the average instanteous cellular [Ca^{++}] accumulation per second ([Ca^{++}]i/second) = $J_T/3$, and is obtained simply by multiplying the inverse volume ratio of the spaces by J_T. We now plug experimental values from the data for multiple trials. Specifically we had to obtain i) the change in the ETS [Ca^{++}], ii) the observed time constant calculated by the Prophet computer "Expfit" Subroutine, iii) the stimulus interval, and iv) the action potential duration.

In 0.050 mM Ca^{++} Ringers the $[Ca^{++}]_i$/second = 0.6 $\pm$ 0.1 micromolar, (n = 14).

In 0.20 mM Ca^{++} Ringers the $[Ca^{++}]_i$/second = 1.9 $\pm$ 0.4 micromolar, (n = 15).

In 1.0 mM Ca^{++} Ringers the $[Ca^{++}]_i$/second = 7.9 $\pm$ 0.9 micromolar, (n = 5).

The average instantaneous net transmembrane Ca^{++} ion flux in picomoles/cm^2/second can be calculated. The surface area/liter of frog ventricular cells is about 1 $micron^{-1}$ (or 10^{15} $microns^2/10^{15}$ $microns^3$), (Page & Niedergerke, 1972). One picomole/cm^2 is equivalent to 10^{-12} moles/10^8 $microns^2$ (or 10^{-5} moles/10^{15} $microns^2$). Hence, each picomole/cm^2 of ion flux will cause a 10 micromolar cytoplasmic [Ion] increase. Thus, in 0.050 to 1.0 mM Ca^{++} Ringers, a 0.5 to 8.8 micromolar cytosolic [Ca^{++}] increase/second can occur by a 0.05 to 0.88 picomole/cm^2/second net Ca^{++} influx. The inverse of Faraday's constant, 1/(96,487 coulombs/mole) = 10^{-5} moles per coulomb. (or ten picomoles/10^{-6} coulombs/second). Hence, 10 picomoles/second of monovalent cations is a 1 microampere inward current. In the case of Ca^{++}, a picomole/cm^2/second flux is 0.2 microampere/cm^2 (or 200 nanoamperes/cm^2) inward current. Therefore,

the instantaneous average Ca^{++} current in 0.050 to 1.0 mM Ca^{++} Ringers would be 10-170 nanoamperes/cm^2 (assuming Ca^{++} influx occurs entirely via Ca^{++} channels).

In frog atrial trabecula a calcium and sodium current has been measured which has a magnitude of 3 to 4 microamperes/cm^2 and a duration of about 20 to 50 millseconds in 1.8 Ca^{++} Ringers (Fischmeister & Horackova, 1983). If this current flux had occurred over a second (3.5 uA/cm^2/50 msec to 3.5 uA/cm^2/20 msec = 0.07-0.18 uA/cm^2), then its flux would be similar to the current magnitude of this study. Due to the slow response rate of the Ca^{++} ion selective microelectrode, the actual duration of the transmembrane Ca^{++} flux could not be quanitatively established. However, the consistent synchronization of the termination of the beat to beat extracellular [Ca^{++}] depletions with the end of the action potential plateau strongly suggests that the Ca^{++} influx persists during the entire action potential plateau.

E. Instantaneous and Steady State Subendothelial Space [Ca^{++}] Depletion

The subendothelial space (SES) is 3 microns wide on the average, and surrounds the trabecular core of muscle cells (Page & Niedergerke, 1972). It is surrounded by the trabecular endothelial cell sheath which is the outer most border of each trabeculum. Changes in the instantaneous extracellular [Ca^{++}]/second are larger in the SES versus ETS by 26/10 (the extracellular space:SES volume ratio). The endothelial sheath delays ion diffusion equilibrium between the ETS and SES with time constant Ts. The change in the $[Ca^{++}]_{SES}$ over time is:

$$[Ca^{++}]_{SES(t)} = (J_T) \times 2.6 \times Ts \times [1 - EXP(-t/Ts)].$$

The mean τ_s was estimated to be 3.3 $\pm$ 1.2 seconds by Page & Niedergerke, (1972) who suggested that their estimate was too high by 20 to 30%. So a mean τ_s of 2.5 $\pm$ 0.9 seconds was used here and in section A of Analysis. Page and Niedergerke (1972) found great histological variability in frog ventricle. The estimated τ_s ranged from 0.3 to 4 seconds. In one second $[Ca^{++}]_{SES} = 2.14\ J_T$ (where J_T was determined in Analysis section D). After one second the $[Ca^{++}]$ depletion magnitude in the SES would be -4, -12, and -49 micromolar lower than the respective ETS $[Ca^{++}]$s of 0.050, 0.20, and 1.0 mM Ca^{++}Ringers.

At steady state, $[1 - EXP(-t/\tau_s)] = 1$. This occurs in about 4 time constants or 10 seconds on the average.

$$\text{The } [Ca^{++}]_{SES,\ (t=10\ \text{seconds})} = 2.6 \times J_T \times \tau_s = 6.5\ J_T.$$

Therefore, the steady state SES $[Ca^{++}]$ depletion is -12, -37, and -150 micromolar lower than the respective ETS $[Ca^{++}]$s of 0.050, 0.20, and 1.0 mM Ca^{++} Ringers. But this would only occur during a voltage clamp or high $[K^+]_o$ contracture since the action potential duration is approximately 1 second.

A table summarizing the estimated changes in the extracellular $[Ca^{++}]$ in the ETS, SES, and IFS is shown below for 1 millimeter diameter frog ventricular strips. The data was determined for times 1, 10 and 240 seconds following initiation of rapid repetitive stimulation with 0.050, 0.20, and 1.0 mM Ca^{++} Ringers. This data is plotted in figure 29.

Time (seconds)	Bath $[Ca^{++}]$	Maximum ETS $[Ca^{++}]$ depletion	Maximum SES $[Ca^{++}]$ depletion	Maximum IFS $[Ca^{++}]$ depletion
1	50	-1 (49)	-4 (45)	-23 (22)
1	200	-4 (196)	-12 (184)	-64 (120)
1	1000	-6 (994)	-50 (944)	-250 (694)
10	50	-6 (44)	-12 (32)	-14 (18)
10	200	-24 (176)	-37 (139)	-44 (95)
10	1000	-50 (950)	-150 (800)	-225 (575)
240	50	-42 (8)	-2 (6)	-3 (3)
240	200	-160 (40)	-7 (33)	-11 (22)
240	1000	-320 (680)	-100 (580)	-145 (435)

In the above table, all $[Ca^{++}]$ are micromolar. In the 3 columns labeled Maximum ETS, Maximum SES, and Maximum IFS, the bracketed numbers are the extracellular $[Ca^{++}]$ in the space at the respective time. The number listed in each of the three columns, to the left of the bracketed number, is the $[Ca^{++}]_o$ gradient between that column's space and the column to its left. The table's numbers were determined as follows: 1) The listed maximal ETS $[Ca^{++}]$ depletions after 240 seconds of rapid stimulation are experimental observations. At 1 to 10 seconds time the ETS $[Ca^{++}]$ depletions are (1-EXP-1/60) = 0.02 and (1-EXP-10/60) = 0.15 fractions of the maximal ETS $[Ca^{++}]$ depletion. 2) The SES $[Ca^{++}]$ gradient at 10 seconds time was calculated in Analysis sections D and E

from experimental data. At 1 second the SES [Ca^{++}] gradient is (1 - Exp -1/2.5) = 0.33 fraction of the 10 second SES [Ca^{++}] gradient. At 240 seconds, the SES [Ca^{++}] gradient is assumed to be the product of the 10 second SES [Ca^{++}] gradient and the % ETS [Ca^{++}] depletion. 3) The IFS [Ca^{++}] gradient at 1 second was calculated in Analysis Section C from experimental data. The IFS [Ca^{++}] gradient at 10 and 240 seconds is assumed to be the product of the 1 second IFS [Ca^{++}] gradient and the % SES [Ca^{++}] depletion at 10 and 240 seconds time.

V DISCUSSION

The variations in the calcium ion concentration of the extracellular spaces in beating frog ventricular muscle strips were studied using Ca^{++} ion selective microelectrodes. Experimental protocols known to cause muscle contraction, also caused significant transient or prolonged extracellular calcium ion depletion depending upon the extracellular location. Extracellular $[Ca^{++}]$ depletion measurements were used to develop a mechanistic model of extracellular $[Ca^{++}]$ depletion based on upon frog ventricle histology. The membrane transport of Ca^{++} was studied using this model.

A. Mechanism of Extracellular $[Ca^{++}]$ Depletion

The extracellular space of the frog ventricle has been studied in detail using electron microscopy by Page and Niedergerke (1972). They described three distinct extracellular compartments: the interfibrillar space (IFS), subendothelial space (SES), and extratrabecular space (ETS) which are found in series between the muscle cell membrane, and the fluid outside the wall of the ventricle. This is depicted in figure 28. The SES and ETS $[Ca^{++}]$ progressively equilibrate by simple diffusion in response to the lowering (depletion) of the $[Ca^{++}]$ in the IFS. The IFS is the immediate extracellular Ca^{++} source to most of the muscle cell membranes. Comprising 4% of the extracellular space, the IFS is formed by the apposition of bordering ventricular muscle cells. As a consequence the IFS is 0.01 to 1 micron wide and tortuous. The sausage-shaped muscle cells are packed, 10 to 100 per trabecula and occupy 74% of the tissue volume. During the action potential the cells accumulate Ca^{++}

Figure 28: Based upon observations of Page and Niedergerke (1972) four drawings of frog ventricular anatomy are presented in cross-section to the long axis of the muscle cells.

In the upper left panel the contour of a 1 millimeter frog ventricular muscle strip is shown.

In the upper right panel is shown a small region of the muscle strip with the extratrabecular space (ETS: extracellular space surrounding muscle trabecula). Note the variability of clefts and trabecular shapes.

Lower left panel shows a single trabecula with a sheath of porous endothelial cells. The shaded region is the subendothelial space (SES; a 1-5 micron wide extracellular space surrounding the tightly packed core of muscle cells). Trabecula are 20-60 microns in diameter.

Lower right panel shows 10 muscle cells and their extracellular cleft space known as the interfibrillar space (IFS). Due to the large cell membrane area:IFS volume, the IFS $[Ca^{++}]$ depletions are very large relative to those in the SES and ETS for short times. The IFS clefts are 0.01-1 micron wide.

Labels to Figure 28:

A = 1000 micron wide Frog Ventricular muscle strip in cross section
B = (200 micron wide cluster of trabecula + ETS)
C = (Single trabecula containing SES + 30 muscle cells)
D = (10 muscle cells + IFS)
E = Single muscle cell (average diameter = 5 microns, cells are 74% tissue volume)
ETS = Extratrabecular space (15% tissue vol., $[Ca^{++}]_o$ diffusive equilibrium Tau = 60 sec.)
SES = Subendothelial space (10% tissue vol., $[Ca^{++}]_o$ diffusive equilibrium Tau = 0.3-4 sec.)
IFS = Interfibrillar space (1% tissue vol., $[Ca^{++}]_o$ diffusive equilibrium Tau = 0.25 sec.)
Sheath = Defines the trabecula. It is made of endothelial cells and has narrow intercellular clefts.

Drawing based upon observations by Page and Niedergerke (1972).

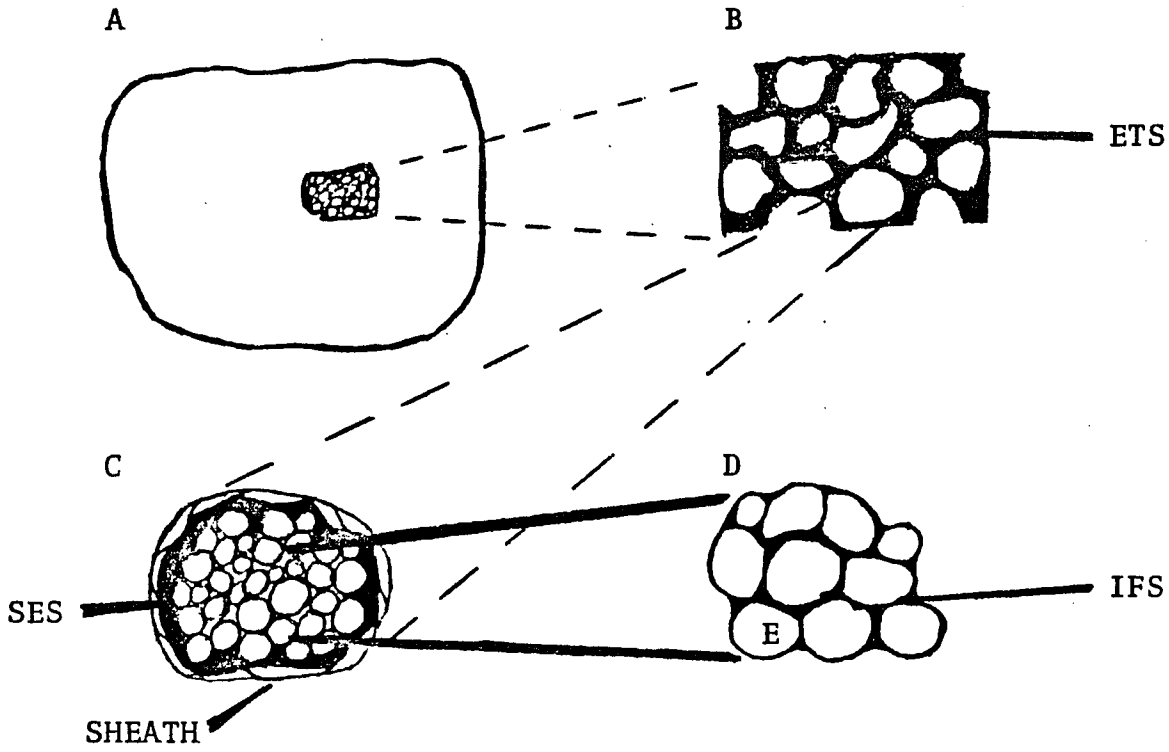
A
B
ETS
C
D
SES
IFS
E
SHEATH

from the IFS, lowering the IFS $[Ca^{++}]$. The SES occupies 38% of the extracellular space and surrounds the perimeter of the muscle cells inside each trabecula. As the IFS $[Ca^{++}]$ falls during the action potential, Ca^{++} from the SES diffuses into the IFS, down $[Ca^{++}]$ gradients in the clefts of the IFS. The SES is several microns wide and is bounded by a sheath of endothelial cells which are the outer surface of each trabecula. The endothelial sheath delays the attainment of ionic diffusion equilibrium between the SES and ETS. The SES $[Ca^{++}]$ falls establishing a $[Ca^{++}]$ gradient across the endothelial sheath. Eighty-five percent of the ventricular wall volume is occupied by trabecula and 15% by ETS. The ETS is 58% of the extracellular volume. As Ca^{++} leaves the ETS by diffusion through pores in the endothelial sheath and enters the SES, ETS $[Ca^{++}]$ depletion takes place. The thicker the ventricular wall, the lower the ETS $[Ca^{++}]$ at the center of the wall may become. Based upon experimental measurements and extrapolation performed in the Analysis section, figure 29 was generated. Figure 29 shows the $[Ca^{++}]$ in the IFS, SES and ETS after 1, 10 and 240 seconds of rapid beating in 0.050, 0.20, and 1.0 millimolar $[Ca^{++}]$ Ringers. Conceptually, this model is derived from the model of extracellular $[K^+]$ accumulation in frog ventricle reported by Kline (1975) and Cohen and Kline (1982).

The IFS, SES and ETS $[Ca^{++}]$ fall (deplete) at different rates and to different steady state concentrations as cellular Ca^{++} uptake occurs. Kline (1975) predicted that the cellular efflux of K^+ would cause rapid $[K^+]$ elevation (accumulation) in the IFS with a time constant of approximately 100 milliseconds. The time constant of the IFS $[Ca^{++}]$ depletion is estimated to be 250 milliseconds since the relative

Figure 29: Model of extracellular [Ca^{++}] depletion at 1, 10, and 240 seconds time after rapid repetitive stimulation. This is shown for 0.05 mM (top panel), 0.20 mM (middle panel), and 1.0mM Ca^{++} Ringers (bottom panel) for a frog ventricular muscle strip (1 millimeter diameter). This is drawn in cross section to indicate the radial dependence of the extracellular [Ca^{++}] depletion. Left Y-axis is $[Ca^{++}]_o$ in micromolar units while right Y-axis indicates the % extracellular [Ca^{++}] depletion.

Figure 29 Labels:
A = Center of IFS and center of ventricular muscle strip
B = SES of trabecula
C = Endothelial sheath of trabecula
ETS = Extratrabecular space not drawn to scale with respect to other radial widths.

In each of the three panels:

Top curve shows the extracellular [Ca^{++}] in ETS, sheath gradient, SES, and IFS after a one second action potential. Note the largest [Ca^{++}] depletion is in the IFS because of the large cell membrane surface area:IFS cleft volume (ratio is 26 times greater than the ETS).

Middle curve is the extracellular [Ca^{++}] after 10 seconds of rapid beating. Note the SES [Ca^{++}] is now significantly depleted and ETS [Ca^{++}] is just beginning to fall. Because of the SES Ca^{++} depletion, the IFS [Ca^{++}] may fall to a new lower level.

Lowest curve is the extracellular [Ca^{++}] after 240 seconds of rapid beating, when ETS [Ca^{++}] attains diffusive equilibrium with the bath. The [Ca^{++}] depletion in the ETS is a radial function and the gradients in other extracellular compartments for trabecula at the center of the strip, are smaller at this time.

MODEL OF THE RADIAL DEPENDENCE OF $[Ca^{++}]_o$ DEPLETION IN A ONE MILLIMETER WIDE STRIP OF FROG VENTRICLE

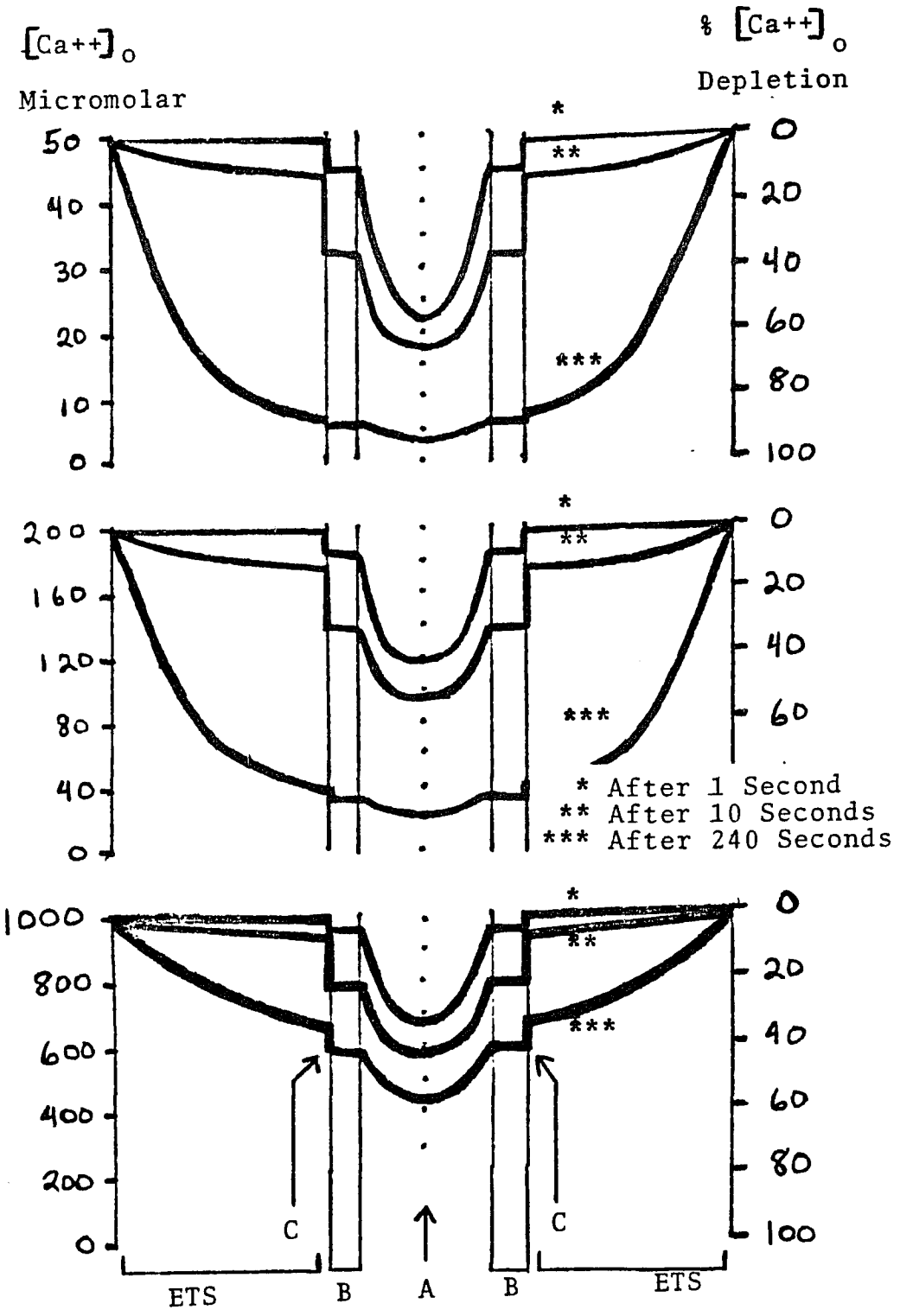

rate of K^+:Ca^{++} diffusion is 2.5 (D_{K+}/D_{Ca++} = 2.5; Wang, 1953; Friedman and Kennedy, 1955). In Analysis section B, the $[Ca^{++}]$ at the center of the IFS was calculated to be 250 micromolar lower than the SES $[Ca^{++}]$ after a one second action potential when the bath $[Ca^{++}]$ is 1.0 millimolar.

The SES $[Ca^{++}]$ has been estimated by Page and Niedergerke (1972) to equilibrate with time constant of 0.3 to 4.4 seconds (average value corrected for 25% overestimation is 2.5 seconds) after an instantaneous change in the ETS $[Ca^{++}]$. In Analysis section E, the SES $[Ca^{++}]$ was calculated to be 50 micromolar lower than the ETS $[Ca^{++}]$ after a one second action potential when the bath $[Ca^{++}]$ is 1.0 millimolar. The SES $[Ca^{++}]$ at steady state would be about 150 micromolar lower than the ETS $[Ca^{++}]$, after 10 seconds of continuous membrane depolarization when the bath $[Ca^{++}]$ was 1.0 millimolar.

The ETS $[Ca^{++}]$ equilibrated with an average time constant of 60 seconds, in 1 millimeter diameter frog ventricular strips bathed in 0.050-1.0 millimolar $[Ca^{++}]$ Ringers. At the center of such strips, the ETS $[Ca^{++}]$ fell by 80% after 3 to 5 minutes of rapid beating with a bath $[Ca^{++}]$ of 0.050-0.20 millimolar. The steady state magnitude of the ETS $[Ca^{++}]$ depletion was less at shallower radial depths but the time constant of the depletion was usually the same. Exceptions to this point were described in Analysis section C. The limited data obtained in 1.0 mM $[Ca^{++}]$ Ringers indicated that ETS $[Ca^{++}]$ depletions of at least 33% occur. The overall principle is that as the ETS $[Ca^{++}]$ falls, the SES $[Ca^{++}]$ falls lower allowing the IFS $[Ca^{++}]$ to fall even further.

B. Experimental Results Supporting the Model

Extracellular [Ca^{++}] depletion was predominantly studied in the ETS, but evidence of [Ca^{++}] depletion in beat to beat locations (SES and IFS) was often obtained. The Ca^{++} ion selective microelectrode tip is smaller than the width of the average ETS and SES clefts. The kinetics of the extracellular [Ca^{++}] depletions and the extracellular [Ca^{++}] increase following stimulation were consistent with the model. The large magnitude of some of the beat to beat [Ca^{++}] depletions and fast time constants of the decay tails, qualitatively suggested that the microelectrode tip was sometimes situated in the IFS .

The attainment of the steady state ETS [K^+] should occur 2 to 3 times faster than the time for attainment of the steady state ETS [Ca^{++}] according to simple diffusion principles (Wang, 1953; Friedmann and Kennedy, 1955). Kline and Morad (1978) and Martin and Morad (1982) observed that the ETS [K^+] attained a quasi-steady state level in 1 to 2 minutes. In the present study the ETS [Ca^{++}] attained a quasi-steady state level in 3 to 5 minutes, 2 to 3 times longer than the time required for [K^+] accumulation. When the Na^+/K^+ ATPase was inhibited by 10^{-6}M Ouabain or 80 mM Li^+, the time to steady state [K^+] accumulation was not significantly altered (Martin and Morad, 1983). Activation of the Ca^{++} extrusion process after 4 to 5 minutes of repetitive stimulation was miminal. Simultaneous measurements of the [K^+] and [Ca^{++}] during prolonged stimulation, qualitatively confirmed separate measurements of the ETS [K^+] and ETS [Ca^{++}] time courses. Thus the relative rates of the attainment of the steady state extracellular [K^+] and [Ca^{++}] are consistent with a model of extracellular [ion] equilibrium by simple diffusion before activation of ion pumps has

significantly begun.

When the extracellular Ca^{++} ion selective microelectrode tip is not in the ETS, then it must be either in the SES or IFS. Since the IFS is narrower than the microelectrode tip, only distorted IFS $[Ca^{++}]$ measurements can be obtained. Stable SES $[Ca^{++}]$ measurements are possible because the SES is 1 to 5 microns wide (Page and Niedergerke, 1972). In 0.20 mM $[Ca^{++}]$ Ringers beat to beat depletions of the extracellular $[Ca^{++}]$ were frequently observed with a magnitude of 50-60 micromolar. This magnitude is in between the magnitude of extracellular $[Ca^{++}]$ depletions expected in the SES and center of the IFS (see Analysis section E). The time course of the beat to beat $[Ca^{++}]_o$ increase (or $[Ca^{++}]_o$ depletion decay tail) following membrane repolarization was mathematically the sum of two exponentials plus a constant. From the analysis of these $[Ca^{++}]_o$ depletion decay tails, average time constants of 0.2-0.4 and 1.7-3.9 seconds (n=7) were obtained for the rapid and slow phases of the $[Ca^{++}]_o$ depletion decay tail. The slower time constant was in the range predicted for the time constant of the SES $[Ca^{++}]$ depletion decay tail. Since the faster time constant is similar to the time constant of the response, of the Ca^{++} ion selective microelectrode to an electrical square pulse, it has little quantitative meaning. However, the presence of this time constant which is 10-fold faster than the SES $[Ca^{++}]$ time constant suggests that the microelectrode tip may have been in the IFS. Although the Ca^{++} microelectrode did not permit quantitative measurements of the IFS $[Ca^{++}]$ depletions, the qualitative beat to beat $[Ca^{++}]$ depletions were consistent with the model. The largest and fastest decaying beat to beat $[Ca^{++}]$ depletions are expected in the IFS. During an action

potential the IFS $[Ca^{++}]$ depletion will be superimposed upon the smaller and slower decaying SES $[Ca^{++}]$ depletions which have a time constant of several seconds. The SES beat to beat $[Ca^{++}]$ depletions will have a smaller magnitude with a monoexponential decay tail of several seconds when the microelectrode tip is in the SES not IFS.

The beat to beat IFS and SES $[Ca^{++}]$ depletions ride on a much slower $[Ca^{++}]_o$ depletion during repetitive stimulation. The slow $[Ca^{++}]_o$ depletion phase is observed with no beat to beat $[Ca^{++}]_o$ depletion when the microelectrode tip is in the ETS. The $[Ca^{++}]$ in the IFS and SES depend upon the SES and ETS $[Ca^{++}]$. During an action potential the IFS $[Ca^{++}]$ would attain steady state if the SES $[Ca^{++}]$ was constant . However, because the SES $[Ca^{++}]$ falls during an action potential, the IFS $[Ca^{++}]$ also falls with the time constant of the SES. Since the maximum % change in the ETS $[Ca^{++}]$ after 10 seconds of rapid stimulation is only about 10%, the steady state SES $[Ca^{++}]$ depletions can often be observed. When stimulation is stopped the SES $[Ca^{++}]$ depletion decays with a time constant of several seconds. For more prolonged periods (several minutes) of repetitive stimulation, the beat to beat $[Ca^{++}]_o$ depletions superimpose upon a slower time course of ETS $[Ca^{++}]$ depletion . A similar observation was made by Kline and Morad (1976, 1978) regarding the beat to beat accumulation of $[K^+]_o$. The beat to beat extracellular $[K^+]$ increases did not fully decay during the interval between the action potentials at high heart rates. The extracellular $[K^+]$ accumulation had SES and ETS time constants of about 1 and 25 seconds respectively (Kline, 1975). A similar slow time constant for $[K^+]_o$ accumulation was observed without beat to beat $[K^+]_o$ fluctuations.

Membrane repolarization stops the beat to beat $[Ca^{++}]_o$ depletions. Similar findings were observed for extracellular $[K^+]$ accumulation in this preparation by Kline (1975). It is evident that membrane repolarization turns off cellular Ca^{++} influx which was activated by membrane depolarization during the action potential. The frog ventricular muscle action potential repolarized in less than 100 milliseconds. It is likely that the cellular influx of Ca^{++} is tightly controlled by the membrane potential in frog ventricle (Morad and Orkand, 1971). When the cellular Ca^{++} influx is turned off in less than 100 milliseconds, the IFS $[Ca^{++}]$ rapidly increases towards the bath $[Ca^{++}]$ due to the diffusion of Ca^{++} down the SES - IFS $[Ca^{++}]$ gradient. Because the SES - IFS $[Ca^{++}]$ gradient rapidly collapses the SES $[Ca^{++}]$ depletion is slowed as the membrane repolarizes. The SES $[Ca^{++}]$ then rises with a time constant of several seconds. During single action potentials the ETS $[Ca^{++}]$ may fall by 1 to 2%. After an action potential the slow disappearance of SES $[Ca^{++}]$ depletion is caused by the diffusion of Ca^{++} down the ETS - SES $[Ca^{++}]$ gradient (established across the endothelial sheath of each trabecula). This gradient produces small sometimes detectable beat to beat ETS $[Ca^{++}]$ depletions (see figure 8) which continue to fall beyond membrane repolarization for a second before they stop and then slowly disappear. Similar behavior for beat to beat ETS $[K^+]$ accumulation was observed (figure 8) and was computor modeled by Kline (1975). See also Cohen and Kline (1982).

While the location of the calcium ion selective microelectrode tip was not determined directly, the measurements of extracellular $[Ca^{++}]$ fluctuations were consistent with a mechanistic model involving three extracellular compartments (see figure 29). This model was generated

from extracellular calcium ion-selective microelectrode recordings and knowledge of frog ventricular histology (Page & Niedergerke, 1972). The present model's principles were extracted from the model of $[K^+]_o$ accumulation in frog ventricle generated by Kline (1975).

Kline's model was based upon detailed evidence of beat to beat extracellular $[K^+]$ accumulation measured by Kline (1975) and Kline and Morad (1976, 1978). The extracellular $[K^+]$ accumulation model was readily converted to a model of extracellular $[Ca^{++}]$ depletion for two reasons. First both cellular K^+ efflux and Ca^{++} influx appear to occur continuously during the action potential. Secondly, the determination of the model's kinetics was facilitated by knowledge of the free diffusion constants of K^+ (Friedmann and Kennedy, 1955) and Ca^{++} (Wang, 1953).

The model of extracellular $[Ca^{++}]$ depletion has to be modified to explain the alteration in the time constant of the time course, of large $[Ca^{++}]$ depletions in 0.050 and 0.20 mM Ca^{++}Ringers (see figure 12 and see Analysis section C). As the % time that the membrane is depolarized is increased by increasing the heart rate, the rate of ETS $[Ca^{++}]$ depletion should proportionately increase. This relation holds for low heart rates, but at high heart rates, less than proportionate increases in ETS $[Ca^{++}]$ depletion occur (see figures 10-12). The time constant of the ETS $[Ca^{++}]$ depletions in 0.050-0.20 mM Ca^{++} Ringers, decrease with increasing heart rate. It is proposed that a portion or all of the cellular uptake of Ca^{++} from the IFS depends upon the IFS/cytoplasmic $[Ca^{++}]$ gradient. As this gradient decreases the rate of cellular Ca^{++} accumulation should decrease. When the gradient was dissipated rapidly at higher heart rates, the time constant of the time course of

extracellular [Ca^{++}] depletion was less. In 0.050 mM Ca^{++} Ringers the time constant of ETS [Ca^{++}] depletion shortened more than in 0.20 mM Ca^{++} Ringers. Recently it has been hypothesized that intracellular [Ca^{++}] accumulation during the frog heart action potential would not turn off the slow inward calcium current measured by voltage clamp (Fischmeister and Horackova, 1983). However, $[Ca^{++}]_o$ depletion may reduce the transmembrane influx of Ca^{++} when the frog ventricle is superfused with low [Ca^{++}] Ringers.

Additional support for this view was the influence of the superfusate [Ca^{++}] on the magnitude of twitch tension as the frog ventricular heart rate was acutely increased (see figure 27). It was shown by Brown and Orkand (1968) that repetitive stimulation of frog ventricular strips superfused in less than 1 mM Ca^{++} Ringers produced a rate-dependent decrease in twitch tension followed by an increase in twitch tension. Lowering the superfusate [Ca^{++}] increased the amount of twitch tension depression. At the same time the action potential duration was not shortened.

In Dr. Penefsky's laboratory we noticed that the duration of the negative twitch tension staircase was greater at low heart rates versus higher heart rates (see figure 27). There was less twitch tension depression at the low rates. While extracellular [Ca^{++}] depletion was greater at high heart rates and was sustained beyond several minutes, the depression of twitch tension was more transient at high heart rates. One important factor of frog ventricular contractility appears to be an intracellular calcium store which dissipates when the transmembrane Ca^{++} influx is low (Orkand, 1968; Chapman and Niedergerke, 1970 a,b). While the time course of extracellular [Ca^{++}] depletion correlates with

the negative phase of staircase tension in frog ventricular strips superfused in low Ca^{++} Ringers, extracellular [Ca^{++}] depletion may be less consequential in experiments conducted in higher than 1 mM Ca^{++} Ringers. However, measurement of extracellular [Ca^{++}] depletion in frog ventricular strips superfused with greater than 1 mM [Ca^{++}] Ringers was not possible due to the strong twitch tension. The absolute size of the depletions in higher [Ca^{++}] Ringers is likely to increase to some maximum value. At the same time the % of the total extracellular [Ca^{++}] that depletes will decrease as the magnitude of the transmembrane Ca^{++} flux per action potential approaches its maximum.

C. Role of Extracellular [Ca^{++}] in Frog Ventricular Muscle Contraction

The small size of frog ventricular muscle cells (average diameter is 5 microns; Staley & Benson, 1968; Page and Niedergerke, 1972), the slow onset and then continuous development of twitch tension during membrane depolarization (Orkand, 1968; Morad and Orkand, 1971), and the rapid and high sensitivity of the twitch tension to the extracellular [Ca^{++}] (Luttgau & Niedergerke, 1968; Kavaler, 1974) are consistent with the hypothesis that extracellular fluid Ca^{++} is the major source of Ca^{++} used to activate contraction during each action potential (Morad & Goldman, 1973). The idea that Ca^{++} more readily enters depolarized cells is at least 25 years old. In 1957 Hodgkin and Keynes found that the nerve action potential caused additional net influx of extracellular $^{45}Ca^{++}$ into axoplasm. The accumulation increased as the extracellular [Ca^{++}] increased. A 10 to 20-fold increase in cellular $^{45}Ca^{++}$ uptake was observed by Niedergerke (1963b) using repetitively

depolarized frog ventricles. In his 1963 study and a later 1968 study (Niedergerke et al.) estimated the transmembrane Ca^{++} flux per action potential in 1 mM $[Ca^{++}]$ Ringers to be 0.13 to 0.2 picomoles/cm^2. This was equivalent to a cellular accumulation of 1.3 to 2 micromolar $[Ca^{++}]$ per action potential. A 1970 $^{45}Ca^{++}$ uptake study by Sands and Winegrad determined that the frog ventricle transmembrane Ca^{++} flux per action potential in 0.3 mM $[Ca^{++}]$ Ringers was 0.08 picomoles/cm^2 (or a cellular accumulation of 0.8 micromolar $[Ca^{++}]$ per action potential). In addition, frog ventricle cellular $^{45}Ca^{++}$ accumulation was increased by Ringers with low $[Na^{+}]$ or high $[K^{+}]$ (Niedergerke, 1963a) or low $[K^{+}]$ (Thomas, 1960). All of these solutions caused muscle contractions.

The amount of Ca^{++} needed to trigger a physiological contraction in frog ventricle has been estimated. Katz (1970) estimated that 50 to 60 micromoles of Ca^{++}/kilogram wet weight of cells was needed to saturate the Troponin-C Ca^{++} binding sites of the cardiac muscle contractile proteins. Using chemically-skinned frog ventricular cells, with buffered $[Ca^{++}]$ Ringers, Winegrad (1971) determined that the free $[Ca^{++}]$ in the cytoplasm during physiological contractions was 10 micromolar. Five to six times more frog ventricular muscle tension than is physiological could be generated by Winegrad's skinned cell method or by the voltage clamp technique (Morad and Orkand, 1971). The normal frog ventricular cell $[Ca^{++}]$ accumulation per action potential is expected to be 10 micromolar/kilogram wet ventricular weight, equal to a 1 picomole per cm^2 per action potential transmembrane Ca^{++} flux. It was evident in the early 1970's that the estimate of beat to beat cytoplasmic $[Ca^{++}]$ accumulation (determined by the radioisotope $^{45}Ca^{++}$ flux) was

underestimated if this transmembrane Ca^{++} flux was to supply all the activator Ca^{++} (Niedergerke and Orkand, 1966; Chapman and Niedergerke, 1970a).

Using extracellular $[Ca^{++}]$ depletion, estimates of the average instantaneous intracellular $[Ca^{++}]$ accumulation have been made in this study (for details, see analysis section D). At steady state, 1 mM $[Ca^{++}]$ Ringers superfused frog ventricular muscle is known to generate 100% physiological twitch tension (Niedergerke, 1956; Luttgau and Niedergerke, 1958; Morad and Orkand, 1971). In the present study the instantaneous, average cellular $[Ca^{++}]$ accumulation per second was calculated to be 6.7 to 8.8 micromolar in 1.0 mM $[Ca^{++}]$ Ringers, 1.5 to 2.3 micromolar in 0.20 mM $[Ca^{++}]$ Ringers, and 0.5 to 0.7 micromolar in 0.050 mM $[Ca^{++}]$ Ringers. These estimates are similar to the quantity proposed to be needed. These measurements also show that the instantaneous, average beat to beat Ca^{++} influx increases as the extracellular $[Ca^{++}]$ increases from 0.050 to 1.0 mM. Twitch tension increases linearly as the Ringers $[Ca^{++}]$ is increased in this range (Niedergerke et al., 1976; Chesnais et al, 1978; Kavaler et al, 1978). The estimates of transmembrane Ca^{++} flux by the ETS $[Ca^{++}]$ depletion method (see section D of Analysis) support the hypothesis that the majority of activator Ca^{++} in frog ventricle, under physiological conditions, arises from an extracellular Ca^{++} pool, rather than from an intracellular Ca^{++} pool during the action potential. This hypothesis was not strongly supported by $^{45}Ca^{++}$ flux studies (Niedergerke, 1963b). The reliability of radioisotope tracer flux studies has been questioned (Niedergerke et al, 1976; Attwell et al., 1979). In addition, evidence has indicated that frog ventricular intracellular pools of

Ca^{++} are insufficient or inactive sources of activator Ca^{++}.

The mitochondria and the sarcoplasmic reticulum of frog ventricular cells, are the only intracellular Ca^{++} pools observed by Winegrad (1973) to accumulate Ca^{++} (or Sr^{++}). In addition, this only occurred when the divalent ion concentration was in the millimolar range. Isolated cardiac mitochondria release Ca^{++} when the intracellular $[Na^{+}]$, 5 to 7 mM (Lee and Fozzard, 1975; Ellis, 1977; Sheu et al., 1980) is increased to 8 mM (Crompton et al., 1976). Since the steady state frog ventricular transmembrane $[Na^{+}]$ influx can not significantly exceed the $[K^{+}]$ efflux per action potential of 10-30 picomoles/cm^2 (Johnson, 1957;Kline, 1975), the cytoplasmic $[Na^{+}]$ increase per beat may not exceed 0.3 millimolar. Thus, the cytosolic $[Na^{+}]$ increase per action potential is insufficient to stimulate Ca^{++} efflux from cardiac mitochondria. In addition, frog ventricular mitochondria accumulate Ca^{++} with a Km of 30 micromolar (Scarpa & Graziotti, 1973). Thus, these mitochrondria lack the capability to lower the cytosolic $[Ca^{++}]$ enough to cause complete twitch tension relaxation.

Frog ventricular sarcoplasmic reticulum (SR) occupies only 0.5% of the cell volume, while mammalian SR occupies about 7.5% of the mammalian heart cellular space (Page et al., 1971; Page and Niedergerke, 1972). The t-tubule system is absent in frog ventricular cells (Page and Niedergerke, 1972). The t-tubule system is believed to coordinate membrane depolarization and SR Ca^{++} release in skeletal muscle and in mammalian cardiac muscle cells (Morad & Goldmann, 1973; Chapman, 1979). The SR Ca^{++} stores are believed to be the major source of activator Ca^{++} in mammalian cardiac muscle (Solaro & Briggs, 1974; Kirchberger, 1974; Fabiato and Fabiato, 1978; Levitsky et al., 1981). The Fabiatos

(1978) have shown that skinned mammalian cardiac cells of many species, twitch upon exposure to a small amount of Ca^{++}. Skinned frog ventricular cells do not twitch with the Fabiato protocol. Skinned cardiac muscle cells from a variety of vertebrate animals have the same $[Ca^{++}]_i$ dependence to generate muscle tension (Fabiato & Fabiato, 1978). The prevailing hypothesis is that action potential dependent transmembrane Ca^{++} fluxes of mammalian heart cells are too small to cause more than 10% of the observed twitch tension (Chapman, 1979). The small Ca^{++} influx by mammalian heart cells is hypothesized to trigger the release of large SR Ca^{++} stores which activate the twitch tension (Chapman, 1979).

The available experimental evidence points to different pathways for the Ca^{+}+ activation of frog ventricle contraction versus the mammalian ventricle contraction. The long frog ventricular action potential permits significant transmembrane Ca^{++} influx. While much remains to be learned about the cytoplasmic handling of Ca^{++} in frog ventricle cells, the mitochondria and sarcoplasmic reticulum do not seem to be important factors in the short term of a single contraction/relaxation cycle. Somewhere within the frog heart cell there is a compartment which can store hundreds of micromoles of Ca^{++}/per liter of cells. In addition there must be a mechanism for twitch tension relaxation which is not solely dependent upon cellular Ca^{++} extrusion. The Ca^{++} extrusion process takes minutes to fully activate while tension relaxes in only a second.

D. Evidence and Role of a Ca^{++} Extrusion Process

Frog ventricular cells can store millmolar quantities of calcium ions without apparent harm when driven by repetitive stimulation (Niedergerke, 1963b; Sands and Winegrad, 1970), which results in extracellular $[Ca^{++}]$ depletion (Dresdner et al., 1982, Dresdner and Kline, 1983). During this time, the twitch tension eventually increases in amplitude but the baseline tension does not increase (Niedergerke, 1956, Chapman & Niedergerke, 1970a, b). The cytoplasmic $[Ca^{++}]$ must be submicromolar between contractions (Winegrad, 1971, Lee et al., 1980, Sheu and Fozzard, 1982). Hence most of the beat to beat cytoplasmic Ca^{++} accumulation must be sequestored within the cell in an inactive state (Niedergerke, 1963a). Niedergerke (1963a) observed that both $^{45}Ca^{++}$ influx and efflux rates were increased during repetitive stimulation to nearly the same amount. Since the capacity of frog ventricular cells to store Ca^{++} must be finite, it is reasonable to predict that a membrane Ca^{++} extrusion mechanism exists to protect the cell from an intracellular $[Ca^{++}]$ overload.

Evidence was obtained during measurements of the extracellular $[Ca^{++}]$ of a Ca^{++} extrusion process. When repetitive stimulation was prolonged beyond 4 minutes, the ETS $[Ca^{++}]$ began to shift from a level of maximum depletion to less depletion. This can only occur if the steady state net transmembrane $[Ca^{++}]$ influx is decreasing. When stimulation was stopped, the ETS $[Ca^{++}]$ increased back to the superfusate $[Ca^{++}]$ and then slowly increased above it. When repetitive stimulation was prolonged for 20 to 30 minutes, the ETS $[Ca^{++}]$ depletion eventually disappeared. When stimulation was then stopped, the ETS $[Ca^{++}]$ greatly increased above the superfusate $[Ca^{++}]$. These

experiments indicated that active Ca^{++} extrusion could be activated. The post-drive ETS $[Ca^{++}]$ overshoot increased for longer periods of repetitive stimulation until its absolute magnitude was the same as the magnitude of the ETS $[Ca^{++}]$ depletion observed after 3 to 4 minutes. Also, the time required for full activation of the ETS $[Ca^{++}]$ overshoot was similar to the time required for the ETS $[Ca^{++}]$ overshoot to decay (20-30 minutes).

The characteristics of the activation of Ca^{++} efflux are similar to the basic features of the Na^+/K^+ ATPase pump activation described in this preparation by Martin & Morad, 1982. Frog ventricle Na^+/K^+ pump activation occurs slowly like Ca^{++} efflux activation. Na^+/K^+ pump activity depends upon the extracellular $[K^+]$ and intracellular $[Na^+]$ (Skou, 1957, 1965; Thomas, 1972; Deitmar and Ellis, 1978; Eisner and Lederer, 1980; Gasby, 1980; Cohen et al., 1981; Glitsch et al., 1981; Martin and Morad, 1982). Na^+/K^+ pump activity also depends on the intracellular ATP, ADP, Pi, and Mg^{++} concentrations (Wang et al., 1977). In cardiac muscle, repetitive stimulation increases the intracellular $[Na^+]$ (Cohen, C.J.et al.;1982;Lee and Dagostino, 1983) and the extracellular $[K^+]$ (Kline, 1975; Kline and Morad, 1976, 1978; Kunze, 1977; Kline et al., 1980; Kline and Kupersmith, 1982; Martin and Morad, 1982). In the present study repetitive stimulation increased the net cellular $[Ca^{++}]$ and activated Ca^{++} efflux. The intracellular $[Ca^{++}]$ must be an important factor since Ca^{++} must bind to the inner cell membrane Ca^{++} efflux process site. The Ca^{++} efflux increased till it matched the Ca^{++} influx per stimulus interval. Similarly, K^+ efflux is balanced by K^+ uptake (Kunze, 1977; Kline et al., 1980; Martin and Morad, 1982).

Prevailing evidence from studies of nerve and muscle cells suggests that Na^+ dependent Ca^{++} exchange and/or a Ca^{++} ATPase are Ca^{++} extrusion processes. The transmembrane $[Na^+]$ gradient has been shown to influence the rate of Ca^{++} efflux from squid axons (Baker, 1972; Blaustein, 1974) but it is a complex, highly regulated process (Blaustein, 1977; Mullins, 1977). In cardiac muscle where the actual transmembrane $[Na^+]$ and $[Ca^{++}]$ gradients are less readily controlled than in the squid axon experiments, evidence of a reversible Na^+ dependent Ca^{++} efflux was demonstrated by Reuter and Seitz (1968) with guinea pig auricles and ventricular trabeculae of sheep and calf hearts. The apparent stoichiometry of the Ca^{++} efflux was 2 Na^+ in per Ca^{++} pumped out of the cells. Lowering the extracellular $[Na^+]$ increased the intracellular $[^{45}Ca^{++}]$ and decreased the rate of $^{45}Ca^{++}$ efflux. Lowering the extracellular $[Ca^{++}]$ also decreased the rate of $^{45}Ca^{++}$ efflux. The greatest inhibition of $^{45}Ca^{++}$ efflux (pumping) occurred with zero extracellular $[Na^+]$ and $[Ca^{++}]$. The $^{45}Ca^{++}$ efflux had a Q_{10} of 1.35 and was not reduced by dinitrophenol (an ATP synthesis inhibitor). These observations indicated that ATP was not directly required as an energy source. Instead the energy was obtained from the transmembrane $[Na^+]$ gradient. Reuter and Seitz (1968) interpreted their data in terms of a bidirectional, facilitated ion exchange mechanism.

The basic problem with the hypothetical Na^+ dependent Ca^{++} exchanger was its thermodynamics. Only enough Na^+ gradient energy was available to transport Ca^{++} out of the cell when the cytoplasmic $[Ca^{++}]$ was greater than 16 micromolar (Glitsch et al., 1970). Controversy grew over this issue and the question of whether a

$2Na^+:1Ca^{++}$, $3Na^+:1Ca^{++}$, or $4Na^+:1Ca^{++}$ ion exchange stoichiometry could be kinetically determined (Mullins, 1979). Evidence of regulation of the resting cytoplasmic $[Ca^{++}]$ by the extracellular $[Na^+]$ was demonstrated by Lee et al. (1980) in rabbit papillary muscles and by Bers & Ellis (1981) in sheep purkinje fibers. These experiments suggested that the Na^+/Ca^{++} exchange stoichiometry was greater than $2Na^+:1Ca^{++}$ because the cytoplasmic $[Ca^{++}]$ was submicromolar. A detailed study of the intracellular $[Na^+]$ and $[Ca^{++}]$, membrane potential and tension by Sheu and Fozzard (1982) proposed that the empirical Na^+/Ca^{++} ion exchange stoichiometry was 2.4 to 2.6.

Bridges and Bassingwaighte (1983) studied the stoichiometry of Na^+/Ca^{++} exchange in rabbit ventricle and obtained a $3Na^+:1Ca^{++}$ stoichiometry in an experiment where the Ca^{++} pump direction was reversed by reversing the Na^+ gradient. First, the cellular potassium concentration was lowered from 132 to 38 mM while the cellular sodium concentration was increased from 15 to 111 mM. This was accomplished by retrograde superfusion of whole rabbit hearts with 10 micromolar acetyl strophanthidin and 50 micromolar $[Ca^{++}]$ Tyrodes solution for 90 minutes. Five to fifteen minutes after the Tyrode's $[Ca^{++}]$ was increased to 12 mM, the intracellular $[Na^+]$ fell from 105 to 84 mM while the intracellular $[Ca^{++}]$ increased from 6.2 to 13.1 mM. The intracellular $[Na^+]$ fell by 21 mM while the intracellular $[Ca^{++}]$ increased 7 mM.

Detailed study of a Na^+/Ca^{++} exchange process was beyond the scope of this thesis. However, a stimulatory effect of low $[Na^+]_o$ Ringers on $[Ca^{++}]_o$ depletion in frog ventricular muscle during repetitive trains of action potential was observed (see figure 19) and this

result is consistent with the Na^+/Ca^{++} exchange hypothesis. Detailed studies by Luttgau and Niedergerke (1958) and Niedergerke (1963a) indicate an important role of the Na^+/Ca^{++} composition of the Ringers. Na^+/Ca^{++} exchange may have several functions since a stoichiometry of $3Na^+:1Ca^{++}$ makes it a voltage-sensitive Ca^{++} transport system. During membrane depolarization Na^+/Ca^{++} exchange may bring Ca^{++} into cells. Membrane repolarization may reverse this process, sending Ca^{++} out of cells (Mullins, 1979). Repetitive stimulation disturbs the intracellular $[Na^+]$ and $[Ca^{++}]$, and extracellular $[Ca^{++}]$, and may alter the net Ca^{++} fluxes carried by Na^+/Ca^{++} exchange at all membrane potentials.

A Ca^{++} stimulated Mg^{++} ATPase has been detected in the frog heart sarcolemma (Morcos, 1981). This Ca^{++} pump is energized by ATP, dependent upon the intracellular $[Ca^{++}]$ and $[Mg^{++}]$, but independent of the intracellular $[Na^+]$ and [K+] (Caroni & Carofoli, 1980; Morcos, 1981; Beage et al., 1981). To date, information on the Ca^{++} ATPase has arisen mostly from membrane vesicle studies. The cardiac intracellular $[Mg^{++}]$ may be relatively constant at about 3mM (Hess and Weingart, 1981; Hess et al., 1982). One problem has been that the Ca^{++} ATPase studies have used subphysiological $[Mg^{++}]$ where the Ca^{++} ATPase sensitivity to Ca^{++} is greater. A second problem is the lack of a specific Ca^{++} ATPase inhibitor. Caroni and Carofoli (1980; 1981) inhibited the Ca^{++} ATPase in vesicles with orthovanadate, lanthanum, or trifluoroperazine, drugs known to have multiple sites of action. The available experimental studies on cardiac Ca^{++} ATPase are insufficient to assess its role in the frog ventricle.

E. Pharmacological Modification of the Transmembrane Ca^{++} Flux

The effect of inorganic Ca^{++} antagonists and catecholamines upon extracellular $[Ca^{++}]$ depletion was examined to help to validate the measurement of extracellular $[Ca^{++}]$ using Ca^{++} ion selective microelectrodes and to test assumptions concerning these agents. Previously, tension, membrane current and $^{45}Ca^{++}$ uptake measurements have been used to study the transmembrane Ca^{++} influx in a less direct manner.

One millimolar managanese ions blocked $[Ca^{++}]_o$ depletion recorded in the ETS - by 56±9% in 5 experiments in 0.20 mM $[Ca^{++}]$ Ringers. Chapman and Ellis (1977a) obtained about a 75% inhibition of low Na^+ contracture tension when the ratio of $[Ca^{++}]_o$ to $[Mn^{++}]_o$ was 0.2 in frog atrial trabeculae. The block of extracellular $[Ca^{++}]$ depletion by Mn^{++} is consistent with the hypothesis that Mn^{++} competitively antagonizes the transmembrane Ca^{++} influx. Mn^{++} has long been known to interfere with membrane ion transport (Fatt and Ginsborg, 1958; Hagiwara & Nakajima, 1966; Rongier et al, 1969; Kohlhardt et al., 1973; Chapman and Ellis, 1977a; Hagiwara and Byerly 1981; Reuter, 1983). One mechanism is that Mn^{++} blocks the voltage-dependent slow inward current carried by Na^+ and Ca^{++} in frog atrium (Rougier et al, 1969) and in cat ventricle (Kohlhardt et al., 1973) without significantly influencing the fast Na^+ current (Rougier et al., 1969). As a result the fast upstroke of the frog ventricular action potential is not altered very much for moderate $[Mn^{++}]$ (Hagiwara and Nakajima, 1965) but the plateau height and action potential duration are reduced. Manganese ion blocks potassium current (Kass and Tsien, 1975). Mn^{++} also blocks frog heart tension development caused by action potentials, low Na^+, and high K+ Ringers (Rougier et al., 1969;

Kohlhardt et al., 1973; Chapman and Ellis, 1977; Anderson et al., 1977). Mn^{++} also slows tension relaxation (Roulet et al., 1979). When high $[Mn^{++}]$ is used, some Mn^{++} may enter frog heart cells and cause contraction (Chapman and Ellis, 1977b). Kavaler et al. (1978) have shown that Mn^{++} rapidly blocks twitch tension in frog ventricle without a significant change in action potential duration. In the present study action potential duration was reduced by only 14%. Mn^{++} was a good agent to use to test the validity of the technique developed in this study because it was rapidly reversible.

Ni^{++} also blocked extracellular $[Ca^{++}]$ depletion but the post-drug control $[Ca^{++}]_o$ depletions were difficult to obtain since Ni^{++} was slow to wash out. Ni^{++} is known to have all the actions of Mn^{++} plus an inhibitory action on the inactivation of the fast sodium channel (Babskii & Donskikh, 1968; Kohlhardt et al., 1973; Chapman & Ellis, 1977). Ni^{++} prolongs the frog ventricular action potential duration and lowers the plateau (Babskii and Donskikh, 1968; Kline, 1975; Morad et al., 1981). The prolongation of the frog ventricular action potential is thought to be due to decreased inactivation of the sodium channel conductance (Babskii and Donskikh, 1968) and a decreased rate of K^+ efflux (Kline and Morad, 1978). Thus Ni^{++} and Mn^{++} are nonspecific Ca^{++} antagonists.

Catecholamines have a positive inotropic effect (Oliver & Schafer, 1895; Elliot, 1905; Graham and Lamb, 1968; Niedergerke et al., 1976; Morad et al., 1981) in the frog heart. The frog ventricular twitch tension in 0.3 mM Ca^{++} Ringers may increase over ten told with moderate doses of epinephrine (Graham and Lamb, 1968). In the present study 50 micromolar epinephrine increased the magnitude and rate of extracellular

$[Ca^{++}]$ depletion 4 to 5 fold. At the same time the action potential duration was tripled and the height of the plateau was increased (see Niedergerke et al., 1976; Morad et al., 1981). The effect of epinephrine on frog ventricular action potential prolongation had an ED_{50} of 20 micromolar. This ED_{50} is similar to the frog ventricle beta receptor K_D determined in competitive binding experiments with [3H] dihydro-alprenolol by Hancock et al. (1979). The ED_{50} of epinephrine in the frog atrium is 10-100 times lower (Stene-Larsen and Helle, 1978.) The positive inotropic action of epinephrine in frog ventricle is neither blocked by alpha antagonists i.e. phetolamine (Morad et al., 1981) nor do alpha agonists have any inotropic effects. Propranolol blocked the actions of epinephrine in the present study. This was consistent with the hypothesis that epinephrine stimulates Beta adrenergic receptors in the frog ventricle (Stene-Larsen and Helle, 1978; Morad et al., 1981). Isoproterenol was about ten times more potent than epinephrine in the present study and in the radioligand binding study of Hancock et al. (1979).

Morad et al. (1981) found that the relaxant effect of catecholamines in the frog ventricle predominated over the inotropic effect after 1 second of prolonged membrane depolarization. The present study indicates that the relaxant effect of catecholamines in the frog ventricle is not due to a net reversal in the transmembrane Ca^{++} flux during action potentials exceeding a one second duration (see figures 23 and 24). Secondly, the present study specifically demonstrates for the first time that the transmembrane Ca^{++} flux is increased although it has been known for a long time that the cardiac slow inward current is increased by catecholamines (Vassort et al., 1969; Reuter, 1974; Reuter & Scholz,

1977). There has been no report suggesting that any effect of catecholamines is mediated via Na^{+}/Ca^{++} exchange. The effect of epinephrine was easily reversible and the preparation did not appear to desensitize to the catecholamine.

The prevailing general hypothesis of catecholamine action in cardiac muscle involves three sites of action. Catecholamines 1) increase the slow inward calcium current, 2) increase the Ca^{++} capacity of the sarcoplasmic reticulum and 3) decrease the affinity of the contractile proteins for Ca^{++} (Rinaldi et al., 1982; LePeuch et al., 1980, 1981; Solaro et al., 1976; Mope et al, 1980; McClellan and Winegrad, 1978, 1980; Kirchberger et al., 1974; Reuter, 1983). In all three cases protein at the site of action is phosphorylated by a Cyclic AMP activated protein kinase (Tsien, 1977). The intracellular [Cyclic AMP]:[Cyclic GMP] ratio is not constant during single frog ventricular action potentials (Wollenberger et al., 1973; Brooker, 1973). During twitch tension development the intracellular [Cyclic AMP] increases and the intracellular [Cyclic GMP] falls.

Singh et al.,(1978) have found that isoproterenol causes a sustained increase in the intracellular [Cyclic AMP] while transiently decreasing the intracellular [Cyclic GMP]. The tension increase due to catecholamine stimulation is linearly proportional to the % change in the intracellular [Cyclic AMP]/% change in the [Cyclic GMP] (Singh et al., 1978). Interestingly, Flitney et al., (1977) have shown that the development of the frog ventricular hypodynamic state is accompanied by a decrease in the intracellular [Cyclic AMP]:[Cyclic GMP] ratio. The application of intracellular cyclic nucleotides can mimic the action of catecholamines (Tsien et al., 1972; Nargeot et al., 1983). Thus, the principal effect

of catecholamine binding to Beta receptors is to increase the rate of synthesis of intracellular Cyclic Amp (Ramussen and Goodman, 1977; Tsien, 1977). The intracellular [Cyclic AMP] is regulated in part by the intracellular [Cyclic GMP] (Flitney and Singh, 1981).

The relationship between the drug concentration and the intracellular cyclic nucleotide concentration is a current area of intensive pharmacological research. It is known that catecholamines elevate the cytosolic concentration of cyclic nucleotides which indirectly increase the slow inward Ca^{++} current and decrease the sensitivity of the contractile elements to the intracellular $[Ca^{++}]$. The effects of catecholamines on the frog heart cell SR are unknown.

Catecholamines increase the rate of relaxation. This effect is still evident in sodium free Ringers (Roulet et al., 1979). This suggests that catecholamines may stimulate a (Na^{+}-independent) Ca^{++} extrusion process if heart cells must extrude Ca^{++} to relax tension. The relaxant effect is also evident in catecholamine experiments with aequorin (Allen & Blinks, 1978). The intracellular $[Ca^{++}]$ is estimated from the light emission of frog atrial cells injected with the calcium sensitive photoprotein, aequorin. The intracellular $[Ca^{++}]$ and tension fall at a much greater rate in catecholamine-stimulated versus control frog atrium (Allen and Blinks, 1978).

The effect of epinephrine on extracellular beat to beat $[Ca^{++}]_o$ depletion was blocked partially by 1 millimolar Mn^{++} and more completely by 1 millimolar Ni^{++}. The action potential was only slightly shortened with Ni^{++}, indicating that Ca^{++} influx can be blocked without causing substantial shortening of the action potential duration. This approach would be a useful method in future studies to dissect out

the important features of catecholamine stimulation. For example, is the enhanced Ca^{++} influx more important than the change in the intracellular [Cyclic AMP]? Ni^{++} has been shown to block the positive inotropic effect of epinephrine and the slow inward current (Morad et al., 1981).

The measurement of the extracellular [Ca^{++}] in frog ventricular muscle has provided results which interpreted with caution, allow the relationships between the transmembrane [Ca^{++}] flux, twitch tension and action potential duration to be studied. The observations of the present study support many of the hypotheses concerning the frog ventricle. The new technique described in this thesis demonstrates that the transmembrane Ca^{++} flux can be specifically studied in a rapid and continuous manner in intact cardiac tissue. The importance of the histology of the tissue can be better understood. Lastly, this approach can be used to study cellular Ca^{++} efflux without regard to whether this efflux generates membrane current.

VI SUMMARY

1. Extracellular calcium ion concentration was measured in the extracellular spaces of frog ventricular muscle strips with a Ca^{++} selective microelectrode (time constant 0.3 - 0.6 seconds; Fluka Ca^{++} neutral carrier exchange cocktail, Simon et al; 1978; of tip diameter 1.5 - 3 microns). The extracellular potential (V_o) was measured when double or triple barrel ion selective microelectrodes were used. The transmembrane potential was measured with a conventional 3M KCl filled microelectrode in the intracellular space of a separate frog ventricular muscle strip.

2. The extracellular $[Ca^{++}]$ was monitored during the course of a single action potential, but the measured change was probably underestimated by 20%. $[Ca^{++}]_o$ depletions of up to 50 micromolar (from 0.20 to 0.15 mM) were seen.

3. During the action potential the extracellular $[Ca^{++}]$ continued to fall indicating net cellular Ca^{++} uptake. Repolarization stopped the depletion which then subsided with a time constant of 1-5 seconds.

4. During sudden increases in heart rate (from 1 to 3-60 per minute) the $[Ca^{++}]_o$ depletion seen during single action potentials summed, resulting in a slowly equilibrating depletion compared with the more rapidly equilibrating extracellular $[K^+]$ accumulation. The slow $[Ca^{++}]_o$ depletions were greater at higher heart rates, bath $[Ca^{++}]$, and at deeper depths in the tissue extracellular space.

5. At high heart rates the $[Ca^{++}]_o$ depletion saturated and the time constant of the depletion decreased several-fold (from 60 to 10 seconds). It is hypothesized that the transmembrane Ca^{++} flux varies with $[Ca^{++}]_o$.

6. After 3-4 minutes of repetitive stimulation, the slow $[Ca^{++}]_o$ depletion attained a minimum level and thereafter slowly subsided during the next 20-30 minutes of stimulation. When stimulation was stopped the $[Ca^{++}]_o$ increased for 20-30 minutes above the bath $[Ca^{++}]$ by roughly the magnitude of the depletion. During brief repetitive stimulation, $[Ca^{++}]_o$ depletion and its time constant were decreased when the Ca^{++} extrusion process had been already activated.

7. Low Na^+ Ringers markely shortened the action potential duration but $[Ca^{++}]_o$ depletions were not proportionately reduced. Either low Na^+ Ringers increases cellular Ca^{++} uptake or cellular Ca^{++} uptake occurs largely in the early phase of the action potential.

8. Continuous membrane depolarization by low Na^+/high K^+ Ringers caused prolonged $[Ca^{++}]_o$ depletion and activated a Ca^{++} extrusion process. Prolonged $[Ca^{++}]_o$ depletion indicates that cellular Ca^{++} uptake is not completely inactivated by membrane depolarization.

9. Manganese ion reversibly blocked $[Ca^{++}]_o$ depletion. Nickel ion blocked $[Ca^{++}]_o$ depletion but was less reversible.

10. Catecholamines in 0.050 mM Ca^{++} Ringers prolonged the action potential duration several-fold and increased the rate and magnitude of beat to beat $[Ca^{++}]$ depletions several-fold. The effect of epinephrine was completely antagonized by propranolol indicating that $[Ca^{++}]_o$ depletion and the action potential duration are modulated by a Beta adrenergic receptor. The relaxant effect of catecholamines (Morad et al., 1981) is not due to a reversal in the transmembrane Ca^{++} flux after 1 second of membrane depolarization. Nickel ion antagonized the augmentation of beat to beat $[Ca^{++}]_o$ depletion induced by catecholamines.

11. The negative phase of twitch tension staircase in low Ca^{++} Ringer (Brown & Orkand, 1968) coincided with the time course of $[Ca^{++}]_o$ depletion. The % twitch tension depression and % $[Ca^{++}]_o$ depletion were similar. For small increments in heart rate, twitch tension depression is prolonged. After sufficient time has passed to activate Ca^{++} efflux, return to a slower heart rate caused a prolonged twitch tension overshoot with a magnitude and duration similar to the tension depression. It is concluded that extracellular $[Ca^{++}]$ depletion has a role in the hypodynamic frog ventricle twitch tension response.

12. The estimated net transmembrane Ca^{++} influx/cm^2 cell membrane in 0.050 - 1.0 mM Ca^{++} Ringers (0.05 - 0.88 picomoles/cm^2/second) increases the cytoplasmic $[Ca^{++}]$ to 0.5 - 8.8 micromolar. It is concluded that sufficient extracellular Ca^{++} enters frog ventricular muscle cells during the action potential to directly cause the observed contraction.

VII REFERENCES

Adrian, R. H. (1956) The effect of internal and external potassium concentration on the membrane potential of frog muscle. J. Physiol. 133; 631-658.

Allen, D. G. & Blinks, J. R. (1978) Calcium transients in aequorin-injected frog cardiac muscle. Nature (Lond.). 273; 509-513.

Anderson, T. W., Hirsch, C. & Kavaler, F. (1977) Mechanism of activation of contraction in frog ventricular muscle. Circ. Res. 41(4); 472-480.

Attwell, D., Eisner, D. & Cohen, I. (1979) Voltage clamp and tracer flux data: effects of a restricted extracellular space. Quart. Rev. Biophys. 12(3); 213-261.

Babskii, E. B. & Donskikh, E. A. (1968) Electrophysiological investigation of action of nickel ions on the myocardium. Dokl. Akad. Nauk. SSSR. 178; 248-251.

Baker, P. F. (1972) Transport and metabolism of calcium ions in nerve. Prog. Biophys. Mol. Biol. 24; 177-223.

Beauge, L., Dipolo, R., Osses, L., Barnola, F. & Campos, M. (1981) A (Ca^{2+}, Mg^{2+})-ATPase activity in plasma membrane fragments isolated from squid nerves. Biochim. Biophys. Acta. 644; 147-152.

Bers, D. M. & Ellis, D. (1981) Changes of intracellular calcium and sodium activities in sheep cardiac purkinje fibers measured with ion selective microelectrodes. J. Physiol. 310; 73P-74P.

Bers, D. M. & Ellis, D. (1982) Intracellular calcium and sodium activity in sheep heart purkinje fibers - Effect of changes of external sodium and intracellular pH. Pflugers Arch. 393; 171-178.

Blaustein, M. P. (1974) The interrelationship between sodium and calcium fluxes across cell membranes. Rev. Physiol. Biochem. Pharm. 70; 33-82.

Blaustein, M. P. (1977) Effects of internal and external cations and ATP on sodium-calcium, and calcium-calcium exchange in squid axons. Biophys. J. 20; 79-11.

Blinks, J. R. & Koch-Weser, J. (1963) Physical factors in the analysis of the actions of drugs on myocardial contractility. Pharm. Rev. 15; 531-599.

Brooker, G. (1975) Implications of cycle nucleotide oscillations during the myocardial contraction cycle. Adv. Cyclic Nuc. Res. 5; 435-452.

Bridge, J. H. B. & Bassingthwaighte, J. B. (1983) Uphill sodium transport driven by an inward calcium gradient in heart muscle. Science. 219; 178-180.

Brown, A. M. & Orkand, R. K. (1968) A down then up staircase in frog ventricle due to altered excitation-contraction coupling. J. Physiol. 197; 295-304.

Burton, R. F. (1975) Ringer Solution & Physiological Saline, Wright & Son LTD., Bristol, U.K.

Caroni, P. & Carafoli, E. (1980) An ATP-dependent Ca^{2+} pumping system in dog heart sarcolemma. Nature. 283; 765-767.

Caroni, P. & Carafoli, E. (1981) The Ca^{2+} ATPase of heart sarcolemma: Characterization, calmodulin dependence, & partial purification. J. Biol. Chem. 256(7); 3263-3270.

Carslaw, H. S. & Jaeger, J. C. (1959) Conduction of heat in solids, 2nd edition Oxford, Claredon Press.

Chapman, R. A. (1979) Excitation-contraction coupling in cardiac muscle. Prog. Biophys. Molec. Biol. 35; 1-52.

Chapman, R. A. & Ellis, D. (1977a) The effect of manganese ions on the contraction of the frog's heart. J. Physiol. 272; 331-354.

Chapman, R. A. & Ellis, D. (1977b) Uptake and loss of manganese from perfused frog ventricle. J. Physiol. 272; 355-366.

Chapman, R. A. & Fry, C. H. (1978) An analysis of the cable properties of frog ventricular myocardium. J. Physiol. 283; 263-282.

Chapman, R. A. & Niedergerke, R. (1970a) Effects of calcium on the contraction of the hypodynamic frog heart. J. Physiol. 211; 389-421.

Chapman, R. A. & Niedergerke, R. (1970b) Interaction between heart rate and calcium concentration in the control of contractile strength of the frog heart. J. Physiol. 211; 423-443.

Chesnais, J., Kavalu, F., Anderson, T. W. & Coraboeuf, E. (1978) Staircase in frog ventricular muscle - Its dependence on membrance excitation and extracellular ionic composition. Circ. Res. 43(b), 917-925.

Clark, A. J. (1913) The action of ions and lipoids upon the frog's heart. J. Physiol. 47; 66-107.

Cohen, I., Falk, R. & Kline, R. (1981) Membrane currents following activity in canine cardiac purkinje fibers. Biophys. J. 33; 281-288.

Cohen, I. & Kline, R. P. (1982) K^+ fluctuations in the extracellular spaces of cardiac muscle: Evidence from the voltage clamp and K^+ selective extracellular microelectrodes. Circ. Res. 50; 1-16.

Cohen, C. J., Fozzard, H. A. & Sheu, S. (1982) Increase in intracellular sodium ion activity during stimulation in mammalian cardiac muscle. Circ. Res. 50(5); 651-662.

Crompton, M., Capano, M. & Carafoli, E. (1976) The sodium-induced efflux of calcium from heart mitochondria: Possible mechanism for the regulation of mitochondrial calcium. Eur. J. Biochem. 69; 453-462.

Deitmar, J. W. & Ellis, D. (1978) The intracellular sodium activity of cardiac purkinje fibers during inhibition and reactivation of the Na-K pump. J. Physiol. 284; 241-259.

Dresdner, K., Kline, R. P. & Kupersmith, J. (1982) Extracellular calcium ion depletion in frog ventricle. Biophys. J. 37(2-2); 239a.

Dresdner, K. & Kline, R. P. (1983) Effects of Epinephrine, Ni^{++}, and Mn^{++}, on extracellular Ca^{++} activity fluctuations in beating frog ventricle using calcium ion selective microelectrodes. Biophys. J. 42(2-2); 75a.

Ebashi, S. & Endo, M. (1968) Calcium ions and muscle contraction. Prog. Biophys. Molec. Biol. 18; 123-183.

Eisner, D. A. & Lederer, W. J. (1980) Characterization of the electrogenic sodium pump in cardiac purkinje fibers. J. Physiol. 303; 441-474.

Elliot, T. R. (1905) The action of adrenaline. J. Physiol. 32; 401-467.

Ellis, D. (1977) The effects of external cations and ouabain on the intracellular sodium activity of sheep heart purkinje fibers. J. Physiol. 273; 211-240.

Ellis, S. (1952) The influence of enzyme inhibitors on the action of epinephrine on the frog's heart. J. Pharmacol. 105; 381-390.

Fabiato, A. & Fabiato, F. (1978a) Calcium-induced calcium release of calcium from the sarcoplasmic reticulum of skinned cells from adult human, dog, cat, rabbit, rat and frog hearts, and from fetal and newborn rat ventricles. Ann. N. Y. Acad. Sci. 307; 491-521.

Fatt, P. & Ginsborg, B. C. (1958) The ionic requirements for the production of action potentials in crustacean muscle fibers. J. Physiol. 142; 516-543.

Fischmeister, R. & Horackova, M. (1983) Variation of intracellular Ca^{++} following Ca^{++} current in heart. A theoretical study of ionic diffusion inside a cylindrical cell. Biophys. J. 41(3), 341-349.

Flitney, F. W., Lamb, J. F. & Singh, J. (1977) Intracellular nucleotides and contractility of the hypodynamic frog ventricle. J. Physiol. 276; 38P-39P.

Flitney, F. W. & Singh, J. (1981) Evidence that Cyclic GMP may regulate Cyclic AMP metabolism, in isolated frog ventricle. J. Molec. Cell. Cardiol. 13; 963-979.

Friedman, M. & Kennedy, J. W. (1955) The self-diffusion coefficients of potassium, cesium, iodide, and chloride ions in aqueous solutions. J. A. Chem. Soc. 77; 4499-4501.

Gadsby, D. C. (1980) Activation of the electrogenic Na^+/K^+ exchange by extracellular K^+ in canine cardiac purkinje fibers. Proc. Natl. Acad. Sci. 77(7); 4035-4039.

Glitsch, H. G., Reuter, H. & Scholz, H. (1970) The effect of the internal sodium concentration on calcium fluxes in isolated guinea-pig auricles. J. Physiol. 209; 25-43.

Glitsch, H. G., Kaupmann, W. & Pusch, H. (1981) Activation of active Na transport in sheep purkinje fibers by external K or Rb ions. Pflugers Arch. 391, 28-34.

Graham, J. A. & Lamb, J. F. (1968) The effect of adrenaline on the tension developed in contractures and twitches of the ventricle of the frog. J. Physiol. 197; 479-509.

Hagiwara, S. & Byerly, L. (1981) Membrane biophysics of calcium currents. Fed. Proc. 40; 2220-2225.

Hagiwara, S. & Nakajima, S. (1965) Tetrodotoxin and manganese ion: Effects on action potential of the frog heart. Science. 149; 1254-1255.

Hancock, A. A., Delean, A. L. & Lefkowitz, R. J. (1979) Quantitative resolution of Beta-adrenergic receptor subtypes by selective ligard binding: Application of a computerized model fitting technique. Molec. Pharm. 16; 1-9.

Hess, P. & Weingart, R. (1981) Free magnesium in cardiac and skeletal muscle measured with ion-selective microelectrodes. J. Physiol. 318; 14P-15P.

Hess, P., Metzger, P. & Weingart, R. (1982) Free magnesium in sheep, ferret and frog striated muscle at rest measured with ion-selective micro-electrodes. J. Physiol. 333; 173-188.

Hodgkin, A. L. & Horowicz, P. (1959) The influence of potassium & chloride ions on the membrane potential of single muscle fibers. J. Physiol. 148; 127-160.

Hodgkin, A. L. & Keynes, R. D. (1957) Movements of labeled calcium in squid giant axons. J. Physiol. 138; 253-281.

International Union of Pure and Applied Chemistry (1976) Recommendation for nomenclature of ion-selective electrodes. Pure. Appl. Chem. 48; 127-132.

Johnson, J. A. (1957) Sodium exchange in the frog heart ventricle. Amer. J. Physiol. 191(3); 487-492.

Johnson, E. A. & Liebermann, M. (1971) Heart: Excitation & Contraction. Ann. Rev. Physiol. 33; 479-532.

Kass, R. S. & Tsien, R. W. (1975) Multiple effects of calcium antagonists on plateau currents in cardiac purkinje fibers. J. Gen. Physiol. 66; 169-192.

Katz, A. (1970) Contractile proteins of the heart. Physiol. Rev. 50; 63-158.

Kavaler, F. (1974) Electromechanical times course in frog ventricle: Manipulation of the calcium level during voltage clamp. J. Cell Molec. Cardiol. 6; 575-580.

Kavaler, F., Anderson, T. W. & Fisher, V. J. (1978) Sarcolemmal site of caffeine's inotropic action on the ventricular muscle of the frog. Circ. Res. 42(2); 285-290.

Kirchberger, M. A., Tada, M. & Katz, A. M. (1974) Adenosine 3':5'-Monophosphate-dependent protein kinase-catalysed phosphorylation reaction, and its relation to calcium transport in cardiac sarcoplasmic reticulum. J. Biol. Chem. 249; 6166-6173.

Kline, R. P. (1975) K^+ efflux and accumulation in frog ventricular muscle. Ph. D. Dissertation. U. Penn. Neurobiology Dept.

Kline, R. P., Cohen, I., Falk, R. & Kupersmith, J. (1980) Activity-dependent extracellular K^+ fluctuations in canine purkinje fibres. Nature. 286; 68-71.

Kline, R. P. & Kupersmith, J. (1982) Effects of extracellular potassium accumulation and sodium pump activation on automatic canine purkinje fibers. J. Physiol. 324; 507-533.

Kline, R. & Morad, M. (1976) Potassium efflux and accumulation in heart muscle: Evidence from K^+ electrode experiments. Biophys. J. 16; 367-372.

Kline, R. P. & Morad, M. (1978) Potassium efflux in heart muscle during activity: Extracellular accumulation and its implications. J. Physiol. 132; 537-558.

Kohlhardt, M., Bauer, B., Krause, H. & Fleckenstein, A. (1973) Selective inhibition of the transmembrane Ca conductivity of mammalian myocardial fibers by Ni, Co, and Mn ions. Pflugers Arch. 338; 115-123.

Kunze, D. L. (1977) Rate dependent changes in extracellular potassium in rabbit atrium. Circ. Res. 41(1); 122-127.

Lamb, J. F. & McGuigan, J. A. S. (1966) Contractures in a superfused frog's ventricle. J. Physiol. 186; 261-283.

Lee, C. O. & Fozzard, H. A. (1975) Activites of potassium and sodium ions in rabbit heart muscle. J. Gen. Physiol. 65; 695-708.

Lee, C. O., Uhm, D. Y. & Dresdner, K. (1980b) Sodium-calcium exchange in rabbit heart muscle cells: Direct measurement of sarcoplasmic Ca^{+2} activity. Science. 209; 699-701.

Lee, C. O. & Dagostino, M. (1982) Effect of strophanthidin on intracellular Na ion activity and twitch tension of constantly driven canine cardiac purkinje fibers. Biophys. J. 40; 185-198.

LePeuch, C. J., Haeich, J. & Demaille, J. G. (1979) Concerted regulation of cardiac sarcoplasmic reticulum calcium transport by cyclic adenosine monophosphate dependent and calcium-calmodulin dependent phosphorylations. Biochem. 18; 5150-5157.

LePeuch, C. J., LePeuch, D. A. M. & DeMaille, J. G. (1980) Phospholamban, activator of cardiac sarcoplasmic reticulum calcium pump. Physiochemical properties and diagonal purifaction. Biochem. 19; 3368-3373.

Levitsky, D. O., Benevolensky, D. S., Levchenko, T. S., Smirnov, V. N. & Chazov, E. I. (1981) Calcium binding rate and capacity of cardiac sarcoplasmic reticulum. J. Molec. Cell Card. 13; 785-796.

Lieb, H. & Loewi, O. (1918) Uber spontanerholung des froschherzens bei unzureichender kationspeisung III Mitteilung. Quanitative mikroanalytische untersuchugen uber die ursache der calciumabage von seiten des herzens. Pflugers Arch. 173; 152-157.

Luttgau, H. C. & Niedergerke, R. (1958) The antagonism between Ca and Na ions on the frogs heart. J. Physiol. 143; 486-505.

Mainwood, G. W. & Lucier, G. E. (1971) Fatigue and recovery in isolated frog sartorius muscles: The effects of bicarbonate concentrations and associated potassium loss. Can. J. Physiol. Pharmacol. 50; 132-142.

Mainwood, G. W. & Worley-Brown, P. (1975) The effects of extracellular pH and buffer concentration on the efflux of lactate from frog sartorius muscle. J. Physiol. 250; 1-22.

Martell, A. E. & Smith, R. M. (1974) Critical Stability Constants Vol.1:Amino Acids Plenum Press, N.Y.; 269-272.

Martin, G. & Morad, M. (1982) Activity-induced potassium accumulation and its uptake in frog ventricular muscle. J. Physiol. 328; 205-227.

Mope, L., McClellan, G. B. & Winegrad, S. (1980) Calcium sensitivity of the contractile system and phosphorylation of troponin in hyperpermeable cardiac cells. J. Gen. Physiol. 75; 271-282.

McClellan, G. B. & Winegrad, S. (1978) The regulation of the calcium sensitivity of the contractile system in mammalian cardiac muscle. J. Gen. Physiol. 72; 737-764.

McClellan, G. B. & Winegrad, S. (1980) Cyclic nucleotide regulation of the contractile proteins in mammalian cardiac muscle. J. Gen. Physiol. 75; 283-295.

Morad, M. & Orkand, R. K. (1971) Excitation-contraction coupling in frog ventricle: Evidence from voltage clamp studies. J. Physiol. 219; 167-189.

Morad, M. & Goldman, Y. (1973) Excitation-contraction coupling in heart muscle: Membrane control of development of tension. Prog. Biophys. Molec. Biol. 27; 257-313.

Morad, M., Sanders, C. & Weiss, J. (1981) The inotropic actions of adrenaline on frog ventricular muscle: Relaxing versus potentiating effects. J. Physiol. 311; 585-604.

Morcos, N. (1981) Isolation of frog heart sarcolemma possessing (Ca^{2+}-Mg^{2+})-ATPase and Ca^{2+} pump activities. Biochim. Biophys. Acta. 643; 55-62.

Mullins, L. J. (1977) A mechanism for Na/Ca transport. J. Gen. Physiol. 70; 681-695.

Mullins, L. J. (1979) The generation of electric currents in cardiac fibers by Na/Ca exchange. Amer. J. Physiol. 236(3); C103-C110.

Nargeot, J., Nerbonne, J. M., Engels, J. & Lester, H. (1983) Time course of the increase in the myocardial slow inward current after a photochemically generated concentration jump of intracellular cAMP. Proc. Natl. Acad. Sci. 80; 2395-2399.

Neher, E. & Lux, H. D. (1973) Rapid changes of potassium concentration at the outer surface of exposed single neurons during membrane current flow. J. Gen. Physiol. 61; 385-399.

Nicholson, C. (1980) Dynamics of the brain cell microenvironment. Neurosci. Res. Prog. Bull. 18(2); 234-292.

Niedergerke, R. (1956) The staircase phenomena and the action of calcium on the heart. J. Physiol. 134; 569-583.

Niedergerke, R. (1957) The rate of action of calcium ions on the contraction of the heart. J. Physiol. 138; 506-515.

Niedergerke, R. (1963a) Movements of Ca in frog heart ventricles at rest and during contractures. J. Physiol. 167; 515-550.

Niedergerke, R. (1963b) Movements of Ca in beating ventricles of the frog heart. J. Physiol. 167; 551-580.

Niedergerke, R. & Orkand, R. K. (1966a) The dual effect of calcium on the action potential of the frog's heart. J. Physiol. 184; 291-311.

Niedergerke, R., Page, S. & Talbot, M. S. (1969b) Calcium fluxes in the frog's heart. J. Physiol. 184; 291-311.

Niedergerke, R., Ogden, D. C. & Page, S.(1976) Contractile activation and calcium movements in heart cells. Symp. Soc. Exp. Biol. XXX; 381-395.

Oehme, M., Kessler, M. & Simon, W. (1976) Neutral carrier Ca^{+2} microelectrode. Chimia 30; 204-206.

Oliver, G. & Schafer, E. A. (1895) The physiological effects of extracts of the Suprarenal Capsules. J. Physiol. 18; 230-276.

Orkand, R. K. (1968) Facilitation of heart muscle contraction and its dependence on external calcium and sodium. J. Physiol. 196; 311-325.

Page, E., McCallister, L. P. & Power, B.(1971) Stereological measurements of cardiac ultrastructures implicated in excitation-contraction coupling. Proc. Natl. Acad. Sci. 68; 1465-1466.

Page, S. & Niedergerke, R. (1972) Structures of physiological interest in the frog heart ventricle. J. Cell Sci. 11; 179-203.

Penefsky, Z. J., Barry, C. R. & Scott, W. N. (1981) Seasonal variations in the electrical and mechanical responses of toad myocardium. Comp. Biochem. Physiol. 69A; 649-658.

Prince, D. A., Lux, H. D. & Neher, E. (1973) Measurement of extracellular potassium activity in cat cortex. Brain Res. 50; 489-495.

Rasmussen, H. & Goodman, D. B. P. (1977) Relationship between calcium and cyclic nucleotides in cell activation. Physiol. Rev. 57(3); 421-509.

Reuter, H. & Seitz, N. (1968) The dependence of calcium efflux from cardiac muscle on temperature and external ion composition. J. Physiol. 195; 451-470.

Reuter, H. (1974) Localization of Beta adrenergic receptors and effects of noradrenaline and cyclic nucleotides on action potentials, ionic currents, & tension in mammalian cardiac muscle. J. Physiol. 242; 429-451.

Reuter, H. & Scholz, H. (1977) The regulation of the calcium conductance of cardiac muscle by adrenaline. J. Physiol. 264; 49-62.

Reuter, H. (1983) Calcium channel modulation by neurotransmitters, enzymes and drugs. Nature. 301; 569-574.

Rinaldi, M. L., Capony, J. & Demaille, J. G. (1982) The Cyclic AMP dependent modulation of cardiac sarcolemmal slow calcium channels. J. Molec. Cell. Cardiol. 14; 279-289.

Ringer, S. (1883) A further contribution regarding the influence of the different constituents of the blood on the contraction of the heart. J. Physiol. 4; 29-42.

Rougier, O., Garnier, D., Gargouil, Y. M. & Coraboeuf, E. (1969) Existence and role of a slow inward current during the frog atrium action potential. Pflugers Arch. 308; 91-110.

Roulet, M., Mongo, K. G., Vassort, G. & Ventura-Clapier, R. (1979) The dependence of twitch relaxation on sodium ions and on internal Ca^{++} stores in voltage-clamped frog atrial fibers. Pflugers Arch. 379; 259-268.

Sands, D. & Winegrad, S. (1970) Treppe and total calcium content of the frog ventricle. Amer. J. Physiol. 218(3); 908-910.

Scarpa, A. & Graziotti, P. (1973) Mechanisms for intracellular calcium regulation in heart I. Stopped flow measurements of Ca^{++} uptake by cardiac mitochondria. J. Gen. Physiol. 62; 756-772.

Scheuer, T. & Kass, R. S. (1983) Slow inactivation in calcium channels of cardiac purkinje fibers. Biophys. J. 41(2-2); 309a.

Sheu, S., Korth, M., Lathrop, D. A. & Fozzard, H. A. (1980) Intracellular and extracellular K^+ and Na^+ activities and resting membrane potential in sheep cardiac purkinje strands. Circ. Res. 47; 692-700.

Sheu, S. & Fozzard, H. (1982) Transmembrane Na^+ and Ca^{++} electrochemical gradients in cardiac muscle and their relationship to force development. J. Gen. Physiol. 80; 325-351.

Simon, W., Ammann, D., Oehme, M. & Morf, W. E. (1978) Calcium selective electrodes. Ann. N. Y. Acad. Sci. 307; 52-70.

Singh, J., Flitney, F. W. & Lamb, J. F. (1978) Effects of isoprenaline on contractile force, and intracellular cyclic 3', 5'-nucleotide levels in the hypodynamic frog ventricle. FEBS LETT. 91(2); 269-272.

Skou, J. C. (1957) Influence of some cations on an adenosine triphosphatase from peripheral nerve. Biochim. Biophys. Acta. 23; 294-401.

Skou, J. C. (1965) Enzymatic basis for active transport of Na^+ and K^+ across cell membrane. Physiol. Rev. 45; 596-617.

Solaro, R. J., Wise, R. M., Shiner, J. S. & Briggs, F. M. (1974) Calcium requirements for calcium myofibrillar activations. Circ. Res. 34; 525-530.

Solaro, R. J. & Briggs, F. N. (1974) Estimating the functional capabilities of sarcoplasmic reticulum in cardiac muscle. Circ. Res. 34; 531-540.

Solaro, R. J., Moir, A. J. G. & Perry, S. V. (1976) Phosphorylation of troponin I and inotropic effect of adrenaline in perfused rabbit heart. Nature. 262; 615-616.

Staley, N. A. & Benson, E. S. (1968) The ultrastructure of frog ventricular cardiac muscle and its relationship to mechanisms of excitation-contraction coupling. J. Cell Biol. 39; 99-114.

Stene-Larsen, G. & Heller, K. B. (1978) Cardiac Beta 2-adrenoceptor in the frog. Comp. Biochem. Physiol. 60c; 165-173.

Thomas, L. J. (1960) Increase of labeled calcium uptake in heart muscle during potassium lack contracture. J. Gen. Physiol. 43; 1193-1206.

Thomas, R. C. (1972) Electrogenic sodium pump in nerve and muscle. Physiol. Rev. 52(3); 563-594.

Tsien, R. W., Giles, W. & Greengard, P. (1972) Cyclic AMP mediates the effects of adrenaline on cardiac purkinje fibers. Nature New Biol. 240; 181-183.

Tsien, R. W. (1977) Cyclic AMP and contractile activity in heart. Adv. Cyclic. Nucleotide. Res. 8; 364-420.

Tsien, R. Y. & Rink, T. J. (1980) Neutral carrier ion selective microelectrodes for the measurement of intracellular free calcium. Biochimi. et Biophys. Acta. 599; 623-638.

Vassort, G., Rougier, O., Garnier, D., Sauviat, M. P., Coraboef, E. & Gargouil, Y. M. (1969) Effects of adrenaline on membrane inward currents during the cardiac action potential. Pflugers. Arch. 309; 70-81.

Walker, J. (1971) Ion specific liquid ion exchanger microelectrodes. Analyt. Chem. 43; 89-93A.

Wang, J. H. (1953) Tracer diffusion in liquids. IV Self-diffusion of calcium ions and chloride solutions. J. Am. Chem. Soc. 75; 1769-1770.

Wang, T., Lindenmayer, G. E. & Schwartz, A. (1977) Steady state kinetic study of magnesium and ATP effects on ligand affinity and catalytic activity of sheep kidney sodium-potassium adenosine triphosphatase. Biochim. Biophys. Acta. 484; 140-160.

Wilbrant, W. & Koller, H. (1948) Die calcium-wirkung am froschherzen ala funktion des ionengleishewichtz zwischen zellmembran und umgelbung. Helv. Physiol. Acta. 6; 208-211.

Winegrad, S. (1971) Studies of cardiac muscle with a high permeability to calcium produced by treatment with EDTA. J. Gen. Physiol. 58; 71-93.

Winegrad, S. (1973) Intracellular calcium binding and release in frog heart. J. Gen. Physiol. 62; 693-706.

Winegrad, S., McClellan, G., Horowit, R., Tucker, M., Lin, L. & Weisburg, A. (1983) Regulation of cardiac contractile proteins by phosphorylation. Fed. Proceed. 42; 39-44.

Wollenberger, A., Babskii, E. B., Krause, E. G., Genz, S., Bolhm, D. & Bogdanova, E. V. (1973) Cyclic changes in levels of Cyclic AMP & Cyclic GMP in frog myocardium during the cardiac cycle. Biochem. Biophys. Res. Comm. 55; 466-452.